MOLECULAR UNDERSTANDING OF FUNCTIONALITY AND UTILISATION OF WHEY PROTEIN IN NOVEL PRODUCT CONCEPTS WITH CHITOSAN AND STARCH

A thesis submitted in fulfilment of the requirements for the degree of

Doctor of Philosophy

Natasha Yang

BSc (Honours) Food Science

School of Applied Sciences

College of Science, Engineering and Health

RMIT University

MELBOURNE - AUSTRALIA

2014

CONTENTS

DECLARATION

I certify that except where due acknowledgement has been made, the work is that of the author alone; the work has not been submitted previously, in whole or in part, to qualify for any other academic award; the content of the thesis is the result of work which has been carried out since the official commencement date of the approved research program; any editorial work, paid or unpaid, carried out by a third party is acknowledged; and, ethics procedures and guidelines have been followed.

Natasha Yang
30th June 2014

ACKNOWLEDGEMENTS

I would like express my utmost gratitude to my primary supervisor Professor Stefan Kasapis for firstly accepting me into this PhD program and granting me the opportunity to take part in his active research group. During this time, his wisdom, knowledge and his demonstrated urgency and commitment to the highest standards of advancing Food Science has motivated and inspired me to continue to completion. It is bittersweet to have arrived at the conclusion of a life-changing experience and I only hope to meet such an influential leader and apply the invaluable lessons I have learnt in my future endeavours.

I would also like to thank my PhD co-supervisor Dr. John Ashton for his challenging questions and reminder to view research on a "practical significance" point of view, and Ms. Elisabeth Gorczyca, for her moral support. Additionally, her creativity and openness to novel ideas has positively influenced me to view the world with more fluidity, to challenge boundaries and question normality. Her wittiness and the personal stories she has shared with me have certainly made my experience more interesting and entertaining.

The whole venture would have been virtually impossible without funding. Thus, I am grateful for the financial support provided by Professor Stefan Kasapis, Sanitarium Health and Wellbeing Company and RMIT University.

I would also like to extend my gratitude to the RMIT Food Science and Microscopy technical staff, Lillian Chuang, Yan Chen, Deesha Makwana and Phil Francis for their assistance and accommodation of my research needs. As for my senior ex-colleagues, Omar Almarhag, Paul George, Vinita Chaudhary, Sobhan Savoodkahi, I would like to acknowledge my appreciation for their support provided in the earlier stages of my development. I would also like to express my appreciation to my current colleagues Naksit Panyoyai, Vilia Paramita, Lita Katopo and Nashi Alqahtani for their contribution in creating a positive and encouraging learning environment.

PUBLICATIONS AND PRESENTATIONS

Most of the work reported in this thesis has previously been presented in the following papers:

Journal Publications

1) Yang, N., Liu, Y. T., Ashton, J., Gorczyca, E. & Kasapis, S. (2013). Phase behaviour and *in vitro* hydrolysis of wheat starch in mixture with whey protein. *Food Chemistry*, 137, 76-82.

2) Yang, N., Luan, J., Ashton, J., Gorczyca, E. & Kasapis, S**.** (2014). Effect of calcium chloride on the structure and *in vitro* hydrolysis of heat induced whey protein and wheat starch composite gels. *Food Hydrocolloids*, http://dx.doi.org/10.1016/j.foodhyd.2014.02.022.

Fully refereed conference proceedings papers

1) Yang, N., Kasapis, S., Ashton, J.F., Pepler, T. & Ginn, P (2011). Investigating the phase morphology of whey protein and wheat starch binary mixtures as a function of processing conditions. In *"Tackling Tomorrow Today" –44th Annual AIFST Convention*, Sydney, July 10-13, pp. 55.

2) Yang, N., Kasapis, S., Ashton, J.F., Pepler, T. & Ginn, P. (2012). Investigating phase morphology of whey protein and wheat starch systems. In Australian Food Science Summer School, The University of Melbourne, Victoria, February 1-3, pp. 37.

3) Yang, N., Liu, Y.T., Ashton, J., Gorczyca, E. & Kasapis, S. (2012). Network formation and microstructure of whey protein and wheat starch systems. In *International Conference on Halal Gums*, Penang, Malaysia, December 5-7, pp. 25.

SUMMARY

Network formation of whey protein isolate (WPI) with native wheat starch (WS) has been examined. The investigation involved small deformation dynamic oscillation in shear, differential scanning calorimetry (DSC), texture profile analysis, environmental scanning electron microscopy (ESEM) and *in vitro* starch digestion. The aqueous systems consisting of 15% WPI, i.e. over the minimum critical gelling concentration of the protein, and increasing concentrations of up 15% WS were heated from 25-85°C, followed by cooling from 85-5°C. From the DSC studies, endothermic peaks reflecting starch gelatinisation and protein denaturation were resolved and the absence of other events exemplifies associative physicochemical interactions lacking between the two polymers.

The rheological profiles of binary mixtures exhibited dramatic increases in G' at temperatures more closely related to those observed for individual WPI (73°C) rather than WS (60°C) systems. This pattern prevailed even at high additions of WS (15%), whereby intense G' values were detected at 70°C. During cooling of the 15 WPI 15 WS system, a significantly higher storage modulus, i.e. greater than the sum of G' from the individual components, was measured. The gel strength apparent with single and binary systems was qualitatively reflected when subjected to single cycle compression tests. In conjunction to all the aforementioned approaches, the SEM micrographs argue for the formation of micro phase separated networks that are WPI continuous and WS discontinuous. The *in vitro* alpha amylase digestion studies demonstrate such phase morphology provides considerable reduction in the rate and extent of starch degradation.

The second set of experiments examined the formation of heat induced WPI and WS gels in the presence of $CaCl_2$ (5-192mM). The study involved similar multidisciplinary approach that was previously undertaken. When the 15% WPI system was heated in the presence of the cation, significant increase in the elastic modulus occurred at much earlier temperatures than when the protein was heated alone (73°C). The trend appeared to be concentration dependent whereby higher concentrations of $CaCl_2$ led to consistently lower onset temperatures of protein aggregation. For example, the phase transition of 15% WPI detected in the presence of

30mM and 120mM $CaCl_2$ appeared at 63°C and 53°C respectively. Micrographs from SEM depict increasingly porous WPI networks with increasing levels of $CaCl_2$ addition.
When undertaking long-deformation texture analysis of $CaCl_2$ incorporated gels, a linear relationship between the salt concentration and measured hardness did not suffice. Rather, greater hardness was measured in the absence of the cation (more elastic gels) and at high concentrations (120mM; more brittle gels) of incorporation. At intermediate levels of $CaCl_2$ incorporation, WPI-WS gels exhibited a clear decrease in the maximum force required for deformation. The latter gels were also the least vulnerable to amylolytic attack during digestion experiments. The investigation proves that $CaCl_2$ promotes the aggregation of WPI and incorporation at 48mM provides the optimum spatial structure for maximum reduction in starch degradation.

In the next part of experiments, WPI-WS preparations with the addition of medium molecular weight chitosan (MMW CHT) as low-to-intermediate solid systems were investigated. The rheological properties of single MMW CHT systems were first analysed at various concentrations (1, 1.5 and 2%) and pH (5.5, 6 and 6.5). Subsequently following heating, systems were cooled from 85°C to 5°C. In the latter stage, the 2% MMW CHT at pH 5.5 showed a smooth development in storage modulus of the highest value and thus was the chosen combination for further analysis in composite mixtures.

During the temperature ramp (25-85°C) in low amplitude oscillation experiments, the presence of the heteropolysaccharide clearly interfered with the aggregation of WPI. The sequences were replicated utilising highly sensitive micro-DSC, and no new thermal events were detected indicating the MMW CHT-WPI interactions were not of a covalent nature. From the ATR-FTIR work, an increased intensity of the absorbance peak at the amide II region was apparent, with samples containing MMW CHT, which represents a higher degree of morphological arrangement in the system. Results of the study evidenced electrostatic interactions as the driving force between MMW CHT and WPI which led to augmentation of infrared spectra.

The previously chosen 2% MMW CHT was incorporated into WPI-WS gels for last set of experiments involving *in vitro* starch digestion. The study included a comparison with gels containing 2% low molecular weight (LMW) under two digestion models, a benign system

with pH controlled at 6.9 throughout the entire experiment and a system with pH adjustments according to those applicable to the human gastrointestinal tract (mouth, stomach, small intestine). Sugar liberated at the end point of benign systems containing 15 WPI 7.5 WS and 15 WPI 7.5 WS 2 CHT corresponded to 69 and 47 mg/g respectively.

Sugar liberated at the end point of benign systems containing 15 WPI 15 WS and 15 WPI 15 WS 2 MMWCHT were 88 and 72.3mg/g respectively. As for 15 WPI 15 WS 2 LMW CHT the corresponding value was 82.7mg/g. The incorporation of both MMW and LMW CHT assisted in the reduction of starch degradation with the former being of greater effect. While adjusting the pH throughout the experiment resulted in greater fluctuations, the qualitative role of CHT in the WPI-WS gels was still realised. Results open new avenues for a detailed investigation of whey protein and chitosan networks as barriers to starch hydrolysis under an experimental protocol that imitates physiological conditions of digestion *in-vitro* and *in-vivo.*

TABLE OF CONTENTS

LIST OF FIGURES

LIST OF TABLES

LIST OF ABBREVIATIONS AND SYMBOLS

RMIT	Royal Melbourne Institute of Technology
USA	United States of America
IUPAC	International Union of Pure and Applied Chemistry
RMMF	RMIT Microscopy and Microanalysis Facility
VIC	Victoria
Ltd.	Limited
cm^2	Square centimetre
kPa	Kilo Pascal
p	Solvent partition
min	Minute
ml	Millilitre
L	Liter
µm	Micrometer
ϕ_2	Volume fraction in dispersed phase
H	Hour
i.e.	That is
o/w	Oil-in-water
sol	Solution
MW	Molecular weight
S-S	Disulfide bonds
-SH	Thiol groups

LIST OF ABBREVIATIONS AND SYMBOLS (continued)

kDa	kilo Dalton
sd	Standard Deviation
~	About
UV	Ultraviolet
NaCl	Sodium chloride
BSA	Bovine serum albumin
vis	Visible
WPI	Whey protein isolate
WPC	Whey protein concentrate
LVR	Linear viscoelastic region
ARG-2	Advanced Rheometer Generation-2
DSC	Differential Scanning Calorimeter
MDSC	Modulated Differential Scanning Calorimeter
SEM	Scanning electron microscopy
FTIR	Fourier Transform Infrared Spectroscopy
DNSA	Dinitro salicyclic acid assay
Pa	Pascal
HCl	Hydrochloric acid
max	Maximum
Na_2SO_4	Sodium sulphate
NaOH	Sodium hydroxide

LIST OF ABBREVIATIONS AND SYMBOLS (continued)

UATR	Universal Attenuated Total Reflectance
My	Moduli of polymer Y
w/w	Weight by weight
w/v	Weight by volume
Mol	Mole
rad	Radian
M	Molar
mM	milli Molar
pI	Isoelectric point
Mx	Moduli of polymer X
$\dot{\gamma}$	Shear rate
σ	Shear stress
η	Viscosity
ω	Angular Frequency
G''	Loss modulus
G^*	Complex modulus
Gy	Modulus of phase Y
G'	Storage modulus
$tan\ \delta$	Phase angle
BSE	Back scattered electrons

LIST OF ABBREVIATIONS AND SYMBOLS (continued)

ΔH	Change in enthalpy
A	Absorbance
in-vitro	Within the glass
in-vivo	Within the living
$CaCl_2$	Calcium chloride
IR	Infra-red
cfu	Colony forming units
Cp, Cs	Heat capacity
se	Standard error
E	Energy
E_a	Activation energy
f	Heat flow
f_0	Fractional free volume
α	Alpha
β	Beta
T	Temperature
t	Time
η^*	Complex viscosity
η'	Dynamic viscosity
ϕ_X	Phase volume of component X
T_d	Denaturation temperature

LIST OF ABBREVIATIONS AND SYMBOLS (continued)

$\AA$	Angstrom
λ	Wavelength
kV	Kilo volt
ϕ_Y	Phase volume of component Y
c_x	Effective concentration (%w/w) of polymers X in the two phases
w	Total weight of water in system
w_x	Weight of water in phase X
w_y	Weight of water in phase Y
atm.	Atmospheric
Ca^{2+}	Calcium ions
GI	Gastrointestinal

Chapter 1 - Introduction

This introduction is organised so that the reader is informed about the characteristics of the main components (starch, whey proteins and chitosan) of this study both in general and in terms of their gelling characteristics, individually. Following this is the background literature for the 'heart' of what was investigated in this study, namely: the literature that exposes and explains the nature of the interactions between these components; firstly in binary format and finally as tertiary dispersion.

1.0 Starch

1.0.1 Structure of starch

It has been well established that starch is a major storage polysaccharide in plants and in its native form exists as semi-crystalline granules, which contain the polymers amylose and amylopectin (Jackson, 2003; Fassler et al., 2006; Tester, Karkalas& Qi, 2004). It is well known that the former is a predominantly linear chain comprised of D-glucose residues connected by α1→4 linkages (with a few α1→6 linkages). This non-ramified structure possesses approximately 4,000 glucose units with an estimated molecular weight ranging from a few thousand to more than a million Daltons (Nelson & Cox, 2008). Amylopectin also consists of (α1→4) glycosidic linkages but it is distinguishable from amylose because it is highly branched via α1→6 linkages every 24 to 30 glucose residues (Nelson & Cox, 2008). The estimate of the molecular weight for amylopectin is about 10^8 Daltons. Interestingly, even though amylose is linear and shorter, it is more extended in its structure than the larger amylopectin molecule which tends to be compact. The chemical structure of both amylose and amylopectin is depicted in Figure 1.1.

Also Figure 1.2 shows both a schematic diagram and a cluster model of amylopectin (Ap) adapted from Gallant, Bouchet, & Baldwin, (1997). This figure shows the relative positioning of the crystalline and amorphous regions of Ap in terms of the reducing and non-reducing ends of Ap. It should be noted that while the amorphous region of starch granules is mainly attributed to amylose, the crystalline portion is completely associated with amylopectin (Hermansson & Svegmark, 1996).

Amylose is structurally incompatible with amylopectin, despite the fact that both have glucose as their base unit. Amylose does consist of a straight glucose chains as does some sections of the Ap molecule. However, amylose generally forms left-handed single helices which have been described as being ‘stiff’. An alternative configuration for amylose is the formation of left-handed but parallel double helix junctions.

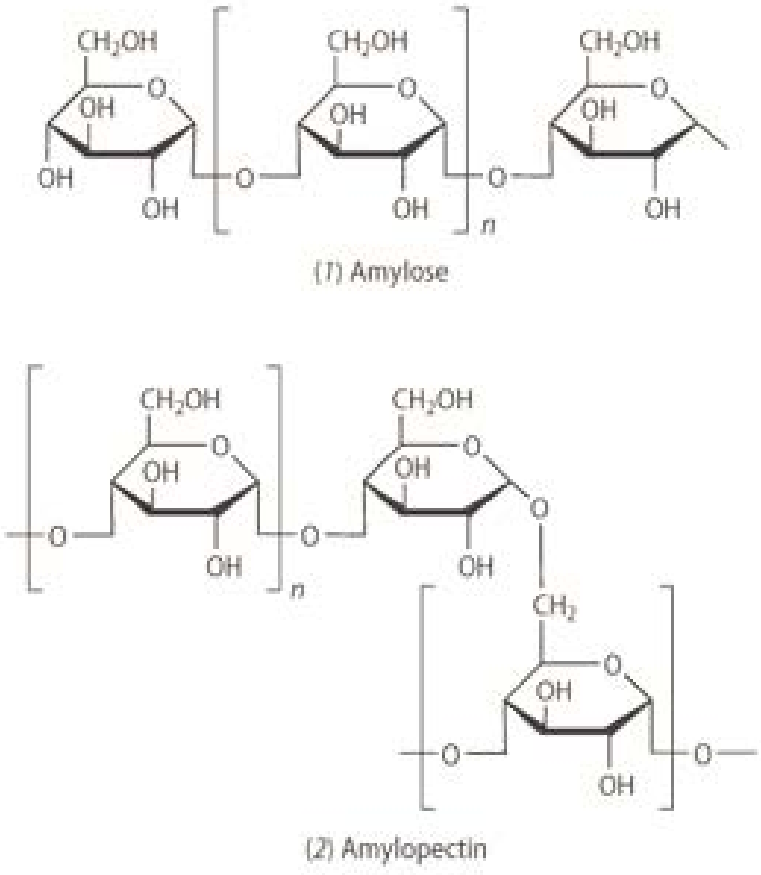

Figure 1.1 Representative structures of amylose (top) and amylopectin (bottom) (Clark & Ross-Murphy, 2009)

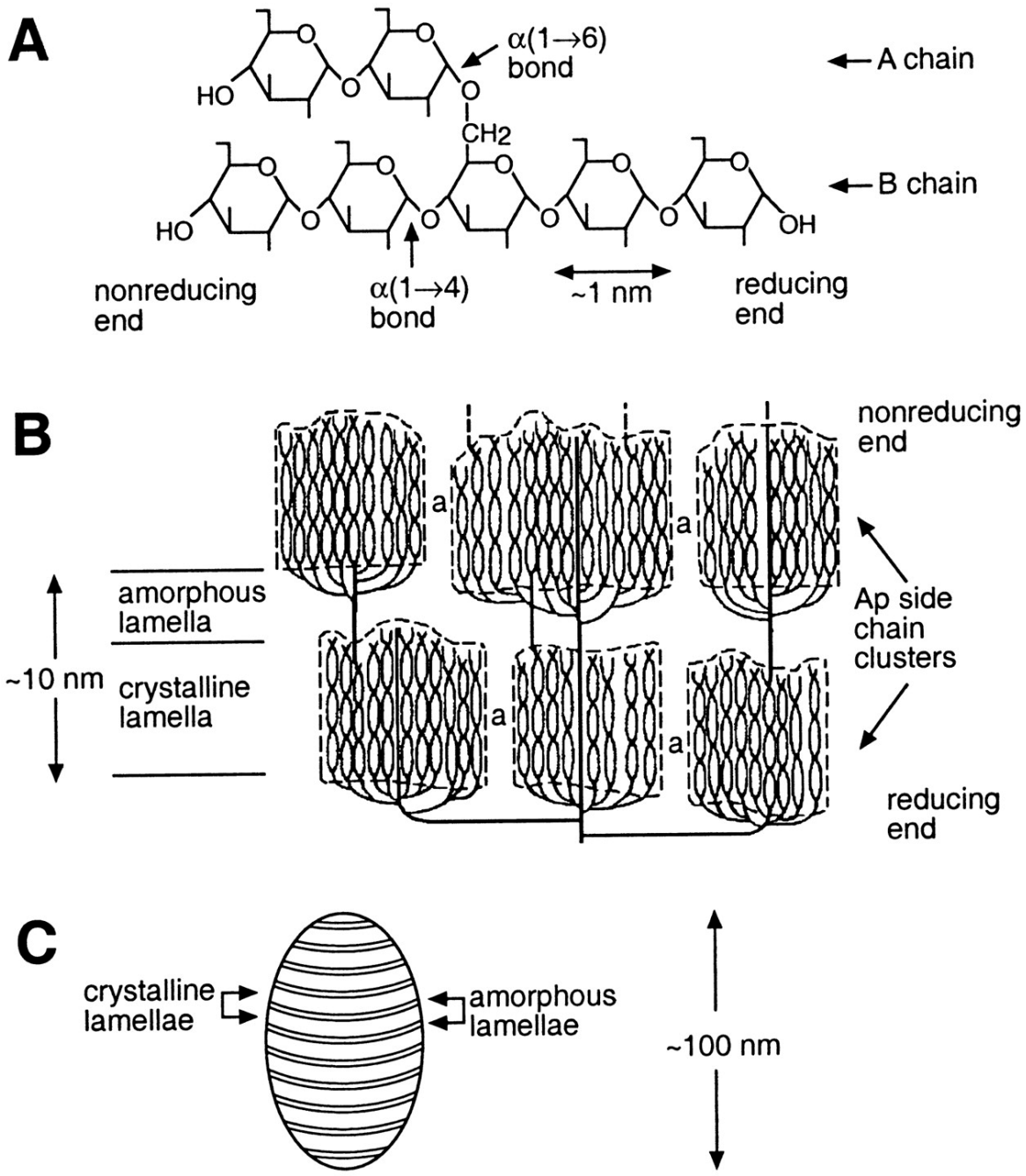

Figure 1.2 Schematic diagrams of amylopectin (Ap) where diagram A shows the reducing end of Ap as well as the linkages; the solid lines in diagram B indicate glucan chains and the dotted lines show Ap clusters and the arrangement of Ap showing the crystalline and non crystalline lamella and C is a schematic of the arrangement of Ap in a granule from Gallant, Bouchet, & Baldwin, (1997*).*

1.0.2 Sources of starch

The major sources of starch that are consumed in the human diet can be classified into two categories, namely: cereal (wheat, rice, maize) and tuber (potato) starches. The high production of wheat sees starch of this origin as the most common source in Australia while in America the same is true for corn (Environmental protection agency, 2013). Differences in the granule morphology and composition can be associated with the botanical source of the granules. However, it should be noted that granules from the same botanical origin can also differ as a result of variation in soil composition and associated climatic conditions (Singh, Singh, Kaur, Sodhi & Gill, 2003). Differentiating characteristics of starch granules include granule size and shape, clustering tendency of granules (i.e. individual granules versus compounding of granules), packing of amylopectin double helices and amylose, ratio of amylopectin to amylose and phosphorus content. The granule sizes of starches from various sources are listed in Table 1.1 (Copeland, Blazek, Salman & Tang, 2009; Lindeboom, Chang & Tyler, 2004).

In general, cereal starches appear to be smaller and possess more porous surfaces as compared with their tuber counterparts (Singh et al., 2003). In some species, such as wheat, the granules possess a bimodal distribution of two types of starch granules referred to as type A and B granules (Hermansson & Svegmark, 1996; Lindeboom et al., 2004). The A type granules are larger and disk-like or lenticular in shape with diameters in the range of 15 to 40mm (Copeland et al., 2009). The smaller B type granules are spherical or polygonal with diameters between 1 to 10mm (Baum & Bailey, 1987; Singh et al., 2003). The significance of this bimodal nature of the starch granules is not comprehended, however, there is an association between granule size and swelling functionality and therefore, ability to thicken a product (Lindeboom et al., 2004).

Table 1.1 Granule sizes of starches from different origins (Copeland, Blazek, Salman & Tang, 2009; Lindeboom, Chang & Tyler, 2004).

Source	Diameter Range [µm]
Bimodal granules	
Barley	2–3 & 12–32
Waxy maize	5-15 & 10–20
Rye	2–3 & 22–36
Triticale	5 & 22–36
Wheat	<10 &10–35
Small granule starch	
Buckwheat	2–14
Cattail	2–15
Oat	2–14
Rice	3-8
Wild rice	2–8
Medium granule starch	
Corn	5-20
Tapioca	5-25
Large granule starch	
Potato	15-75

The amylose and amylopectin ratio in starch can vary substantially within and between botanical sources and the latter is demonstrated in Table 1.2 (Fedriksson, Andersson, Eliasson & Aman, 1998). Native starches generally possess a higher proportion of amylopectin (65-75%) as compared with amylose (25-35%). The level of amylose can be further reduced by chemical modification and the term "waxy" starch essentially refers to starches with little to no amylose (Jackson, 2003). In regards to native wheat starch, the amylose content can range from 18 to 30% (Deatherage, MacMasters, & Rist, 1955; Medcalf & Gilles, 1965; Singh et al., 2003; Soulaka & Morrison, 1985).

Table 1.2 Amylose and amylopectin content from different starch sources (Fedriksson et al., 1998).

Starch Source	Amylose content (%)	Amylopectin content(%)
Wheat	25	75
Potato	24	76
Tapioca	17	83
Rice	17	83
Waxy maize	<1	>99
High amylose	50/75	50/25

It should also be noted that phosphorus is a significant non-carbohydrate component of starch (Singh et al., 2010). In potato starch, phosphorus is present as phosphate monoesters, which are covalently bound to amylopectin (Singh et al., 2003) or form hydrogen bonds with some of the hydroxyl groups. This increases the hydrophilicity of the starch and therefore its ability to swell. In cereal starches, the phosphorus is present as phospholipids that form complexes with both amylose and amylopectin (Singh et al., 2003).

1.0.3 Processing of starch

Starches are not only naturally present in plant foods but they also form a component of our staple foods; foods such as bread, noodles, pastas and rice. As well as this, starch has become 'entrenched' in the food industry because of its low cost (compared with other ingredients used in a similar manner), no detectable flavour at low concentrations (2-5%) and functional versatility (Pangborn & Szczesniak, 1974; Saha & Bhattacharya, 2010). Its versatility has resulted in a myriad of applications such as emulsifiers, colloidal stabilisers and bulking agents. Included in the list of possible applications is their effectiveness as thickeners and gelling agents providing body for food products such as sauces, soups, gravies and salad dressings (Burey, Bhandari, Howes & Gidley, 2008). The processes used by food manufacturers as well as the initial characteristics (composition and morphology) of the native granule determine the ultimate functionality of the starch. Despite the diversity of applications, a common and well documented component of most of these involve the process of gelatinisation and in some cases gelation of starches (Zeng, Morris, Batey, & Wrigley, 1997).

Briefly, gelatinisation, which occurs in the presence of sufficient moisture and heat, is heavily influenced by the presence of sugars, acids and agitation (Donald, 2004). The sugars are associated with effective water binding (sugars bind water more effectively than starch does) causing a decrease in the availability of water and thereby reducing the rate or extent of gelatinisation. Addition of acids whilst heating results in acid hydrolysis of starch to produce dextrins (shorter chain polysaccharides) which will bind less water; thus reducing the extent of gelatinisation. By contrast, agitation whilst heating allows the granules to swell independently resulting in a more even mix; this is provided the agitation is not too severe to cause granule rupture. Thus, the main event in gelatinisation is water intake where water diffuses through what Hermansson & Svegmark (1996) describe as the equatorial groove and centre of the starch granule.

Subsequently, the starch granules begin to swell radically, firstly in the amorphous regions (Figure 1.2) due to the weaker hydrogen bonding of water to hydroxyl groups of both the linear and branched starch fractions (Singh et al., 2003). What is apparently happening is that the kinetic energy of the heated water results in a hydrogen bond exchange. So the weaker hydrogen bonding within the starch is replaced by hydrogen bonding between the water and the starch, which in turn allows additional water uptake further in the granule to cause granule

swelling. The result of the swelling of the granules is an increase in viscosity which is paralleled with the thickening of the material. The amylose component of starch is also associated with the increase in viscosity not because it is hydrophilic, in fact the centre of the helical structure of amylose is relatively hydrophobic but because of its extended conformation. Another consequence of this gelatinisation process is the loss of the crystalline structure within the granules. The gelatinisation temperature of starch is normally between 50-78°C depending on the starch type as listed in Table 1.3 (Baks et al., 2007).

Table 1.3 Gelatinisation temperature of a number of commonly available starches (Baks et al., 2007).

Starch type	Gelatinisation temperature (^{o}C)
Corn	62-72
Wheat	58-64
Potato	50-68
Rice	68-78
Tapioca	58-70

The event following swelling is the rupture of the starch granules due to excessive swelling (Blazek & Gilbert, 2010). Amylose is able to 'escape' because of its linear conformation whereas amylopectin, given its branched and compact conformation is trapped within the imploded granule. In summary the event can be described as either an explosion or an implosion of the granule. In either case, amylose leaches out of the granule and there is an associated decrease in viscosity of the material.

Upon cooling the heated starch dispersion forms a three dimensional network through cross linking of the polymer chains. This cross linking related to primarily the amylose chains is described as the process of gelation as it is associated with the increase in viscosity produced by gel formation. The cross linking of wheat starch was monitored in the rheological experiments conducted by Yang, Irudayaraj, Otgonchimeg & Walsh (2004). In their experiments, it could be seen that as the pure wheat starch was cooled from 85 to 25°C, the G' increased. It is the amylose component that contributes to gelation. Due to the highly

branched structure of amylopectin, close intermolecular associations cannot be formed and instead this polymer provides a stabilising effect. Thus, high amylose starches can build a three dimensional network to enhance fat and water holding capacities whereas waxy starches would be added as thickeners to provide viscosity.

1.0.4 Starch digestion

The first question is why starch digestion is scientifically and socially of interest. The interest was spurred on by the fact that carbohydrate containing foods have been classified according to their glycaemic index (GI) which was introduced by Jenkins et al. (1981) 33 years ago, as a way of classifying foods based on the postprandial rise in blood glucose. The problem arises because a diet rich in high GI foods has been directly associated with obesity and Type 2 diabetes (Better Health Channel, 2014). The latter metabolic disorder also known as diabetes mellitus is characterised by hyperglycaemia due to insulin resistance and insulin deficiency. Since the modern western diet is associated with foods high in GI, it comes as no surprise that alarming increases in the prevalence of these diet-related illnesses have become apparent (Tanamas et al., 2014). While sufferers of obesity are more obvious, it has been estimated that some 940,000 Australians have diabetes and about half of those are not aware that they have the condition (*Health Insite*, September 2008). Furthermore, the World Health Organisation recently reported that at least 347 million people worldwide suffer from diabetes (Kumar & Prabhasankar, 2014).

On the other hand, studies have shown that a low GI diet can provide a desirable reduction in meal-associated hyperglycemia and cardiovascular diseases (Lehmann & Robin, 2007). The difference between a high GI and low GI food is that the latter releases glucose into the blood at a lower level or at slower rate. The latter may come about through a lower rate of starch degradation (digestion); an issue forming the main focus of early studies (Englyst et al., 1999; Jenkins et al., 1980, 1982, 1988, 2002).

This now leads to questions around the process of the digestion of starches. The digestion of foods occurs in three key compartments of the human gastrointestinal tract, namely: the mouth, the stomach and the small intestines. For starch and carbohydrate containing foods, enzymatic degradation initially occurs in the mouth but due to the short retention time in the mouth, most of the hydrolysis occurs in the duodenum and jejunum where pancreatic alpha-

amylase (α-amylase) is available (Kong & Singh, 2008). Gray (1992) explains that the hydrolytic activity of the enzyme involves binding of the starch polymer's five glucose residues adjacent to the terminal reducing glucose unit to specific catalytic sub sites on the α-amylase. This is then followed by cleavage between the second and third α1→4 linked glucosyl residue. However, α-amylases have no specificity for α1→6 branch links in amylopectin, and furthermore, their capacity to hydrolyse α1→4 links adjacent to the branching point is decreased mainly due to steric hindrance (Koh, Kasapis, Lim & Foo, 2009).

Enzymatic degradation is also affected by the size of starch granules in that small starch granules such as those from oats and rice exhibit greater digestibility than do the larger starch granules from maize, wheat and potato (Bednaret al., 2001; Manelius & Bertoft, 1996). Starch digestibility is also enhanced in foods that have undergone gelatinisation-the degree of which can be hindered by amylose complexes with lipids. Since the degree gelatinisation can be hindered by amylose complexes with lipids, such complexes also indirectly affect starch digestibility.

The result of α-amylases activity is the production of maltose and branched dextrins, which is not the final stage of digestion. In the small intestine, further enzymatic hydrolysis occurs at the apical plasma membrane of the enterocytes to which the relevant enzymes are attached; i.e. these enzymes are not found in the lumen of the intestine. It is for this reason that the terminal stage of carbohydrate digestion is carried out by enzymes that are referred to as brush border enzymes. Thus, the final hydrolysis to glucose by brush border enzymes occurs as they (maltose and branched dextrins) cross the mucosa and enter the bloodstream, whilst the undigested starch moves onto the large intestine.

Earlier in this introduction, the nutritional significance of the rate of glucose production was emphasised. So, it comes as no surprise that further studies led to the classification of starches by their rate of digestion: rapidly digestible starch, slowly digestible starch and resistant starch (Englyst, Kingman, & Cumming, 1992). Where, rapidly digestible starch (RDS) was the portion of starch that was hydrolysed to glucose during the first 20min of digestion (Englyst, Englyst, Hudson, Cole & Cummings, 1999). Slowly digestible starch (SDS) was the portion of starch associated with glucose release between 20 and 120 min of digestion. The resistant starch (RS) is the portion of the starch that is not enzymatically degraded by

digestive enzymes and is defined as the difference between the total starch and the amount of glucose released within 120 min of digestion (Englyst et al., 1999).

The purpose of starch digestion is to provide metabolic value to the consumer and according to several authors (Copeland et al., 2009;Frei, Siddhuraju & Becker, 2003), it currently is responsible for approximately 50-70% of the energy consumed in the human diet. However, starch is classified as a high GI food that causes a rapid influx of sugar into blood serum (Brand-Miller et al., 2002; Frei et al., 2003). To compound the problem, heating (cooking) of starch increases the rate of hydrolysis by gelatinising the starch and making it more easily available for enzymatic attack. So, the long-term consumption of starch is not ideal with respect to prevention and management of Type 2 diabetes (Jenkins et al., 2002). On the other hand, starch is ubiquitous and as explained earlier, it has many food applications and consequently, total elimination of the polysaccharide would not be a credible solution to the problem of its poor GI status.

A more practical and feasible approach would be the selection of better starch sources and or the use of other ingredients in the food matrix in combination with starch to hinder the digestibility of starch and thereby lower the GI. So, what evidence is there, that this approach is feasible and effective? According to Colonna et al., (1992), the addition of protein, fibre and other food components can interact with starch and interfere with the enzymatic hydrolysis of starch. It is suggested (Singh, Dartois & Kaur, 2010) that the macromolecule, like proteins, create a physical barrier to reactive enzyme substrate sites and thereby slow starch digestibility. As explained earlier, co-solutes (which can include proteins) can compete with starch for water and given the essential role played by water in gelatinisation, effectively slow down or restrict the degree of gelatinisation and consequently starch hydrolysis. This situation was exemplified in the work done by Kim et al. (2008). Pasta is a case in point, as it was found that the presence of gluten in the dough limited starch digestibility by several mechanisms. Firstly, the protein glutenin and gliadin compete for water, thereby restricting gelatinisation. Secondly, the development of the gluten network created a physically barrier, blocking the enzyme from access to starch. Thirdly, it was also concluded that the protein itself may interact with α-amylase, thus decreasing the potential starch- enzyme interactions (Kim et al., 2008). Another interesting effect is demonstrated with whey proteins which have been shown in several studies (Belobrajdic, McIntosh & Owens, 2004; Berti et al., 2004; Gannon, Nuttall, Neil, & Westphal, 1988; Juntunen et al., 2002; Luhovyy, Akhavan &

Anderson, 2007) to stimulate the release of insulin resulting in a lower postprandial rise in blood glucose beneficial in the management of Type 2 diabetes.

Interestingly, post-gelatinisation including refrigerated storage can also lead to a decrease in starch digestibility as a result of the process of retrogradation (Singh, Dartois & Kaur, 2010). Where retrogradation involves re-association and re-crystallisation of the starch chains in the amorphous material after gelatinisaton. Retrogradation of amylose can occur within 24h after processing whereas amylopectin retrogration can take up to a few days (Singh, Dartois & Kaur, 2010). Aggregation and re-crystallisation of starch chains from amylose and amylopectin leads to structures that resist digestion by amylases (Singh, Dartois & Kaur, 2010). According to Zobel and Kulp (1996) and Goodfellow and Wilson (1990), the retrogradation process for amylose involves two major steps, the first of which is a change from a random coil formation post-gelatinisation to a re-ordering to form double helices. These helices would then aggregate to form crystalline structures. A similar, but slower process was noted for amylopectin with particularly the outer branched chains crystallizing.

As discussed, the digestibility of carbohydrate containing foods can vary significantly as a result of many variables and it is in the interest to the food industry to develop products with SDS. The next issue to discuss is how it can be established that a SDS food matrix has been developed. Obviously, some form of a digestion-type study needs to be carried out. The choices a researcher has is to undertake an *in vivo* or an *in vitro* study. Unmistakably, an *in vivo* study, even if it is an animal study, is the more meaningful of the two. This is the case, even though an animal feeding study is not identical to a feeding trial involving digestion through the human gut; a trial which would not be ethically permissible. The limitations of an *in vivo* study are clear: cost, time, specialised facilities, appropriate feed type and rate, timely sampling and so on. Consequently, an *in vivo* study would only be warranted after substantial evidence of a significant break-through has been obtained. Thus, much of the research and development of food products to date (Hur, Lim, Decker & McClements, 2011) have been conducted using *in vitro* studies to monitor the rate and extent of hydrolysis of specific food matrices. The experimental parameters that need to be defined when implementing an *in vitro* digestion trial include the following: the enzyme (type, source, concentration in international units, appropriate pH and time of addition), sample (form, dimensions, and composition) and operational set-up (closed versus open system, temperature, sampling time, when and how to change the pH, type and concentration of co-solutes and the nature of the applied shear force

as well as the flow rate). The hydrolytic enzymes used *in vitro* digestion trial have been sourced directly from human subjects as well as extracted from plants, animals and moulds. At this point in time, there is no evidence that the enzymes sourced from humans produce more meaningful data than the equivalent enzymes from alternate sources (Hur et al., 2011). However, there is agreement that freshly prepared enzymes is required and that for the *in vitro* experiment to be conducted at the temperature of the human body i.e. 37 ±1°C (U.S. National Library of Medicine, 2014). To more closely mimic the human GI tract, appropriate incubation times and pH adjustment can be made. In this way, the ability of a selected food matrix can be evaluated in terms of its capacity to withstand the acidic conditions of the stomach and the rate and extent of starch hydrolysis in the *in vitro* small intestines. The latter is usually monitored by using the 3,5dinitrosalicyclic acid (DNSA) assay (Bernfeld, 1955).This method measures the total amount of reducing sugars (carbonyl group) through an oxidation-reduction process which involves the functional group of the sugar molecule reducing 3,5 dinitrosalicyclic acid (Pangborn & Szczesniak, 1974). Subsequently, the reaction is measured colormetrically via absorbance at 540nm.

What is essentially missing from most *in vitro* models of the GI tract is the natural micro flora present in the gut, the feedback mechanism used to control the delivery of the enzymes, other GI components and the appropriate shear forces that a food would experience (Hur et al., 2011). Despite this, an *in vitro* study can provide qualitative trends that may occur *in vivo* for low GI foods made with appropriate processing of starch in mixtures with ingredients such as whey protein and chitosan as is the interest of this research.

1.1 Whey protein (WP)

1.1.1 Sources of whey protein

The consumption of bovine milk is recognised as a part of a balanced diet and has been known to contribute to the health and well-being of individuals (Fox & McSweeney, 2003). An important constituent in milk is its proteins, present at 32g/L and comprised of 80% caseins and 20% whey proteins (Fox & McSweeney, 2003). According to Walstra, Wouters & Geurts, (2006), one way to describe the difference between these two groups of proteins is that casein proteins are insoluble even at milk pH whereas WP has traditionally been defined as soluble proteins. The reason being that WP remain ‘dissolved’ in the bovine milk serum

after coagulation of the casein proteins at pH 4.6 (and ≈ 20°C), at its isoelectric pH (pI). While both proteins possess a net negative charge at the pH of milk, the distribution of charges on the whey protein are more uniform (Damodaran, Parkin & Fennema, 2008). Another, often highlighted, difference between casein and whey protein is their rate of digestion. As caseins proteins form clots during digestion (given the pH of the stomach), the hydrolysis of the amino acids on the casein protein is delayed in comparison with the digestion of the amino acids of the whey proteins. Given their more rapid digestion, whey proteins are particularly appealing to post-exercise consumption for athletes and body builders (Fox & McSweeney, 2003; Tipton et al., 2004). The nutritional quality of a protein has been stressed as more important than the quantity (Dubois, 2013) and while both milk proteins score high in the former, whey proteins contain more sulfur amino acids and therefore possess a higher biological value (1.0) than casein proteins (0.8) (Damodaran et al., 2008).

The main whey proteins in descending order (quantity) are β-lactoglobulin, α-lactalbumin, bovine serum albumins, immunoglobulins and lactoferrins. The tertiary structure of proteins determines whether they are fibrous, disordered or globular and whey proteins belong to the globular group (Walstra et al., 2006). These proteins are compact globular proteins that have been classified based on the primary sequence of amino acids in their polypeptide chains (Fitzsimons, Mulvihill & Morris, 2007; Kazmierski, & Crredig, 2003). In Figure 1.3, an illustration shows size comparisons between whey proteins and the casein micelle (De Wit, 1998).

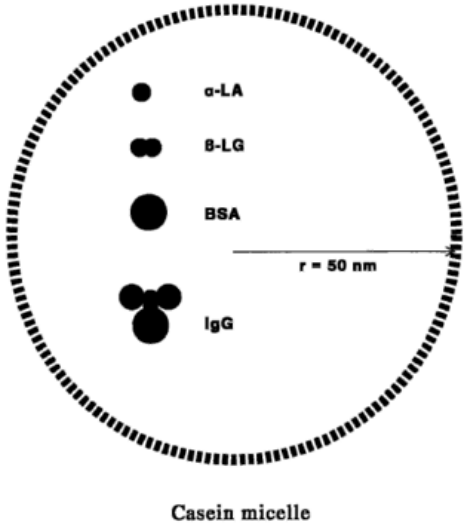

Figure 1.3 Size comparison of whey proteins with casein micelle (De Wit, 1998)

1.1.2 Production of whey protein products

The first step in the manufacture of whey protein involves separating it from the casein proteins and depending on the method used may produce what is called sweet or acid whey. The difference is a result of the method of coagulating the casein proteins: using coagulating enzyme (rennet) or an acid (lactic acid). Sweet whey would be produced by using rennet which also results in retaining more lactose as compared with the acid coagulated approach (Dissanayake, 2011). While the exact content varies, whey generally contains 0.6% whey protein (Foegeding& Luck, 2002). Again depending on the processing method, it is possible to produce various types of whey protein products, namely: whey protein concentrate, isolate and hydrolysates. Whey protein concentrate (WPC) are produced by using ultrafiltration and diafiltration during which low MW components such as lactose and minerals are separated from the retentate. The product can be further concentrated *via* ion exchange chromatography or enzymatically pre-digestion to produce whey protein isolate (WPI) or whey hydrolysates (WH), respectively. Depending on the required characteristics, these products are incorporated providing nutritional and versatile functional roles in various food and pharmaceutical products (Farrell et al., 2004). The compositions of these whey protein powders are summarised in Table 1.4.

Table 1.4 Composition of whey protein powders (Farrell et al., 2004).

Whey protein powders	Protein Concentration	Fat, Lactose, Mineral Content
Whey protein isolate	90-95%	Negligible
Whey protein concentrate	25-89% most common~ 80%	Some fat / lactose / minerals which decrease as protein
Whey Protein hydrolysate	Variable Hydrolysis used to cleave peptide bonds, creating smaller peptide fractions Reduces allergic potential compared with non-hydrolysed	Varies with protein concentration

Whey which is a by-product of cheese production was once considered waste destined solely for the "cheapest gutter" (Smithers, 2008). However with the advances in research and technology, whey derivatives have become increasingly valued. According to De Wit, in 1998 the worldwide production of whey stood at approximately 118 million tonnes. Such an amount could have potentially produced 7 million tonnes of concentrated whey solids however, only about 4.3 million tonnes (10% whey protein content) or 62% of the potential amount was produced (De Wit, 1998). By 2009, 25% of whey production in Australia found its way into domestic manufacture, with the remainder being "off-loaded" abroad as a cost-effective management of the waste of cheese processing (Dairy Australia, 2009). The worldwide production of whey protein in that year according to Thompson et al. (2009) as cited by Dissanayake (2011) was slightly over 0.5 million tonnes. Thus, a great potential for the production of whey derivatives useful in the medical, pharmaceutical and food industry at that point in time still remained to be discovered. The increasing value of whey derivatives between 1950s and 2000s is exhibited in Figure 1.4 (Smithers, 2008).

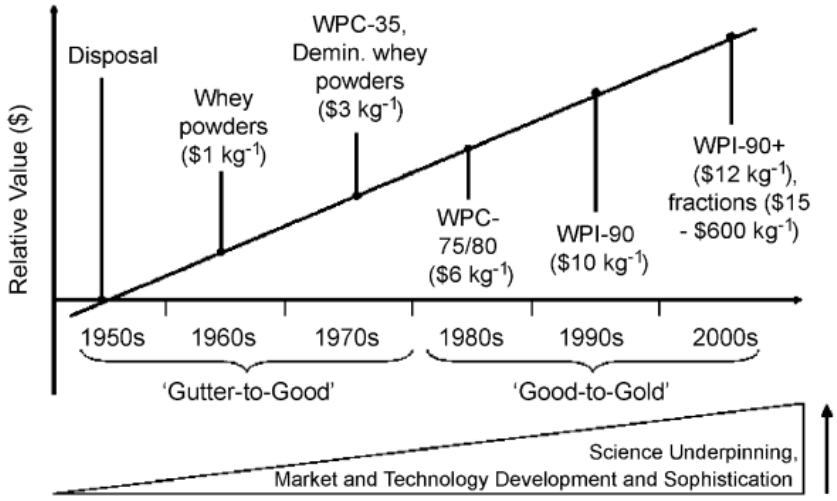

Figure 1.4 Value of whey and whey derivatives over time (Smithers, 2008)

There are many incentives for the production of whey powders and incorporation into food products. Besides being granted GRAS status (Hu, McClements & Decker, 2003) and providing basic nutrition, the uses for whey protein powders and its derivatives span both the nutritional and functional applications. An increasing number of physiological benefits are being associated with individual protein fractions. For example, peptides derived from the

enzymatic hydrolysis of β-lactoglobulin and α-lactalbumin in the intestinal lumen possess antimicrobial activity against Gram positive bacteria (Chatterton, Smithers, Roupas & Brodkorb, 2006). Furthermore, the lactokinins α-lactorphin, β-lactorphin and β-lactotensin exhibit antihypertensive effects by inhibiting the activity of angiotensin converting enzyme (ACE) (Chatterton et al., 2006). In the regulation of blood pressure, ACE plays an important role in monitoring blood pressure. ACE inhibition leads to a decrease in the level of the vasoconstricting peptide, angiotensin II, and a corresponding increase in the level of the vasodilatory peptide, bradykinin, thereby yielding an overall reduction in blood pressure according to Donkor et al., (2007). The antiviral role and cancer preventing bioactive compounds of whey protein have also been well documented (Chatterton et al., 2006; McIntosh et al., 1998; Fox & McSweeney, 2003). As for serum albumin, α-lactalbumin and lactoferrin, their value is associated with their ability to synthesise glutathione which is known to combat free radical damage and cancer (Fox & McSweeney, 2003).

Whey proteins also can exhibit excellent functional properties which are directly related to their molecular characteristics, functional properties such as: hydration, surface activity, protein-protein interactive potential and organoleptic properties (Damodaran et al., 2008). Current functional applications of whey protein include its use as an emulsifier, gelling and foaming agent. According to Barbut (1995) heat induced whey protein gels are added as functional ingredients to sausages. Such applications are often in combination with other ingredients and/or appropriate processing with isolation of specific whey protein fractions since each exhibits its own unique qualities and characteristics. The whey proteins can also be used collectively and incorporation of WPC and WPI in products can impart flavour and colour due to the presence of lactose which can be involved in a Maillard reaction. To produce whey protein products of physiological benefit and desired functionality, knowledge of the structure-function relationships of natural whey powders in relation to processing parameters and subsequent storage is imperative.

1.1.3 The structure of the whey proteins

(a) β-Lactoglobulin

β-Lactoglobulin (β-Lg) is a major whey protein fraction and accounts for about half of the total whey protein available. The MW of β-Lg is 18,000 Da (Eigel et al., 1984; Morr & Ha, 1993) incorporates a primary amino acid sequence of 162 amino acid residues which has the

following sequence: ASP 10 ASN 5 THR 8 SER 7 GLU 16 GLN 9 PRO 8 GLY 4 ALA 15 CYS 5 VAL 9 MET 4 ILE 10 LEU 22 TYR 4 PHE 4 LYS 15 HIS 2 TRP 2 ARG 3 (Morr& Ha, 1993). In terms of the primary structure, many genetic variants of β–Lg have been identified and these differ in their properties including thermal stability (Dissanayake, 2011; Fox &McSweeney, 2003; Walstra et al., 2006). Two main genetic variants are β–Lg A and β –Lg B which possess differences in the amino acid sequence at two positions. The latter form has GLY 64 and ALA 118 residues instead of ASP 64 and VAL 118 (Foegeding et al., 2002). The secondary structure of β-Lg consists of predominantly beta sheets (51.2%), as well as α-helices (6.8%), beta turns (10.5%) and remainder described as random coils (Damodaran et al., 2008). The main feature of the secondary structure is that one α-helix and anti-parallel β-sheets have been formed by nine strands; eight of which create the somewhat flattened, conical barrel or calyx (Croguennec et al., 2004; Dissanayake, 2011; Fox &McSweeney, 2003).

The tertiary structure of β-Lg is largely maintained by two disulfide bonds between the side chains of Cys66-Cys160 and Cys106-Cys119 formed through oxidation of thiol groups (Croguennec et al., 2004). The tertiary structure of β-Lg is affected by pH in that between 5.2 and 7.5, β-Lg is above its isoelectric point and under these conditions β-Lg exists as dimers. These dimers consist of two spheres with radii of 17.9 Å and a distance from centre to centre of 33.5 Å joined to create a two-fold rotation or dyad axis of symmetry (Kasapis, 2010). As the pH decreases below3.5 or increase above 7.5, the dimer dissociates into expanded monomers. β-Lg can also exist as an octamer when the pH is in the range of 3.5 to 5.2 (Morr & Ha, 1993).

Like other proteins, β-Lg loses its secondary structure during sufficient heat treatment. The exposure of highly reactive SH and amino groups pushes for the aggregation of protein chains and formation of a polymeric network. Although thermal transition has been identified to be ~73°C (Yang et al., 2013), the use of optical rotatory dispersion provides evidence that the quaternary structure commences dissociation at temperatures as low as 20°C (Fox and McSweeney, 2003; Morr & Ha, 1993). It should be noted that this protein is highly resistant to low pH values such as those found in the human stomach. It is believed (De Wit, 1998; Papiz et al., 1986) that the stability of the molecule in an acidic environments is related to its biological role as a carrier of retinol from the cow to the calf.

(b) α-Lactalbumin

α-Lactalbumin (α-La) is the second most abundant protein fraction occupying 20% of the total whey protein content (Morr& Ha, 1993). The MW of α-La is 14,174 Da (Kasapis, 2010) incorporates a primary amino acid sequence of 123 amino acid residues which has the following sequence: ASP 9 ASN 12 THR 7 SER 7 GLU 8 GLN 5 PRO 2 GLY 6 ALA 3 CYS 8 VAL 6 MET 1 ILE 8 LEU 13 TYR 4 PHE 4 LYS 12 HIS 3 TRP 4 ARG 1 (Morr & Ha, 1993). Two genetic variants α-La A and α-La B are commonly known and both possess roughly α-helices (26%), β-sheets (14%) and the remainder has an unordered structure (Dissanayake, 2011). The highly compact structure of α-La can be attributed to the presence of 4 disulfide bonds which is double that of β-Lg (Morr & Ha, 1993). In contrast to β-Lg, α-La exists as nearly spherical monomers of about 2.2 x 4.4 x 5.7 nm when it is above its pI of 4.2 to 4.5 (Eigel et al., 1984; Morr & Ha, 1993). At pH values below the pI, α-lactalbumin associates to form dimers and trimers, which results in the formation of a polymeric network (Kasapis, 2010). Furthermore, α-La is generally known to be more heat stable than b-Lac, which was explained to be a result of more covalent bonds and the presence of a Ca^{2+} binding site (Fox & McSweeney, 2003). In previous research, scientists (Morr & Ha, 1993) found that α-La exhibited a high degree of re-naturation as the calcium binding site promoted unfolding of α-La. Consequently, the flexibility of the molecule maybe assisting its heat resistance (Dissanayake, 2011; Morr & Ha, 1993). The thermal transition of this protein occurs at 61-61.5°C (Aguilera & Rojas, 1996).

(c) Bovine Serum Albumin

Containing 582 amino acid residues and a MW of ≈ 66, 433 Da, bovine serum albumin (BSA) possesses the longest polypeptide chain of all the whey proteins. The amino acid sequence of BSA is ASP 39, ASN 12, ASX 3, THR 34, SER 28, GLU 59, GLN 19, GLX 1, PRO 28, GLY 16, ALA 46, CYS 35, VAL 36, MET 4,ILE 14, LEU 61, TYR 19, PHE 27, LYS 59, HIS 17, TRP 2 and ARG 23 (Considine et al., 2007; Morr & Ha, 1993). The secondary structure of BSA does not contain beta-sheets but does contain α-helices (66%), β-turns (10%) and 23% extended chains (Carter & Ho, 1994; Considine et al., 2007; Gelamo et al., 2002; Gelamo & Tabak, 2000; Reed et al., 1975; Wetzel et al., 1980). The shape of this protein is described as being oblate often folding into two or more domains which has been associated with its biological function (De Wit, 1998). The role of BSA which interestingly is similar to that of blood serum albumin, is the binding of insoluble free fatty acids (FFA) (De Wit, 1998). In the

case of blood serum albumin, this binding would result in transportation of insoluble FFA to vital organs *via* the bloodstream. With respect to temperature sensitivity, the conformational changes in BSA are reversible between 42 and 50°C, whereas at temperatures above 52°C, unfolding of the α-helices is irreversible (Considine et al., 2007).

(d) Immunoglobulins

Immunoglobulins exist in minor amounts as compared with the aforementioned whey protein fractions. These antibodies can be classified into the different types, namely IgM, IgA and IgG. The most common immunoglobulin in whey is IgG which comprises 80% of the total immunoglobulin content. The large glycoprotein is identical to that found in human blood serum with a characteristic Y shape and a radius axis of approximately 6 nm. The immunoglobulins have a tendency to bind to other specific molecules (Horowitz & Pigman, 1977).

1.1.4 Effect of food processing on whey protein characteristics

Besides the primary structure, steric effects, secondary binding forces (electrostatic, hydrogen and hydrophobic), and disulfide bridges responsible for the size, shape and configuration of the protein, molecular associations are also influenced by the external environment including temperature, pH, shear and composition (e.g., presence of calcium ions and other macromolecules) of the dispersing medium. These external factors are manipulated by the food industry to provide desirable protein functionality. For example, the pH of an aqueous medium around the pI would reduce protein solubility as a result of lowered electrostatic repulsion (Damodaran et al., 2008). Furthermore, through application of heat, the large number of hidden hydrophobic residues would ultimately unravel, resulting in protein denaturation, aggregation and development of heat-set gels capable of entrapping water and other food materials.

(a) Denaturation and aggregation

Protein denaturation is the significant breakdown of quaternary, tertiary and secondary structures without affecting the peptide bonds between the amino acids. Denaturation is an endothermic process which may occur via the application of appropriate physical agents (heat,

light) or chemical agents (urea or acids). The formal definition of denaturation according to Kauzmann (1959) is that denaturation is the "process (or sequence of processes) in which the spatial arrangement of polypeptide chains within the molecule is changed from that typical of the native protein to a more disordered arrangement (the terms configuration, conformation and state of folding can be substituted for spatial arrangement in this definition)". Damodaran et al., (2008) explains that hydrogen bonds are unstable in high temperatures and therefore are easily disrupted and in addition, the free energy in the system can ultimately induce the unfolding of the protein which in turn results in the exposure of the previously hidden hydrophobic groups. Thermal denaturation of whey proteins can be reversible or irreversible depending on the temperature i.e. generally speaking <70°C and > 75°C, respectively (De Wit, 1998; Livney, Corredig & Dalgleish, 2003; Morr & Ha, 1993). The heat stability of the whey proteins in descending order is α–La (most resistant) >BSA>immunoglobulins> β-Lg (Fox and McSweeney, 2003). Protein concentration is also important to note here as a higher protein concentrations results in a decrease in denaturation temperature (Livney, Corredig & Dalgleish, 2003).

After irreversible denaturation, as De Wit (1998) explains, aggregation commences when more than half of the total protein (60%) has unfolded (irreversibly denatured) provided that the protein concentration is above the gelation threshold. Aggregation involves formation of a network through intermolecular bonding between protein chains involving covalent specifically disulphide bonds by sulfydryl-disulfide interchange and non-covalent bonding such as hydrogen bonding, electrostatic interactions or hydrophobic interactions (Livney, Corredig & Dalgleish, 2003). It should also be noted that although there is a low degree of aggregation occuring in isolated native α–La there is in conjunction with β-Lg, synergistically beneficial aggregation (Livney, Corredig & Dalgleish, 2003). Interestingly Livney, Corredig & Dalgleish (2003), suggests that the driving force for aggregation, more particularly large aggregates, is the need for thermodynamic stability which in this case requires reducing the exposure of hydrophobic regions of the structure. Ultimately there is an increase in beta sheets in exchange for a decrease in alpha helices.

The presence of different types of salts and co-solutes will influence the degree and rate of aggregation. For example, Barbut (1995) reported that low levels of sodium and calcium resulted in clear and opaque WPI gels, respectively and that the difference in the gels was

directly related to the degree of aggregation. The basic argument is that calcium (more so than sodium)is particularly efficient in reacting with charges to establish bridges (calcium bridges) between and within polypeptide chains. Pappas and Rothwell (1991) concluded that the calcium bridging occurred with the free carboxylic groups of aspartic and glutamic acids, particularly as phosphorus was not present in either β-Lg or α-La. When heated in the presence of calcium, β-Lg aggregated completely but failed to do so in the same time (30 min) and temperature (80°C) regime in the absence of the divalent ion (Pappas and Rothwell, 1991). Also, according to Pappas and Rothwell (1991), calcium has a greater binding capacity with β-Lg than α-La.

The addition of salt at low ionic strength (less than 200mM) enhances electrostatic interactions and structural stability, irrespective of the type of salt (Dissanayake, 2011). On the other hand at higher concentrations (>1M), cations increase the denaturation temperature of whey proteins more so than anions with the ability to influence the structural stability of proteins following the Hofmeister series (Damodaran et al., 2008). During the cooling phase after heating, protein-protein interactions continue to occur and are prominent between 40-60°C (Cheftel, Cuq, & Lorient, 1985; Niwa, 1992; Yang, Irudayaraj, Otgonchimeg & Walsh, 2004). For example, Yang et al. (2004) observed an increase in G' of starch and WPI systems during the cooling period when temperatures were between 65 to 30°C and associated this with hydrophobic interactions. The different combinations of the aforementioned factors ultimately result in producing protein gels with different textural characteristics.

1.2 Chitosan

1.2.1 Chitosan structure and source

Chitosan is derived from the partial alkaline deacetylation of the linear β-1, 4 linked N-acetyl-D-glucosamine polymer chitin (Chang, Lin & Chen, 2003). The linear polysaccharide consists of N-acetyl-D-glucosamine and D-glucosamine polymers with β-(1→4) linkages as shown in Figure 1.5. The polymer was first discovered in 1859 by Rouget after boiling chitin in potassium hydroxide although it was not named “chitosan” until 1894 (Alishahi& Aider, 2012; Torres, Beppu & Arruda, 2006). While chitosan is ubiquitous, it is mainly sourced from the shells of crustaceans, in the exoskeletons of arthropods and cell walls of fungi (Cho et al., 2006).

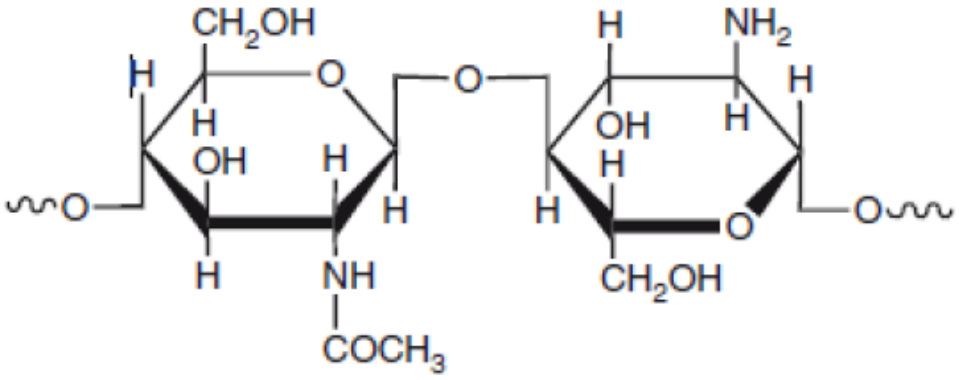

Figure 1.5 Acetylated and deacetylated units of chitosan (Wandrey et al., 2010)

The main functional groups of chitosan include an amino group at the C-2 position and primary and secondary hydroxyl groups at the C-3 and C-6 positions respectively (Thongngam & McClements, 2004). The molecule is positively charged below the pKa value of ~6.5 (Mounsey, O' Kennedy, Fenelon & Brodkorb, 2008). In contrast to chitin, chitosan is soluble in acidic medium whereby the amine groups are protonated to $–NH_3^+$ (Bastos et al., 2010) and it also is capable of forming soluble, insoluble complexes, coacervates and hydrogels, often *via* electrostatic interactions with anionic molecules. This was noted by Thongngam and McClements (2004) when characterising the interactions of chitosan with a model anionic surfactant, sodium dodecyl sulfate (SDS). In their study insoluble complexes of SDS-chitosan were formed and the researchers concluded that the interaction was electrostatic in origin since it was significantly weakened in the presence of 100mM NaCl. Similarly, electrostatic interactions were associated with a whey protein isolate and chitosan complex, according to the isothermal titration calorimetry measurements conducted by Bastos et al. (2010). Additionally, Honary et al. (2009) endorsed electrostatic bondingin an alginate and chitosan mix when investigating the properties of alginate/chitosan microparticles containing prednisolone. In the FTIR component of Honary's et al. work, the disappearance of the N-H bending vibration at 1570 cm^{-1} attributed to the non-acrylated 2-aminoglucose primary amines of chitosan and the –C-O stretching at 1407cm^{-1} of sodium alginate was taken as indicative of an electrostatic bond between them.

A similar scenario is to be found in biological investigations. Pujana's et al., (2012) study of the mucoadhesion of cationic chitosan to negatively charged mucosal surfaces for enhanced drug penetration across the mucosa is a case in point. Honory et al. (2009) using a rat gut loop

found that electrostatic interactions were imperative for effective mucoadhesion of the alginate/chitosan microparticles.

The development of a cold-set gel of chitosan with chicken salt- soluble proteins (SSP) by Kachanechai, Jantawat & Pichyangkura (2008) also supports the presence of chemical bonding.The authors concluded after examining the influence of chitosan on the physicochemical properties of chicken salt soluble proteins, that the interaction between the cationic polysaccharide and SSP did involve disulfide bonds even though the interaction was mainly physical. A covalent relationship was associated with the formation of xyloglucan and chitosan hydrogels in which it was suggested that a covalent interaction occurred between the former aldehyde and latter amino group (Simi & Abraham, 2010). Pujana et al. (2012) noted that aldehydes were among one of the more common covalent cross-linkers used in the development of chitosan nanoparticles. Indeed the applications involving chitosan may also be dependent on molecular interactions *via* hydrogen as well as covalent bonding albeit exhibited to a lesser extent.

1.2.2 Chitosan properties

The properties of chitosan can be attributed to variation in factors such as: MW, degree of deacetylation, distribution of the acetylated residues along the backbone, pH and ionic strength of the external environment (Bastos et al., 2010; Cho et al., 2006; Claesson & Ninham, 1992; Kubota & Kikuchi, 1998; Lamarque, Lucas, Viton & Domard, 2005; Mounsey et al., 2008; Stevens, 1996). In terms of the degree of polymerisation of the chitosan chemical structure, chitosan can be classified as being low (<50 kDa), medium (50-150 kDa) or high (>150 kDa) MW (Coma, 2012; Goy, de Britto & Assis, 2009; Stamford et al., 2013). The degree of deacetylation refers to the percentage of glucosamine present in the molecule which, although does not usually reach 100%, is typically at least 40-60% (Franca, Freitas & Lins, 2011). The higher degree of deacetylation equates to a higher ratio of amino to acetyl groups and consequently a positive charge density (when below the pKa value).

The spatial distribution of N-acetyl groups affects the solubility of the polymer due to flexibility of the structure. Franca et al. (2011) explored the chitosan molecular structure with varying degrees of deacetylation and distribution of N-acetyl groups along the biopolymer chain using a model system. They concluded that a high degree of deacetylation and a

uniform distribution of N-acetyl groups along the linear chain afforded the greatest mobility with a preference for the relaxed two-fold helix and five-fold helix motifs. As previously mentioned, chitosan molecular interactions are predominantly electrostatic and the stability of such would be affected by electrostatic repulsive and attractive forces governed by the pH and ionic strength (Pujana et al., 2012). While whey protein contains anionic patches on its surface, positive charges are also prevalent (Hong & McClements, 2007). In the study by Bastos et al. (2010) it was exemplified that even though whey protein contains both positive and negative charges, coacervates can still be formed with chitosan by appropriate manipulation of ionic strength and pH to screen electrostatic repulsions while retaining electrostatic attractions. In their study, at pH 4, 6 and high ionic strength of 250mM HAc/NaAcbuffer, both electrostatic attractive and repulsive forces between WPI and chitosan are screened. Meanwhile at low ionic strengths of 100mM HAc/NaAC buffer, the screening of electrostatic repulsive forces is the predominant effect leading to a greater amount of WPI-chitosan aggregate formation (Bastos et al., 2010; Wang et al., 2007). Many authors have acknowledged that a pH range of 5.2-6.5 would provoke effective electrostatic interactions between β-Lg and chitosan (Mounsey et al., 2008). This is because the protein above its pI possesses sufficient negative charges to interact with the cationic polysaccharide. As the pH is increased above the chitosan pKa value, there is a reduction in the positive charges and consequent protein polysaccharide electrostatic interactions. This was found to be the case in the study on complex coacervation of β-lg-chitosan mixtures by Mounsey et al. (2008). At pH 8, only 52.5% of insoluble complexes were formed in comparison to the amount at the initial pH of 6.5 (Mounsey et al., 2008). Traditional coacervates are sensitive to changes in pH and ionic strength. This was displayed in the experiment by Mounsey et al. (2008) by the ease at which bound β-Lg to chitosan was replaced by polyanions introduced into the system. Taking this into account, modifications in the form of heat application have been implemented to accompany the traditional coacervation process and enhance stability (Hong &McClements, 2007).

In addition to the versatile functional groups, chitosan is biodegradable and biocompatible, further heightening its appeal in industrial applications. The polysaccharide exhibits preservation properties and is currently used in forming films for preservation of foods (Aider, 2010; Alishahi & Aider, 2012). For example, seafood is prone to oxidative

degradations due to presence of polyunsaturated fatty acids. Chitosan was used to extend the shelf life of the seafood which according to Alishahi & Aider, (2012) was effective because of chitosan's radical scavenging ability. The biopolymer also exhibits antibacterial activity. For example, with 5g/L incorporation, the shelf life of oysters was extended from 9 days to up to 15 days (Alishahi & Aider, 2012; Cao et al., 2009). It should be noted the preservative effectiveness of chitosan is dependent on its physical state. Several researchers (Alishahi & Aider, 2012; Kok & Park, 2007; Lopez-Caballero et al., 2005) found that solubilised chitosan exhibited antibacterial activity when incorporated into fish balls, but the powdered form was not effective when incorporated into similar fish products. The antimicrobial mechanism associated with chitosan is essentially *via* cell lysis which occurs when chitosan binds to the negatively charged surface of bacteria (Alishahi & Aider, 2012).High MW chitosan forms a layer on the surface of the microorganism and thus creating a physical barrier for the entry of nutrients required for bacterial survival (Alishahi & Aider, 2012). By contrast, low MW chitosan is capable of entering the cytosol of microorganisms, binding to DNA and disturbing the synthesis of proteins (Alishahi & Aider, 2012).

Some controversy exists around the effectiveness of the antibacterial activity of chitosan against Gram positive and Gram negative bacteria. Raafat & Sahl (2009) demonstrated thatthe antibacterial activity of chitosan against Gram positive organisms was more effective that against Gram negative bacteria. Whereas a later study by Kong et al. (2010) found the opposite effect. As most studies showing antimicrobial properties have been undertaken *in vitro*, Alishahi & Aider, (2012) recommended *in vivo* studies for further validation.

1.2.3 Processing of chitosan

Chitosan is also used in diet supplements as it is associated with reduced absorption of fat when taken prior to meal consumption. More than one mode of action has been proposed and traditionally it was explained by the direct binding of chitosan to the lipid which obstructed lipid digestibility (Helgason et al, 2008). Upon examining the interaction of chitosan with the oil-in-water emulsions, Helgason et al. (2008) suggested that chitosan forms a secondary emulsion around the oil-in-water emulsion in the stomach. As bile salts are introduced at the duodenum stage, they form strong electrostatic bonds with chitosan and as a result cause the aggregation of the chitosan secondary emulsion. The aggregation results in more coalescence

due to close packing of the oil inside the gel structure, reducing access of digestive enzymes to the lipids (Helgason et al, 2008).

Chitosan is also used to treat poultry wastewater because it binds to the surface of specific molecules which eases removal of suspended solids from the processing of poultry products (Alishahi & Aider, 2012).

The main obstacles for the oral supply of bioactive compounds include the harsh acidic environment of the stomach, degradation by digestive enzymes and the physical barrier of the epithelial cells (Alishahi et al., 2012; Schep et al., 1999). Nevertheless, chitosan has been increasingly investigated as an encapsulant for bioactive compounds. The reason is, as previously mentioned, that chitosan has demonstrated that it possesses mucoadhesion properties and is also able to withstand an acidic environment such as that found in the stomach (Rodriguez & Albertango, 2005).

In the experiments conducted by Belscak-Cvitanovic et al. (2011), electrostatic extruded alginate-chitosan beads exhibited high encapsulation efficiency of extracts from raspberry leaf, hawthorn, ground ivy, yarrow, nettle and olive leaf. Furthermore, chitosan provided a second coating around shark liver oil which had a primary alginate-calcium encapsulatant. The chitosan-alginate polyelectrolyte complex helped to mask the unpleasant taste of the shark liver oil which could prevented given the greater permeability of the primary alginate-calcium barrier (Peniche et al., 2004).

1.3 Biopolymer mixtures

By the end of the 1970s, a good understanding of single polymer systems from solution to gel had been gained and the focus of researchers had moved onto the dynamics of mixed polymer systems (Kasapis, 2008). Saha & Bhattacharya (2010) pointed out that gels could be formed when the two polymers were used together but when used individually it was not possible. The main point was highlighted when Kasapis (2008) pointed out that often the single biopolymer systems was limited to being a viscoelastic liquid or a solid-like material with brittle or elastic textures that had limited functionality and were unsuitable as fat replacers, for example. By contrast, the three dimensional network formed by mixed polymer systems had

the potential to attain alternative texture profiles with desirable mouth-feel (Kasapis, 2008). Consequently, the combining of polymers such as xanthan with galactomannan also allowed synergistic interactions to occur.

1.3.1 Segregative interactions

Biopolymer mixtures consist of two or more different types of biopolymers and the classic combination is a protein paired with a polysaccharide. The mixing of biopolymers in aqueous solutions may result in either associative or segregative interactions (Morris, 2009). Segregative interactions are those in which individual molecules prefer to be surrounded by like molecules; i.e. rather than the other polymer. This type of behaviour has been coined as "thermodynamic incompatibility" in which the driving force may be the differences in charges, structure and conformation and/or MW (Schorsch, Jones, & Norton, 1999; Zeman & Patterson, 1972). In a protein and polysaccharide mixtures, the basis of the molecular phenomena is mainly steric exclusion which means there is a preference for macromolecules to be surrounded by others of the same type, promoting separation into co-existing phases. To further explain, Tolstoguzov (1995) described the development of separate phases as 'membrane-less osmosis'; in which the interfacial surface of the two immiscible aqueous solutions of biopolymers was in itself the membrane through which water diffused. The overall result of this thermodynamic incompatibility is the ultimate rise to phases where one is rich in polymer "X" and other is rich in polymer "Y". In terms of structural arrangement, either polymer may form the continuous phase in which the other polymer is dispersed through as the discontinuous filler. This 'water-in-water emulsion' can be identified visually by the increase in turbidity of the solution (Grinberg & Tolstoguzov, 1972, 1997; Polyacov et al., 1997). In non-gelling biopolymer mixtures the 'water-in-water emulsion' is unstable and eventually resolves into two distinct layers due to a density differences between the phases (Bansil, 1993). In the case of gelling biopolymers the 'water-in-water' emulsion may be preserved and a micro-phase separated network may be formed.

1.3.2 Composite networks

Given the right circumstances, i.e. sufficient moisture and heat, gelling biopolymer mixtures become solvent swollen polymer networks, i.e. gels. Various networks can be formed by the

biopolymer mixture: interpenetrating, coupled separated and phase separated networks. Interpenetrating and coupled separated networks could be described as opposite extremes whereas phase separated networks serve as the intermediate. In the case of the interpenetrating scenario, independent biopolymer networks are formed and as the name suggests, these networks interpenetrate into each other. At the other end of the spectrum is the coupled separated networks whereby the different biopolymers form a single network as a result of covalent bonding, co-operative junction zones and/or ionic interactions. Due to thermodynamic incompatibility, phase separated networks are those in which biopolymers are predominantly rich in their own polymeric domain. The topology of the interpenetrating, coupled separated and phase separated networks are illustrated in Figure 1.6 (Richardson &Kasapis, 1998).

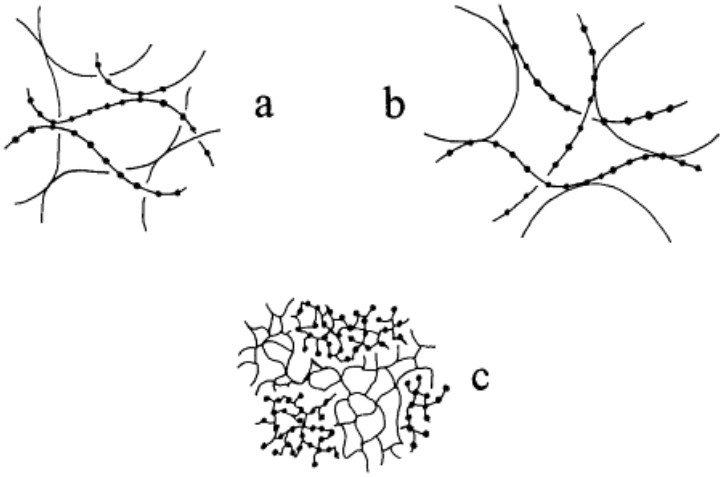

Figure 1.6 Three possible network topologies for binary gelling system a) interpenetrating b) coupled separated c) phase separated (Richardson & Kasapis, 1998)

1.3.3 Identifying composite networks

Using the thermal transitions of heated biopolymer mixtures in calorimetric studies can provide an indication of the type of network formed. If the biopolymers undergo solution to gel transition at temperatures similar to the single systems (and thus two endothermic reactions are clearly observed) it is unlikely a coupled network has been formed. In other words, if there was a specific interactions between the two entities of a coupled network, it would distort the peaks of the individual fractions and new thermal events could be identified (Kasapis, 2008; William et al., 1992). Furthermore, measuring the heat flow during

differential scanning calorimetry (DSC) may also provide an indication of the thermodynamic incompatibility phenomenon. When the samples are heated during calorimetric studies, thermodynamic incompatibility of β-Lg and polysaccharides exhibited a raised denaturation temperature and also delayed the protein aggregation heating profile of β-Lg studied alone (Baeza & Pilosof, 2002; Livney, Corredig & Dalgleish, 2003). In conjunction with DSC, following the elastic and viscous moduli during heating during dynamic oscillation in shear experiments may provide further understanding of the interactions. Provided experiments are within the linear viscoelastic region (LVR), the occurrence of a single-phase transition in mixed protein-polysaccharide systems indicates the absence of bi-continuous networks. This is because to create a bi-continuous networks, two phase transition events are likely to have occurred and therefore, detectable. Validation of a phase-separated network can be further confirmed by the fact that they possess higher storage moduli and associated strength than the sum of the individual components. This is due to solvent partitioning and the effective concentration of biopolymers in both phases. As pointed out by Tolstoguzov (1995), a vast increase in the storage modulus can be seen with even small additions of a biopolymer. In dynamic oscillation tests, the temperature of the phase transition reflects the dominant fraction which constitutes the continuous phase. In fact, many physico-chemical properties of bi-phasic systems resemble the continuous phase (Tolstoguzov, 1995).

The rheological studies can be complemented with texture analysis studies. Measuring the hardness of gels in single cycle compression tests can qualitatively validate observed storage modulus trends. Morphology of the system can also be visualised in scanning electron microscopy and Fourier transform infrared spectroscopy (FTIR) studies are also useful in determining the nature of the developed network. The superimposition of data from individual components in binary systems and the absence of new bands indicate the absence of covalent bonding and consequently confirm the absence of the formation of coupled networks. This, in turn, would suggest the formation of bi-continuous or possibly phase separated networks have occurred.

1.3.4 Phase separated networks

To form protein and polysaccharide phase separated gels, certain conditions must be met and these are summarised in Figure 1.7, which shows the co-solubility of protein and polysaccharide mixtures. The thick solid line (DFGE) is the bimodal curve and conditions that

fall below this curve (AB_1) represent a single-phase system while above it is the two-phase system (AB).

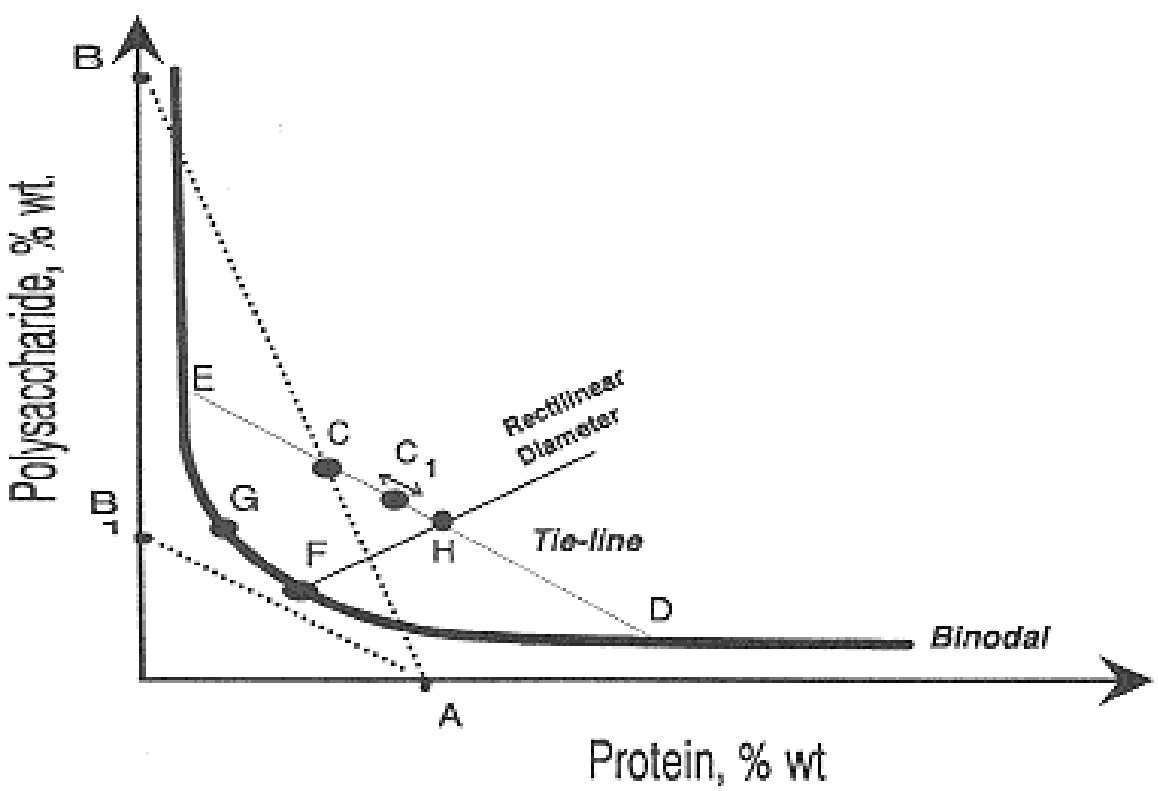

Figure 1.7 Typical phase diagram for protein - polysaccharide- water system adapted (Tolstoguzov, 1995, 1997)

The biopolymers in solution must exceed the existing concentration threshold to phase separate. Such concentration is denoted by (G) on the bimodal curve and according to literature varies from a total solids of 4% for gelatin and linear anionic polysaccharides, to more than 12% in the presence of globular proteins (Tolstoguzov, 1995). It should be noted that different combinations of hydrocolloids may phase separate at varying concentrations and lower thresholds result from cases of greater incompatibility (Tolstoguzov, 1995). Greater incompatibility can occur in the presence of ions as pointed out by Considine et al. (2007) in discussing the outcome of protein-starch systems. Cakir & Foegeding (2011) examined the gel microstructure of a fixed 13%w/v WPI system with varying concentrations of κ-carrageenan and ionic strength. Micro phase separated networks that were protein continuous, bi-continuous and carrageenan continuous were developed depending on the polysaccharide and salt concentration. In their studies, phase separated protein continuous polysaccharide

discontinuous particulate gels were formed at low salt (50 and 100mM NaCl) and κ-carrageenan concentrations (0.1, 0.2%). The higher additions of salt (250mM NaCl) resulted in neutralizing electrostatic repulsion and consequently enhancing protein aggregation. Whereas, lowering the carrageenan threshold resulted in the formation of micro phase-separated protein continuous gels. Moreover, higher MW polymers lead to overlapping and transition from dilute to semi-dilute solutions that also translate to lower critical limits for phase separation (Tolstoguzov, 1995). The tie line (ED) in Figure 1.7 connects the binodal points (D and E) corresponding to the composition of the coexisting phases (Tolstoguzov, 1995). The example mixture (C) is obtained by combining polysaccharide and protein concentration (BC) and (AC). Following the tie line (ED), and a result of water redistribution to the polysaccharide and proteins, the ultimate concentration turns into (E) and (D) respectively.

As previously mentioned, biopolymers in mixtures can lead to one of the polymers forming a continuous phase while the other polymer is dispersed through it as a discontinuous "filler". The stronger component could be attributed to either phases. The Takayanagi blending laws (Fitzsimons, Mulvihill & Morris, 2008) are used to describe these different situations. According to the blending laws, an isostrain condition occurs when the polymer exhibiting greater strength exists as the continuous phase. The main characteristic of the isostrain condition is that a parallel arrangement occurs so both materials are subject to equal deformation (strain). When the opposite is true, i.e. the polymer exhibiting lesser strength acts as the continuous phase, an isostress condition is applicable. The latter series arrangement sees both components subjected to the same force (stress) but the weaker component in the continuous phase limits the force subjected to the discontinuous stronger component phase. The isostrain and isostress equations (Fitzsimons, Mulvihill & Morris, 2008) are shown below:

$$\text{(Isostrain):} \quad G_C = G_X\phi_X + G_Y\phi_Y$$

$$\text{(Isostress):} \quad G_C = (\phi_X/G_X + \phi_Y G_Y)^{-1}$$

The modulus of composite gels (G_C) can be related to the moduli of individual phases (G_X and G_Y) using the equations mentioned above where ϕ_X and ϕ_Y refer to the phase volume of components X and Y, respectively and $\phi_X + \phi_Y = 1$ (Fitzsimons, Mulvihill & Morris, 2008).

The next improvement after Takayanagi blending laws was the development of the water partitioning 'p' factor by Clark (1987). As has been discussed earlier, mixed biopolymers in aqueous solutions undergo a diffusive process of membrane-less osmosis for which the 'p' factor equation was developed to distinguish the solvent partitioning between the two phases and as a result to determine the effective phase volumes. As highlighted in the previous discussion on the binodal curve, the final concentrations of the two polymers in a co-existing system, i.e. (E) and (D), are not equivalent to those which were initially introduced to the system, i.e. (BC) and (AC). It is the former concentrations that correspond to the real moduli of each hydrocolloid. The 'p' factor equation appears below whereby X and Y denote the weight of polymers X and Y. Additionally, the total amount of water is the sum of water X and water Y. The water partitioning is equivalent to the ratio of water/polymer in one phase divided by the corresponding ratio in the other phase.

$$p = \frac{water_X/polymer_X}{water_Y/polymer_Y}$$

The rheological properties of biphasic co-gels have been summarised by Morris (2009) as the following:

- The continuous phase determines the strength of composites.
- The dispersed phase has little direct influence on the moduli of biopolymer composites. However, it can contribute an indirect effect, by occupying part of the total volume, and hence increasing the polymer concentration in the continuous phase.
- Overall moduli can be calculated using the Takayanagi blending laws.
- Melting of a strong dispersed gel phase is unlikely to reduce the overall moduli by more than about a factor of 4.
- Any larger change would indicate a bi-continuous network structure.

Phase separation phenomena between protein and polysaccharide molecules, as described in this section, remains one of the basic tools of achieving the required structural properties and textural profile in food product formulations. As ever, the industrialist is faced with the challenge of innovation in an increasingly competitive market in terms of ingredient cost, product added-value, and expectations of a healthy life-style to mention but a few. It appears, however, that a gap persists between fundamental knowledge and direct application to food

related concepts with a growing need for scientific input. The blending laws described in the aforementioned equations are designed to bridge the gap between applications and research that can advance understanding of phase separation phenomena between food ingredients.

Therefore, this research was designed with the following objectives:

- To acquire molecular understanding and functionality of binary and tertiary polymer systems
- To identify the optimum conditions for the development of novel products with superior nutritional properties i.e. reduced glycemic index.

Typical preparation concentrations reflecting those found in commercial food products are used in the project.

1.4 References

Aguilera, J. M., & Rojas, E. (1996). Rheological, thermal and microstructural properties of whey protein–cassava starch gels. *Journal of Food Science,* 61, 962–966.

Aider, M. (2010). Chitosan application for active bio-based films production and potential in the food industry: a review. *LWT- Food Science and Technology, 43,* 837-842.

Alishahi, A., & Aider,M. (2012). Applications of chitosan in the seafood industry and aquaculture: A review. *Food and Bioprocess Technology,* 5, 817-830.

Baeza RI, Pilosof A.M. R. (2002). Calorimetric studies of thermal denaturation of b-lactoglobulin in the presence of polysaccharides. *Lebens- Wiss u-Technol, 35,* 393-9.

Baks, T., Ngene, I.S., van Soest, J.J.G., Janssen, A.E.M., & Boom, R.M. (2007). Comparison of methods to determine the degree of gelatinisation for both high and low starch concentrations. *Carbohydrate Polymers, 67,* 481-490.

Bansil, R. (1993). Phase separation in polymer solutions and gels. *Journal de Physique, 3,* 225-235.

Baum, B. R., & Bailey, L. G. (1987). A survey of endosperm starch granules in the genus Hodeum: a study using image analytic and numerical taxonomic techniques. *Canadian Journal of Botany, 65,* 1563–1569.

Barbut, S. (1995). Effect of calcium level on the structure of pre-heated whey protein isolate gels. *LWT-Food Science and Technology, 28,* 598-603.

Bastos, D.S., Barreto, B.N., Souza, H.K.S., Bastos, M., Rocha-Leao, M.H.M., Andrade, C.T., & Goncalves, M.P. (2010). Characterisation of a chitosan sample extracted from Brazillian shrimps and its application to obtain insoluble complexes with a commercial whey protein isolate. *Food Hydrocolloids, 24,* 709-718.

Bednar, G.E., Patil, A.R., Murray, S.M., Grieshop, C.M., Merchen, N.R., Fahey Jr. & G.C. (2001). Starch and fiber fractions in selected food and feed ingredients affect their small intestinal digestibility and fermentability and their large bowel fermentability *in vitro* in a canine model. *Journal of Nutrition, 131,* 276–286.

Belobrajdic, D.P., McIntosh, G.H., & Owens, J.A. (2004). A high whey protein diet reduces body weight gain and alters insulin sensitivity relative to red meat in Wistar rats. *American Society of Nutritional Science*, 1454-1458.

Belscak-Cvitanovic, A., Stojanovic, R., Manojlovic, V., Komes, D., Cindric, I.J., Nedovic, V., & Bugarski, B. (2011). Encapsulation of polyphenolic antioxidants from medicinal plant extracts in alginate-chitosan system enhanced with ascorbic acid by electrostatic extrusion. *Food Research International, 44*, 1094-1101.

Bernfeld, P. (1955). Amylases, α and β. In S.P. Colowick, & N.O. Kaplan (Eds.), *Methods in enzymology* (pp. 149-158). New York: Academic Press.

Berti, C., Patrizia, R., Monti, L. D., & Porrini, M. (2004). *In vitro* starch digestibility and in vivo glucose response of gluten-free foods and their gluten counterparts. *European Journal of Nutrition, 43*, 198-204.

Better Health Channel, 2014. Sugar. Retrieved 26 June 2014, <http://www.betterhealth.vic.gov.au/bhcv2/bhcarticles.nsf/pages/Sugar>.

Blazek, J., & Gilbert, E.P. (2010). Effect of enzymatic hydrolysis on native starch granule structure. *Biomacromolecules, 11*, 3275-3289.

Brand-Miller, J. C., Holt, S. H. A., Pawlak, D. B., & McMillan, J. (2002). Glycemic index and obesity. *American Journal of Clinical Nutrition, 76*, 281S–285S.

Burey, P., Bhandari, B.R., Howes, T., & Gidley, M.J. (2008). Hydrocolloid gel particles: formation, characterisation and application. *Critical Reviews in Food science and Nutrition, 48*, 361-377.

Cao, R., Xue, C.H., & Liu, Q. (2009). Change in microbial flora of pacific oysters (Crassotera gigas) during refrigerated storage and its shelf life extension by chitosan. *International Journal of Food Microbiology, 131*, 272-276.

Carter, D. C., & Ho, J. X. (1994). Structure of serum albumin. *Advances in Protein Chemistry, 45*, 153−203.

Chang, K.L.B., Lin, Y.-S., & Chen, R.H. (2003). The effect of chitosan on the gel properties of tofu (soybean curd). *Journal of Food Engineering, 57*, 315-319.

Chatterton, D.E.W., Smithers, G., Roupas, P., & Brodkorb, A. (2006). Bioactivity of β-lactoglobulin and α-lactalbumin - technological implications for processing. *International Dairy Journal, 16,* 1229-1240.

Cheftel, J. C., Cuq, J. L., & Lorient, D. (1985). Amino acids, peptides, and proteins. In O. R. Fennema (Ed.), *Food Chemistry* (pp. 245–370). New York: Marcel Dekker.

Cho, J., Heuzey, M., Begin, A., &Carreau, P.J. (2006). Viscoelastic properties of chitosan solutions: Effect of concentration and ionic strength. *Journal of Food Engineering, 74*, 500-515.

Claesson, P.M., & Ninham, B.W. (1992). pH-Dependent interactions between adsorbed chitosan layers. *Langmuir, 8,* 1406-1412.

Clark, A. H., & Ross-Murphy, S. B. (2009). Biopolymer network assembly: Measurement and Theory. In S. Kasapis, I. T. Norton & J. B. Ubbink (Eds.), *Modern Biopolymer Science: Bridging the Divide between Fundamental Treatise and Industrial Application (pp.* 1-27*).* San Diego: Elsevier.

Clark, A. H. (1987). The application of network theory to food systems. In J. M. V. Blanshard & P. Lillford (Eds.), *Food Structure and Behaviour* (pp. 13-34). London: Academic Press.

Considine, T., Patel, H. A., Anema, S. G., Singh, H., & Creamer, L. K. (2007). Interaction of milk proteins during heat and high hydrostatic pressure treatments. *Innovative Food Science and Emerging Technology, 8*, 1-23.

Colonna, P., Leloup, V., & Bule´on, A. (1992). Limiting factors of starch hydrolysis. *European Journal of Clinical Nutrition, 46*, S17-S32.

Coma, V. (2012). Recent developments in chitin and chitosan bio-based materials used for food preservation. In Y. Habibi and L. A. Lucia (Eds.), *Polysaccharide building blocks: a sustainable approach to renewable materials* (1st ed., pp. 143-175). New Jersey: John Wiley & Sons, Inc.

Copeland, L., Blazek, J., Salman, H., & Tang, M.C. (2009). Form and functionality of starch. *Food Hydrocolloids, 23*, 1527-1534.

Correia, P., Cruz-Lopes, L., &Beirão-da-Costa, L. (2012). Morphology and structure of chestnut starch isolated by alkali and enzymatic methods. *Food Hydrocolloids, 28*, 313-319.

Croguennec, T., Molle, D., Mehra, R., Bouhallab, S. (2004). Spectroscopic characterisation of heat-induced nonnative β –lactoglobulin monomers. *Protein Science*, 13, 1-7.

Dairy Australia, 2009, Our dairy industry statistics. Retrieved 20 January 2011, <http://www.dairyaustralia.com.au/Our-Dairy-Industry-Statistics/Casein-and-Whey>

Damodaran, S., Parkin, K. L., Fennema, O. R. (2008). *Fennema's Food Chemistry, 4th ed.*, CRC Press, Taylor and Francis Gp, Boca Raton, FL.

De Wit, J.N. (1998). Nutritional and functional characteristics of whey proteins in food products. *Journal of Dairy Science, 81*, 597-608.

Deatherage, W. L., MacMasters, M. M., & Rist, C. E. (1955). A partial survey of amylose content in starch from domestic and foreign varieties of corn, wheat, and sorghum and from some other starch bearing plants. *Transactions of American Association of Cereal Chemistry, 13*, 31–33.

Dissanayake, M. (2011). Modulation of functional properties of whey proteins by microparticulation, PhD thesis, Victoria University.

Donald, A. M. (2004). Understanding starch structure and functionality. *Starch in Food, 156*, 184.

Donkor, O. N., Henriksson, A., Singh, T. K., Vasiljevic, T., Shah, N. P. (2007). ACE inhibitory activity of probiotic yoghurt. *International Dairy Journal, 17*, 1321-1331.

Dubois, S. (2013). Which is more important: the quantity or quality of protein?, Livestrong. Retrieved 28 June 2014, <http://www.livestrong.com/article/1002324-important-quantity-quality-protein/>.

Eigel, W. N., Butler, J.E., Ernstrom, C.A., Farrell, H.M., Jr., Harwalker, V.R., Jenness, R., & Whitney, R.McL. (1984). Nomenclature of proteins of cow's milk: fifth revision. *Journal of Dairy Science, 67*, 1599.

Englyst, K.N., Englyst, H.N., Hudson, G.J., Cole, T.J., & Cummings, J.H. (1999). Rapidly available glucose in foods: an *in vitro* measurement that reflects the glycemic response. *The American Journal of Clinical Nutrition, 69*, 448-454.

Englyst, H.N., Kingman, S.M., & Cummings, J.H. (1992). Classification and measurement of nutritionally important starch fractions. *European Journal of Clinical Nutrition, 46,* s33-50.

Environmental Protection Agency 2013, Major Crops Grown in the United States, U.S. Environmental Protection Agency. Retrieved 24 June 2014, <http://www.epa.gov/oecaagct/ag101/cropmajor.html>

Farrell, H.M.Jr., Jimenez-Flores, R., Bleck, G.T., Brown, E.M., Butler, J.E., Creamer, L.K., Hicks, C.L., Hollar, C.M., Ng-Kwai-Hang, K.F. & Swaisgood, H.E. (2004). Nomenclature of the Proteins of Cows' Milk - Sixth Revision. *Journal of Dairy Science, 87*, 1641-1674.

Fassler, C., Arrigoni, E., Venema, K., Brouns, F., & Amado, R. (2006). *In vitro* fermentability of differently digested resistant starch preparations. *Molecular Nutrition Food Research, 50,* 1220–1228.

Fitzsimons, S.M., Mulvihill, D.M. & Morris, E.R. (2007). Denaturation and aggregation processes in thermal gelation of whey proteins resolved by differential scanning calorimetry. *Food Hydrocolloids, 21,* 638-644.

Foegeding, E. A., Davis, J. P., Doucet, D., McGuffey, M. K. (2002). Advances in modifying and understanding whey protein functionality. *Trends in Food Science and Technology, 13*, 151-159.

Foegeding, E. A., & Luck, P. J. (2002). Whey protein products. In: H. Roginski, P.F. Fox, & J.W. Fuquay (Eds.), Encyclopedia of Dairy Sciences. London: Academic Press

Fox, P. F., & McSweeney, P. L. H. (2003). *Advanced Dairy Chemistry – Proteins*, 3rd edition, Kluwer Academic/Plenum Publishers, NY, USA.

Fredriksson, H., Silverio, J., Andersson, R., Eliasson, A. C., & Aman, P. (1998). The influence of amylose and amylopectin characteristics on gelatinisation and retrogradation properties of different starches. *Carbohydrate Polymers, 35*, 119–134.

Frei, M., Siddhuraju, P., Becker, K., (2003). Studies on the *in vitro* starch digestibility and the glycemic index of six different indigenous rice cultivars from the Philippines. *Food Chemistry, 83*, 395–402.

Franca, E.F., Freitas, C.G., & Lins, R.D. (2011). Chitosan molecular structure as a function of N-acetylation. *Biopolymers, 95,* 448-460.

Gallant, D.J, Bouchet, B, &Baldwin, P.M (1997). Microscopy of starch: evidence of a new level of granule organisation. *Carbohydrate Polymers 32***:** 177-191.

Gannon, M. C., Nuttall, F. Q., Neil, B. J., & Westphal, S. A. (1988). The insulin and glucose responses to meals of glucose plus various proteins in type II diabetic subjects. *Metabolism, 37,* 1081-1088.

Gelamo, E. L., Silva, C. H., Imasato, H., & Tabak, M. (2002). Interaction of bovine (BSA) and human (HSA) serum albumins with ionic surfactants: Spectroscopy and modelling. *Biochimica et Biophysica Acta, 1594*, 84−99.

Gelamo, E. L., & Tabak, M. (2000). Spectroscopic studies on the interaction of bovine (BSA) and human (HSA) serum albumins with ionic surfactants, Spectrochimica Acta Part A. *Molecular and Biomolecular Spectroscopy, 56*, 2255−2271.

Goodfellow, B. J., &Wilson, R. H. (1990). A Fourier transform IR study of gelation of amylose and amylopectin. *Biopolymers, 30*, 1183-1189.

Goy, R. C., de Britto, D., & Assis, O. B. G. (2009). A review of the antimicrobial activity of chitosan. *Polimeros Ciencia e Technologia, 19*, 241–247.

Gray, G. M. (1992). Starch digestion and absorption in nonruminants. *Journal of Nutrition, 122*, 172-177.

Grinberg, V. Y., & Tolstoguzov, V. B. (1972). Thermodynamic compatibility of gelatin with some -glucans in aqueous media. *Carbohydrate Research, 25*(2), 313-321.

Grinberg, V. Y., & Tolstoguzov, V. B. (1997). Thermodynamic incompatibility of proteins and polysaccharides in solutions. *Food Hydrocolloids, 11*(2), 145-158.

Guzey, D., & McClements, D.J. (2006). Characterisation of β-lactoglobulin-chitosan interactions in aqueous solutions: A calorimetry, light scattering, electrophoretic mobility and solubility study. *Food Hydrocolloids, 20,* 124-131.

Health Insite, An Australian Government Initiative, Reviewed September 2008. "Diabetes Facts", Publisher: Nutrition Australia, <http://www.healthinsite.gov.au/topics/Diabetes_Statistics>

Helgason, T., Weiss, J., McClements, D.J., Gislason, J., Einarsson, J.M., Thormodsson, F.R., & Kristbergsson, K. (2008). Examination of the interaction of chitosan and oil-in-water emulsions under conditions simulating the digestive system using confocal microscopy. *Journal of Aquatic Food Product Technology, 17,* 216-233.

Hermansson, A., & Svegmark, K. (1996). Developments in the understanding of starch functionality. *Trends in Food Science & Technology, 7,* 345–353.

Honary, S., Maleki, M., & Karami, M. (2009). The effect of chitosan molecular weight on the properties of alginate/chitosan microparticles containing prednisolone. *Tropical Journal of Pharmaceutical Research, 8,* 53-61.

Hong, Y., & McClements, D.J. (2007). Modulation of pH sensitivity of surface charge and aggregation stability of protein-coated lipid droplets by chitosan addition. *Food Biophysics, 2,* 46-55.

Horowitz, M.I., & Pigman, W. (1977). The Glycoconjugates, Vol. 1, *Mammalian Glycoproteins and Glycolipids,* Academic Press, New York.

Hur, S.J., Lim, B.O., Decker, E.A., & McClements, D.J. (2011). *In vitro* human digestion models for food applications. *Food Chemistry, 125,* 1-12.

Hu, M., McClements, D.J. & Decker, E.A. (2003). Impact of whey protein emulsifiers on the oxidative stability of salmon oil-in-water emulsions. *Journal of Agricultural and Food Chemistry, 51,* 1435-1439.

Jackson, D. S. (2003). Starch: Structure, Properties, and Determination. In C. Editor-in-Chief: Benjamin (Ed.), *Encyclopedia of Food Sciences and Nutrition (Second Edition)* (pp. 5561-5567). Oxford: Academic Press.

Jenkins, D.J.A., Kendall, C.W.C., Augustin, L.S.A., Franceschi, S., Hamidi, M., Marchie, A., Jenkins, A.L., & Axelsen, M. (2001). Glycemic index: overview of implications in health and disease. *American Journal of Clinical Nutrition, 76,* 266-273.

Jenkins, D.J., Ghafari, H., & Wolever, T.M. (1982). Relationship between rate of digestion of foods and post-prandial glycaemia. *Diabetologia, 22,* 450-455.

Jenkins, D.J., Wolever, T.M., & Buckley, G. (1988). Low glycemic-index starchy foods in the diabetic diet. *American Journal of Clinical Nutrition, 48,* 248-254.

Jenkins, D.J., Wolever, T.M., Taylor, R.H., Barker, H.M., Fielden, H (1980). Exceptionally low blood glucose response to dried beans: comparison with other carbohydrate foods. *British Medical Journal, 281,* 578-580.

Jenkins, D.J., Wolever, T.M., Taylor, R.H., Barker, H., Fielden, H., Baldwin, J.M., Bowling, A.C., Newman, H.C., Jenkins, A.L., & Goff, D.V. (1981). Glycemic index of foods: a physiological basis for carbohydrate exchange. *American Journal of Clinical Nutrition, 34,* 362-366.

Juntunen, K. S., Niskanen, L. K., Liukkonene, K. H., Poutanen, K. S., Holst, J., & Mykkanen, H. M. (2002). Postprandial glucose, insulin, and incretin responses to grain products in healthy subjects. *American Journal of Clinical Nutrition, 75,* 254-262.

Kachanechai, T., Jantawat, P., & Pichyangkura, R. (2008). The influence of chitosan on physico-chemical properties of chicken salt-soluble protein gel. *Food Hydrocolloids, 22,* 74-83.

Kasapis, S. (2008). Phase separation in biopolymer gels: A low- to high-solid exploration of structural morphology and functionality. *Critical Reviews in Food Science and Nutrition, 48,* 341-359.

Kasapis, S. (2010). Aims and background. ARC Research grant proposal, RMIT University.

Kavanagh, G.M., Clark, A.H., & Ross-Murphy, S.B. (2000). Heat induced gelation of globular proteins: Part 3 Molecular studies on low pH β-lactoglobulin gels. *International Journal of Biological Macromolecules, 28,* 41-50.

Kauzmann, W. (1959). Some factors in the interpretation of protein denaturation. *Advances in Protein Chemistry, 14,* 1-63.

Kazmierski, M. & Crredig, M. (2003). Characterisation of soluble aggregates from WPI. *Food Hydrocolloids, 17,* 685-692.

Kim, E.H.J., Petrie, J.R., Motoi, L.M., Morgenstern, M.P., Sutton, K.V., & Mishra, S. (2008). Effect of structural and physicochemical characteristics of the protein matrix in pasta on *in vitro* starch digestibility. *Food Biophysics, 3,* 229-234.

Koh, L.W., Kasapis, S., Lim, K.M., & Foo, C.W. (2009). Structural enhancement leading to retardation of *in vitro* digestion of rice dough in the presence of alginate. *Food Hydrocolloids, 23,* 1458-1464.

Kong, F. & Singh, R.P. (2008).Disintegration of solid foods in human stomach. *Journal of Food Science, 73,* 67-80.

Kok, T.N., & Park, J.W. (2007).Extending the shelf life of set fish ball. *Journal of Food Quality, 30,* 1-27.

Kong, M., Chen, X.G., Xing, K., & Park, H.J. (2010). Antimicrobial activity of chitosan and mode of action: A state of the art review. *International Journal of Food Microbiology, 144,* 51-63.

Kubota, N., & Kikuchi, Y. (1998). Macromolecular complexes of chitosan. In S. Dumitriu (Ed.), *Polysaccharides: Structural, diversity and functional versatility* (pp. 595-628). New York: Marcel Dekker.

Kumar, S.B., & Prabhasankar, P. (2014). Low glycemic index ingredients and modified starches in wheat based food processing: A review. *Trends in Food science and Technology, 35,* 32-41.

Lamarque, G., Lucas, J.-M., Viton, C., & Domard, A. (2005). Physicochemical behavior of homogenous series of acetylated chitosans in aqueous solution: role of various structural parameters. *Biomacromolecules, 6,* 131-142.

Lehmann, U., & Robin, F. (2007). Slowly digestible starch-its structure and health implications: a review. *Trends in Food Science and Technology, 18,* 346-355.

Lindeboom, N., Chang, P. R., & Tyler, R. T. (2004). Analytical, biochemical and physicochemical aspects of starch granule size, with emphasis on small granule starches: a review. *Starch - Stärke, 56* (3-4), 89-99.

Livney, Y.D., Corredig, M. & Dalgleish, D.G. (2003). Influence of thermal processing on the properties of dairy colloids. *Current Opinion in Colloid and Interface Science, 8,* 359-364.

Lopez-Caballero, M.E., Gomez-Guillen, M.C., Perez-Mateos, M., & Montero, P. (2005). A chitosan-gelating blend as a coating for fish patties. *Food Hydrocolloids, 19,* 303-311.

Luhovyy, B.L., Akhavan, T., & Anderson, G.H. (2007). Whey proteins in the regulation of Food Intake and Satiety. *Journal of the American College of Nutrition, 26,* 704S-712S.

Manelius, R. & Bertoft, E., (1996). The effect of calcium ions on the alpha-amylolysis of granular starches from oats and waxy-maize. *Journal of Cereal Science, 24,* 139–150.

McClemments, D.J. (2002). Modulation of globular protein functionality by weakly interacting co-solvents. *Critical Reviews in Food Science and Nutrition, 42,* 417-471.

McIntosh, G. H., Royle, P. J., Le Leu, R. K., Regester, G. O., Johnson, M. A., Grinsted, L.R, Kenwar R. S., Smithers, G.W. (1998). Whey proteins as functional Food Ingredients? *International Dairy Journal*, *8,* 425-434.

Medcalf, D. G., & Gilles, K. A. (1965). Wheat starches. I. Comparison of physicochemical properties. *Cereal Chemistry, 42,* 558–568.

Morris, E. R. (2009). Functional interactions in gelling biopolymer mixtures. In S. Kasapis, I. T. Norton & J. B. Ubbink (Eds.), *Modern Biopolymer Science: Bridging the Divide between Fundamental Treatise and Industrial Application* (pp. 167-198). San Diego: Elsevier.

Morr, CV. & Ha, EY. (1993). Whey protein concentrates and isolates: processing and functional properties. *Critical reviews in Food Science and Nutrition, 33,* 431-76.

Mounsey, J.S., O'Kennedy, B.T., Fenelon, M.A. & Brodkorb, A. (2008). The effect of heating on β-lactoglobulin-chitosan mixtures as influenced by pH and ionic strength. *Food Hydrocolloids, 22,* 65-73.

Nelson, D.L. & Cox, M.M. (2008). Carbohydrates and glycobiology. *Lehninger Principles of Biochemistry* (5 ed., pp. 239-267). New York: W.H. Freeman & Co Ltd.

Niwa, E. (1992). The chemistry of surimi gelation. In T. C. Lanier & C. M. Lee (Eds.), *Surimi technology* (pp. 389–427). New York: Marcel Dekker.

Pangborn, R. M. & Szczesniak, A. S. (1974). Effect of hydrocolloids and viscosity on flavor and odor intensities of aromatic flavor compounds. *Journal of Texture Studies,4*, 467-482.

Papiz, M. Z., L. Sawyer, E. E. Eliopoulas, A. C. North, J. B., Findlay, R. Sivaprosadaro, T. A. Jones, M. E. Newcomer, and P. J. Kraulis (1986). The structure of β-lactoglobulin and its similarity to plasma retinol-binding protein. *Nature (Lond.) 324*:383–385.

Pappas, C.P. & Rothwell, J. (1991). The effects of heating, alone or in the presence of calcium or lactose, on calcium binding to milk proteins. *Food Chemistry, 42*, 183-201.

Peniche, C., Howland, I., Carrillo, O., Zaldivar, C. & Arguelles-Monal, W. (2004). Formation and stability of shark liver oil loaded chitosan/calcium alginate capsules. *Food Hydrocolloids, 18*, 865-871.

Polyacov, V. I., Grinbereg, V. Ya, & Tolstoguzov, V. B. (1997). Thermodynamic incompatibility of proteins. *Food Hydrocolloids, 11*, 171-180.

Pujana, M.A., Perez-Alvarez, L., Iturbe, L.C.C., & Katime, I. (2012). Water dispersible pH-responsive chitosan nanogels modified with biocompatible crosslinking-agents. *Polymer, 53*, 3107-3116.

Raafat, D., & Sahl, H.G. (2009).Chitosan and its antimicrobial potential - a critical literature survey, *Microbial Biotechnology, 2*, 186-201.

Reed, R. G., Feldhoff, R. C., Clute, O. L., & Peters, T., Jr. (1975). Fragments of bovine serum albumin produced by limited proteolysis. Conformation and ligand binding. *Biochemistry*, *14*, 4578−4583.

Richardson, R. K., & Kasapis, S. (1998). Rheological methods in the characterisation of food biopolymers.In D. L. B. Wetzel, & G. Charalambous (Eds.), *Instrumental methods in food and beverage analysis*. Elsevier, p 23.31-44.

Rodriguez M.S., Albertengo, L.E. (2005). Interaction between chitosan and oil under stomach and duodenal digestive chemical conditions. *Journal of Bioscience, Biotechnology and Biochemistry, 69*, 2057–2062.

Saha, D. & Bhattacharya, A.S. (2010). Hydrocolloids as thickening and gelling agents in food: A critical review. *Journal of Food Science and Technology, 47,* 587-597.

Schep, L.J., Tucker, I.G., Young, G., Ledger, R., & Butt, A.G. (1999). Controlled release opportunities for oral peptide delivery in aquaculture. *Journal of Controlled Release, 59,* 1-14.

Schorsch, C., Jones, M. G., & Norton, I. T. (1999). Thermodynamic incompatibility and microstructure of milk protein/locust bean gum/sucrose systems. *Food Hydrocolloids, 13,* 89-99.

Simi, C.K., & Abraham, T.E. (2010). Transparent xyloglucan-chitosan complex hydrogels for different applications. *Food Hydrocolloids, 24,* 72-80.

Singh, J., Dartois, A., & Kaur, L. (2010). Starch digestibility in food matrix: a review. *Trends in Food Science & Technology, 21,* 168-180.

Singh, N., Singh, J., Kaur, L., Sodhi, N.S., & Gill, B.S. (2003). Morphological, thermal and rheological properties of starches from different botanical sources. *Food Chemistry, 81,* 219-231.

Smithers, G. W. (2008). Whey and whey proteins – from gutter-to-gold. *International Dairy Journal, 18,* 695–704.

Soulaka, A. B., & Morrison, W. R. (1985). The amylose and lipid contents, dimensions and gelatinisation characteristics of some wheat starches and their A- and B- granule fractions. *Journal of the Science of Food and Agriculture, 36,* 709–718.

Stamford, T.C.M., Thatiana, M.S., Horacinna, M.C, Macedo, R.O & Galba, M.C. (2013). Microbiological chitosan: Potential application as anticariogenic Agent, practical Applications. In Biomedical Engineering, Dr. Adriano Andrade (Ed.). Retrieved 24 June 2014, <http://www.intechopen.com/books/practical-applications-in-biomedical engineering/microbiological-chitosan-potential-application-as-anticariogenic-agent>

Stevens, W. F. (1996). Chitosan: A key compound in biology and bioprocess technology, Proceedings of 2nd Asia Pacific Symposium, Bangkok, Thailand.

Tanamas, S.K., Magliano, D.J., Lynch, B., Sethi, P., Willenberg, L., Polkinghorne, K.R., Chadban, S., Dunstan, D., & Shaw, J.E. (2014). The Australian diabetes, obesity and lifestyle study, Australian Policy Online. <http://apo.org.au/research/australian-diabetes-obesity-and-lifestyle-study>

Tester, R.F., Karkalas, J. & Qi, K. (2004). Starch structure and digestibility: Enzyme-substrate relationship. *World's Poultry Science Journal, 60,* 186-194.

Thompson, A., Boland, M., & Singh, H. (2009). Milk Proteins from expression to food, Elsevier Inc, San Diego, CA, USA.

Thongngam, M., & McClements, D.J. (2004). Characterisation of interactions between chitosan and an anionic surfactant. *Journal of Agricultural and Food Chemistry, 52,* 987-991.

Tipton, K.D., Elliott, T.A., Cree, M.G., Wolf, S.E., Sanford, A.P., & Wolfe, R.R. (2004). Ingestion of casein and whey proteins result in muscle anabolism after resistance exercise. *Medicine & Science in Sports & Exercise, 36,* 2073-2081.

Tolstoguzov, V.B. (1995). Some physico-chemical aspects of protein processing in foods. Multicomponent gels. *Food Hydrocolloids, 9,* 317-332.

Tolstoguzov, V. B. (1997). Protein-polysaccharide interactions. In S. Damodaran & A. Paraf (Eds.), *Food Proteins and their Applications* (pp. 171-198). New York: Marcel Dekker.

Torres, M.A., Beppu, M.M., Santana, C.C., &Arruda, E.J. (2006). Viscous and viscoelastic properties of chitosan solutions and gels. *Brazilian Journal of Food Technology, 9,* 101-108.

Ulleberg, E.K., Comi, I., Holm, H., Herud, E.B., Jacobsen, M., & Vegarud, G.E. (2011). Human gastrointestinal juices intended for use in *in vitro* digestion models. *Food Digestion, 2,* 52-61.

U.S. National Library of Medicine 2014, Body temperature normals. Retrieved 24 June 2014, <http://www.nlm.nih.gov/medlineplus/ency/article/001982.htm>

Verheul, M., Roefs, S. P. F. M. (1998). Structure of whey protein gels studied by permeability, scanning electron microscopy and rheology. *Food Hydrocolloids, 12,* 17-24.

Walstra, P., Wouters, J. T. M., Geurts, T. J. (2006). *Dairy Science and Technology*, 2nd ed., Tailor and Francis Group, LLC, Boca Raton, FL.

Wandrey, C., Bartkowiak, A., & Harding, S. E. (2010). Materials for encapsulation. In N. J. Zuidam & V. A. Nedovic (Eds.), *Encapsulation technologies for active food ingredients and food processing* (pp. 31-100). New York: Springer.

Wang, X., Lee, J., Wang, Y.-W., & Huang, Q. (2007). Composition and rheological properties of β-lactoglobulin/ pectin coacervates: effects of salt concentration and initial protein/polysaccharide ratio. *Biomacromolecules, 8,* 992-997.

Wetzel, R., Becker, M., Behlke, J., Billwitz, H., Böhm, S., Ebert, B., et al. (1980). Temperature behaviour of human serum albumin. *European Journal of Biochemistry*, 104, 469−478.

Williams, P. A., Clegg, S. M., Langdon, M. J., Nishinari, K., and Phillips, G. O. (1992). Studies on the synergistic interaction of konjac mannan and locust bean gum with kappa carrageenan. In Gums and Stabilisers for the Food Industry 6, eds. Phillips, G. O., Wedlock, D. J., and Williams, P. A., IRL Press, Oxford, pp. 209–216.

Yang, H., Irudayaraj, J., Otgonchimeg, S. & Walsh, M. (2004). Rheological study of starch and dairy ingredient-based food systems. *Food Chemistry, 86*, 571-578.

Yang, N., Liu, Y., Ashton, J., Gorczyca, E., & Kasapis, S. (2013). Phase behavior and *in vitro* hydrolysis of wheat starch in mixture with whey protein. *Food Chemistry, 137*, 76-82.

Zeman, L., & Patterson, D. (1972). Effect of the solvent on polymer incompatibility in solution. *Macromolecules, 5*(4), 513-516.

Zeng, M., Morrise, C.F., Batey, I.L., & Wrigley, C.W. (1997). Sources of variation for starch gelatinisation, pasting, and gelation properties in wheat. *Cereal Chemistry, 74*, 63-71.

Zobell, H. F., &Kulp, K. (1996). The staling mechanism. In: Baked goods freshness, Technology, evaluation and inhibition of staling. Eds, R.E Hebeda and H.F. Zobel, pp 1-64. New York, USA: Marcel Dekker.

Chapter 2 - Materials and Method

2.0 Materials

Whey protein isolate (WPI)

Whey protein isolate powder was supplied as a 25 kg lot by Fonterra Co-operative Group Ltd., New Zealand. The 25kg was subdivided into 1kg lots which were vacuum packed and refrigerated (4±1°C) until required. As stated in the certificate of analysis from the supplier, the powder consisted of 88.71% protein, 0.93% fat, 4.83% moisture and 3.3% ash (w/w). The WPI was used at a constant concentration of 15% (w/v). Such concentration is above the minimum threshold for gelation to occur.

Wheat starch (WS)

Native wheat starch powder, with the following composition: 94.1% starch, 0.3% ash, 0.1% fat and 5.5% moisture (w/w), was obtained from National Starch and Chemical Co., Thailand. This material was refrigerated (4±1°C) until required. The WS was used at concentrations between 5 to 15% (w/v). The chosen range reflects those typically found in a wide range of food products.

Calcium chloride

Calcium chloride as anhydrous white granules (<7.0mm, >93%), was purchased from Sigma Aldrich Chemicals, Castle Hill, Australia product number C1016, and stored at room temperature (22±2°C).

Chitosan

Medium molecular weight chitosan powder (product number 448877) with 75-85% degree of deacetylation was purchased from Sigma Aldrich Chemicals, St. Louis, MO, USA. The powder was stored in the freezer (-20°C) and was dissolved in 1% (w/v) acetic acid solution when required. The chitosan was used at typical preparation concentrations of 1 to 2% (w/v) which can be dissolved effectively in acidic medium (Gomez- Estaca, Gomez-Guillen, Fernandez-Martin & Montero, 2011; Hou et al., 2012; Mathew, Brahmakumar & Abraham, 2006).

α-Amylase (1,4-α-D-Glucan-glucanohydrolase)

α-Amylase, lyophilised powder, 150-250 units/mg protein (biuret), derived from the filamentous fungus *Aspergillus oryzae*, product number A6211, was purchased from Sigma Aldrich Chemicals, Castle Hill, Australia.

2.1 Sample preparation

The samples required for this thesis were aqueous mixtures and gels formed by the combination of WS, WPI, chitosan and calcium chloride. For rheology and DSC studies, powders were weighed according to desired concentrations, dissolved in distilled water at ambient temperature and gently stirred prior to loading onto the instrument. For microscopy, texture profiling, FTIR and *in vitro* starch digestion, self-supported gels were required. The challenge with the composite gels was to avoid bulk phase separation of the member components during sample preparation and consequently the formation of a 'layered' gel. To combat this, the required dispersions (well stirred) were pipetted into preheated (45°C) aluminium moulds, which were immediately sealed in aluminium foil and then placed into a pre-heated (85±1°C) water bath for 75 min.

Other issues that affected the quality of the gels prepared included: ease in the release of intact gels, and effective sealing of samples. The gels studied must be intact and uniform in size and shape to conduct an accurate texture profile analysis. Since samples often became wedged in the mould, additional preparation steps were included for the gels required for texture profile analysis. Specifically, the walls of the moulds were lightly coated with silicon oil and then the bottom and sides of the mould were fitted with baking paper. A 'clean' release of the gel was obtained as the oil ensured that the baking paper remained in place whilst the sample was being removed. Initially the moulds (sealed in aluminium foil) were placed directly into the water bath. The concern was that the sealing may not be effective and as a result allow the ingress of water into the mould from the water bath. An alternative approach was trialled in which the sealed mould was placed into a small beaker which in turn was placed into the water bath. Although this addressed the problem of water ingress, it created a more serious problem which was separation of the dispersions and as a result the formation of a bulk phase separated gel. This occurred because the heat transfer rate from

water through the air (which has low thermal conductivity) in the beaker and then to the gel was slow enough to allow the dispersions to settle according to their respective densities. The problem was addressed by returning to the practice of placing the mould directly into the water bath with the requirement of meticulous sealing of the mould with aluminium foil before doing so.

The question is what is the order of the events during heating that are associated with forming a gel from single, binary or multicomponent dispersions? The answer requires information from the literature, temperature data from a calibrated thermocouple placed at the centre of the sample gel during heating and heat flow data on the single component gels from the differential scanning calorimeter (DSC). As mentioned above, the heat transfer from the pre-heated water bath to the dispersions in the mould was responsible for the increase in temperature inside the moulds. It was noted that in the first 9 min, the temperature of the gel reached between 20 and 45°C at which point according to (George, 2012), β-lactoglobulin dissociates from the quaternary conformation (dimer). In about the next 3min (≈12min total heating time), the centre of the sample reached 60°C which was the lowest temperature recorded by DSC in the present thesis for WS samples to commence gelatinisation. According to the literature (Seib, 1994; Singh, Singh, Kaur, Sodhi & Gill, 2003) B-type starch granules undergo gelatinisation at a lower temperature than A-type starch granules. Nonetheless the WS is undergoing gelatinisation in this temperature range.

According to the thermocouple, the centre of the sample reached 68°C in the following minute, i.e. after 13 min in the water bath. This is the lowest temperature for whey proteins to commence denaturation, according to DSC heat flow data for WPI samples in the present thesis. At this stage the whey protein secondary conformation is disrupted and increased hydrophobicity is exhibited. Following partial unfolding of the protein domains, whey protein molecules aggregate to form a gel. The latter aggregation step starts after the time (after 13 min.) WPI denaturation temperature has been reached and continues during the remainder of the time (~62 min) the samples were held at 85°C±1°C. Thus, the key polymers (WS & WPI) underwent phase transition within the first 15 min of heating according to the thermocouple temperature data and heat flow data from MDSC. Samples taken out of the heated water bath after 75min were allowed to cool at room temperature and then refrigerated (4±1°C). During the cooling period, retrogradation of starch polysaccharides, and further aggregation of the

whey proteins occurred (Hermansson & Svegmark, 1996). All gel samples were used within 1-2 days after being prepared.

2.2 Rheology

Rheology is the study of flow and deformation of matter (Rao, 1999). Viscosity is the most common rheological parameter used to quantify the flow of a material. Honey and commercial pasteurised skim milk would be examples of highly viscous and comparatively low viscous materials, respectively. Viscosity is defined as the resistance of a material to flow and is represented by the symbol η *(eta)* and measured in Pascals per second ($Pa.s^{-1}$). Measuring the resistance of a material to flow has many industrial applications. For example, knowing the viscosity of ketchup will help to determine the force required to pump the ketchup from one work station to another. That force would need to be enough to relocate the ketchup but ideally be less than the threshold force that can result in breaking the network and thus compromising the sensory aspects of the ketchup. Viscosity characteristics are also pertinent to the packaging of this product, in that the force applied by the consumer using squeeze-bottled ketchup should allow for effortless release of the product but not cause the condiment to flow uncontrollably out of the bottle. The measurement of viscosity normally involves the use of a Brookefield viscometer and/or rheometer. The uni-directional shear applied in viscosity measurements eventually breaks down the sample and thus is considered a large deformation test.

Besides viscosity, other key rheological parameters include: stress, strain, and shear rate. Stress, denoted as σ (sigma), is the force per unit of area. Stress is a measure of pressure for which the SI units are Pascals (Pa). Whereas, strain, denoted as ε (epsilon), is the relative deformation in shear and expressed without units because it is a measure of the changed length over original length or it can be γ (gamma) which is measured in radians. What often is important is the rate at which the deformation occurs (Rao, 2007). Shear rate, denoted as $\dot{\gamma}$, is the speed of strain per unit time and expressed as the reciprocal of time (s^{-1}).

The rheological parameters can be measured in various materials ranging from solids through to liquids. The knowledge we have today has been built on the study of two extremes, namely solids by and liquids by Newton (Jones, 2002). Both the Hookean solid and Newtonian

liquids are highly idealised examples of the behaviour of materials as both form a linear law based on direct proportionality between stress and strain or stress and shear rate, irrespective of force applied and amount of stress. So, the Hookean solid, according to its definition, possesses a purely elastic response with a direct proportional relationship between the stress applied and the consequential strain. Similarly, the Newtonian fluid exhibits a stress that is directly proportional to the rate of strain (Rao, 2007), but in this case, according to its definition, Newtonian fluids possess a purely viscous response.

However, in reality, most food products only exhibit Hookean solid or Newtonian liquid behaviour within a limited range of stresses. More commonly, food materials will exhibit a combination of solid-like and liquid-like behaviour in response to deformation that fits in between these two classical extremes (Hookean solid and Newtonian liquid). Therefore, the term viscoelastic is used to describe most foods as neither the term solid–like nor liquid–like is appropriate. Viscoelasticity can be measured by small-scale deformation using a rheometer. Unlike viscosity measurements, the viscoelasticity of materials is measured with a bi-directional (oscillating) shear. In an oscillation test, a sinusoidal stress or strain is applied. The main characteristic of a small-scale deformation (oscillation) experiment is that the applied stress or strain is carried out within what is called 'the linear viscoelastic region' (LVR). The predetermined LVR is within the domain where the magnitude of stress and strain are related linearly and the rheological behaviour of samples within this region is independent of applied stress and strain. Meaning that both the applied stress (or strain) and associated response follow a sine wave and although, the sample is being 'excited', the strain is never enough to destroy the elastic structure. For this to occur the deformation of the sample is low or slow enough so that the sample's structure is never far from equilibrium and as a result is not deformed permanently during the test. Permanent deformation is what occurs during large-scale deformation measurements as used for viscosity measurements.

In relation to viscoelasticity and to interpret the results of relevant tests, the following terms: storage modulus, loss modulus, tan delta and complex viscosity must be defined. The storage modulus (G') represents the solid like properties of a sample and the strength of a given network and therefore the gel's ability to resist deformation under applied pressure. It accounts for the number and strength of molecular interactions within the sample. The loss modulus (G'') represents the liquid like properties of a sample and accounts only for the number of molecular interactions within the sample. Thus if $G' > G''$, than the material is

more solid than liquid. The converse is also true. The storage and loss moduli can be can be combined to form the complex modulus, G^* which is regarded as indicating the overall resistance of a sample to oscillatory shear. The complex modulus G^* is mathematically = (G'^2 + G''^2)^{½}, with units for all moduli being pascals (Pa). An alternative method for evaluating the relative importance of G' and G'' is to calculate the phase angle (tan δ) which is equal to G''/G' and is deemed to be a measure of the viscoelasticity. So samples with a tan δ above 1 are highly viscous where tan δ values indicate that the sample possess more elastic properties. Significantly, viscosity of a sample can also be determined by using the same small-scale deformation test, but in this case, the viscosity is referred to as complex viscosity and denoted by η* (eta star).and is equal to G^*/ω, i.e. the division of the complex modulus by the deformation frequency (ω).

In this thesis, the Advanced Rheometer Generation 2 (AR-G2) by TA instruments was used to generate results from small-scale deformation oscillation experiments (Figure 2.1). This rheometer is able to qualitatively and quantitatively measure the viscoelasticity of fluids, semi-solids and solids (under appropriate examination conditions). Keeping all parameters constant, but varying the following (one at a time): time, temperature, frequency and strain can provide valuable information about the system under examination:

Figure 2.1 TA Instruments AR-G2 Magnetic Bearing Rheometer at RMIT

Strain sweep

Strain sweep is normally the first experiment conducted on the rheometer. The purpose of the strain sweep is to determine the LVR. To determine the LVR, the amplitude of either stress or strain is varied over a range. In the case of the AR-G2, a strain sweep is used. The resulting graph can indicate the stability of a sample in that the longer the LVR region the more stable the product. In using the AR-G2, the optimum strain, which lies well within the LVR, is determined and used consistently for subsequently conducted tests.

Time sweep

The time sweep consists of monitoring the sample during a specified period of time while holding other variables (including frequency and strain) constant, and enables the user to determine whether the properties of a sample change with time. The time sweep can identify clearly the time needed for the sample to reach an equilibrium state and can also provide insights into storage stability of a product.

Temperature ramp

As the name suggest, a temperature sweep requires the sample to be exposed to a range of temperatures with all other possible variables remaining constant. As a result, this type of experiment allows us to monitor any changes in the sample's properties as a function of temperature e.g. gelation, denaturation, gelatinisation. It should be noted that the scan rate can significantly affect the results. For example, gelation temperature, homogeneity of the network and size of the pores are all affected by the heating rate (Stading & Hermansson, 1990; Stading, Langton & Hermansson, 1993). A scan rate of 1°C/min and 2°C/min is most commonly cited in the analysis of food samples (Cakir & Foegeding, 2011; Noisuwan et al., 2008; Sun & Arntfeld, 2010; Yang et al., 2004)

Frequency sweep

Frequency is the time required to complete one oscillation and is expressed as the inverse of time; where a high frequency would correspond to a shorter time and a low frequency to a longer time to complete one oscillation, respectively. The resulting spectrum of a frequency

sweep provides information to classify the type of system under examination i.e. weak gel, strong gel, dilute solution, entangled solution (Richardson & Kasapis, 1998).

2.3 Modulated Differential Scanning Calorimetry

Differential scanning calorimetry (DSC) is a micromolecular thermal analysis technique designed to measure a sample's heat flow in response to time and change in temperature. The behaviour of the sample is displayed in a thermograph which can be seen on connected computer software. The absorption of heat and release of energy is seen as resulting peaks and troughs in the thermograph with heat flow (mW) labelled on the y axis against temperature displayed on the x axis. In addition to identifying endothermic and exothermic reactions, the area of the peaks and troughs can be measured and is directly proportional to the change in heat enthalpy. Examples of endothermic reactions include the denaturation of protein and gelatinisation of starch. As for exothermic reactions, these may include aggregation of protein and retrogradation of starch.

The instrument contains a chamber into which a sample and/or an inert reference (most commonly an empty pan) are placed. Depending on the layout of the instrument, i.e. heat flux DSC or power compensation DSC, the sample and reference may be contained within the same or in separate chambers (Coleman & Craig, 1996). Either way, the general concept is the same, the two entities are placed on a platform that is heat controlled and the differences in heat flow are registered by thermocouples (Reading et al., 1994). Both low and high solids systems can be investigated using the DSC. The former case is of relevance to this thesis

Like all techniques, there are a number of relevant issues to consider. In this case, it is the need to initially purge the chamber with gas (commonly nitrogen) to allow for uniformity in the thermal environment and correction of the baseline. Whereas in interpreting the resultant plot, the sensitivity and resolution power are important. Sensitivity is the ability to detect thermal transitions while resolution allows separate transitions to be distinguished. Without good sensitivity and resolution thermal transitions may not be detected and/or a number of close transitions may be deduced as a single event. In DSC, higher sensitivity is afforded with

increased sample size and /or higher scan rates but the latter offsets resolution which is improved with slower scan rates (Chiu & Prenner, 2011). Thus, the ideal scan rate is an optimum balance between resolution and sensitivity which would be unique to the sample under investigation. For example, a single solute solution may not require as much resolution as a composite system where one would be expecting various thermal events to occur. Another issue is the range of temperature used. Ideally heating should not exceed 95°C because excessive pressure arising at such temperatures may cause the cell containing the sample to burst. On the other hand, cooling should go below 0°C since the formation of ice crystals may fracture the junction zones of any preformed matrix.

The DSC was followed by the development of an enhanced version of the thermal analytical technique, namely modulated differential scanning calorimetry (MDSC). The distinguishing characteristic between the DSC and MDSC is that the latter includes a heating and cooling sinusoidal modulation applied in addition to the standard linear temperature program of the conventional DSC (Rabel et al., 1999). Thus, while also exhibiting the total heat flow of a sample, the MDSC provides the convenience of separating this into reversing and non-reversing heat flow. According to Gill et al. (1993), reversing heat flow corresponds to heating-rate dependent transitions which can be reversed by some modification in heating and cooling. By contrast, non-reversing heat flow corresponds to absolute temperature dependent transitions which cannot be reversed by heating/cooling once activated (Gill et al., 1993). Despite manipulating scan rate and sample size, the interpretation of overlapping thermal transitions using standard DSC is regarded as being quite difficult. In MDSC, however, enhanced sensitivity in such situations is provided by the separation of thermal transitions into non-reversing and reversing transitions. This scenario is best explained with an example such as the heating of polycarbonate and PET film mentioned by Gill et al. (1993). The resulting thermograph of the polycarbonate and PET blend depicted in Figure 2.2 clearly shows a reaction occurring between 130°C and 150°C as a single thermal transition from a conventional DSC. However, when observing the non-reversing and reversing heating curves generated by a MDSC it is clear that such assessment is not complete. From MDSC, it is apparent the polycarbonate and PET film undergoes two transitions, PET crystallisation and polycarbonate glass transition.

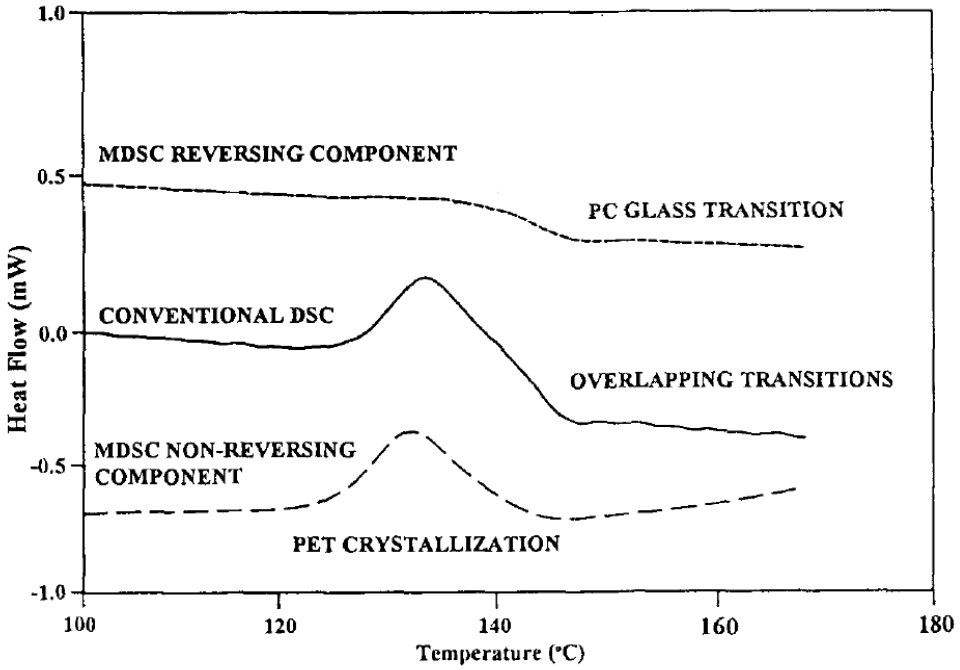

Figure 2.2 Thermograph of polycarbonate/ PET film (Gill et al., 1993)

In this thesis, the TA Instruments Q2000 modulated DSC andSetaram VII micro DSC were used for thermal assessment of samples. The Q2000 provided faster throughput, i.e. more samples could be analysed in a given timeframe, and also achieved separation of reversing and non-reversing heat flow, whereas a higher sensitivity was achieved with the Setaram VII. The modulated DSC and micro DSC can be seen in Figures 2.3 and 2.4 respectively.

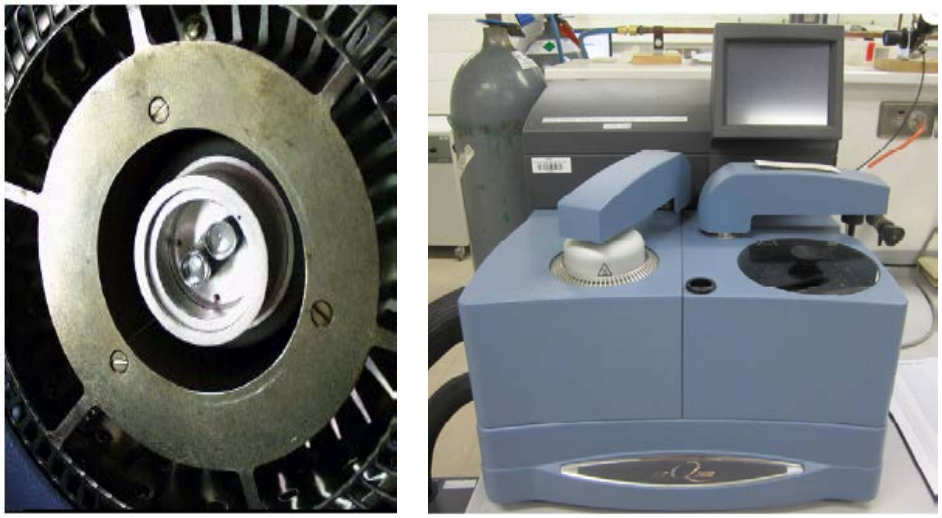

Figure 2.3 TA Instruments MDSC Q2000 with autosampler

Figure 2.4 Setaram VII Micro DSC

2.4 Texture profile analysis

The texture of foods can be measured by undertaking sensory and objective tests. Sensory tests are carried out by using taste panellists and involve oral (smelling and tasting) and non-oral, (touching and visual) evaluation of foods (Bourne, 2002). Objective tests, on the other hand, involve using instruments to generate data that can be used to assess the foods qualitatively and quantitatively. Examples of this is the colourmeter and the texture profile analysis (TPA). The TPA approach was originally developed by General Foods in the 1960's and has improved over time. For this thesis, TA-XT2 Texture analyser by Stable Micro Systems was the instrument used in this thesis as it is Stable Micro Systems' flagship texture analysis instrument (Figure 2.5). This instrument basically comprises of a probe attached to a moving arm (cross head). With the assistance of the arm, the probe moves downwards to come in contact with the sample which is placed on the base of the texture analyser. The texture analyser is connected to a computer software program which facilitates both the programming of the appropriate experimental conditions as well as the interpretation of results.

The aim of the experiment must be clear as it affects the choices that can be made; choices such as type of probe as well as the shape and diameter of the probe. Many fixtures are available to complement the sample under investigation including cone, cylinder, rounded end and puncture probes (Texture Technologies, 2014). With respect to the diameter of the probe, according to Pons and Fiszman (1996) forces registered from a probe diameter smaller than

the sample diameter are largely derived from a puncture which is a combination of compression and shear. When the diameter of the compressing unit is equal to or larger than the sample diameter, the forces registered are mainly due to uniaxial compression. While both puncture and compression tests have been conducted and reported, the latter is more prominent in recent literature (Pons and Fiszman, 1996).

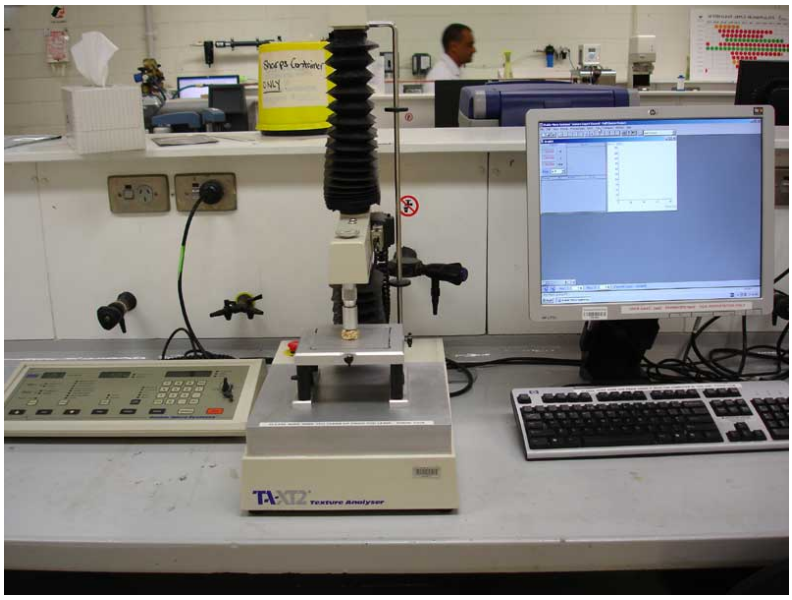

Figure 2.5 Stable Micro Systems TA-XT2 Texture analyser

The rate at which the probe moves towards the sample i.e. the cross-head speed will influence the force required to achieve a set amount of deformation. More specifically, previous authors have noted that when a high cross-head speed was adopted, greater force was required to deform a gel sample of the same type when compared with a low cross-head speed experiment (Pons and Fiszman, 1996). The results were explained by the suggestion that greater relaxation of the gel would be possible at the lower rate of contact. The situation can perhaps be likened to the basis of small deformation oscillation experiments (as previously discussed). Similarly to the rheology experiments, a slow rate of deformation is opted for to measure characteristics of the sample as close as possible to its equilibrium state. In Pons and Fiszman's review (1996) they also noted that experiments conducted with higher cross-head speed correlated better with sensory tests on mechanical hardness. This finding has encouraged scientists to adopt higher cross-head speeds for their texture analysis experiments (Huang et al., 2007). In the experiments by Huang et al., (2007) a cross-head speed of 50 mm/min was used to analyse rice starch gels with gellan, carrageenan and glucomannan.

Depending on the objective of the experiment, a low rate of compression can also be desirable. A low rate of compression, such as 0.1mm/sec, means the gel is closer to its equilibrium position and can provide information on characteristics such as gel strength of a product in its natural state. However, if the objective is correlation to taste panel data which involves assessing the experience in the mouth during mastication then as mentioned above, a higher rate of compression is required for that test.

Texture analysis experiments may involve single cycle or two cycle compression tests. The information that can be obtained when undertaking single cycle compression tests include firmness, hardness, brittleness and adhesiveness. Further information can be obtained with a two cycle deformation test, including elasticity and cohesiveness. For single cycle compression tests, the compression can be high to enable fracture on first go. In two cycle compression tests, to obtain valuable information about the gel in the second stage of the experiment, minimal initial compression, e.g. 25% of the original sample height is used. An example of a texture profile analysis graph is exhibited in Figure 2.6 and the definitions of the texture parameters are listed below in Table 2.

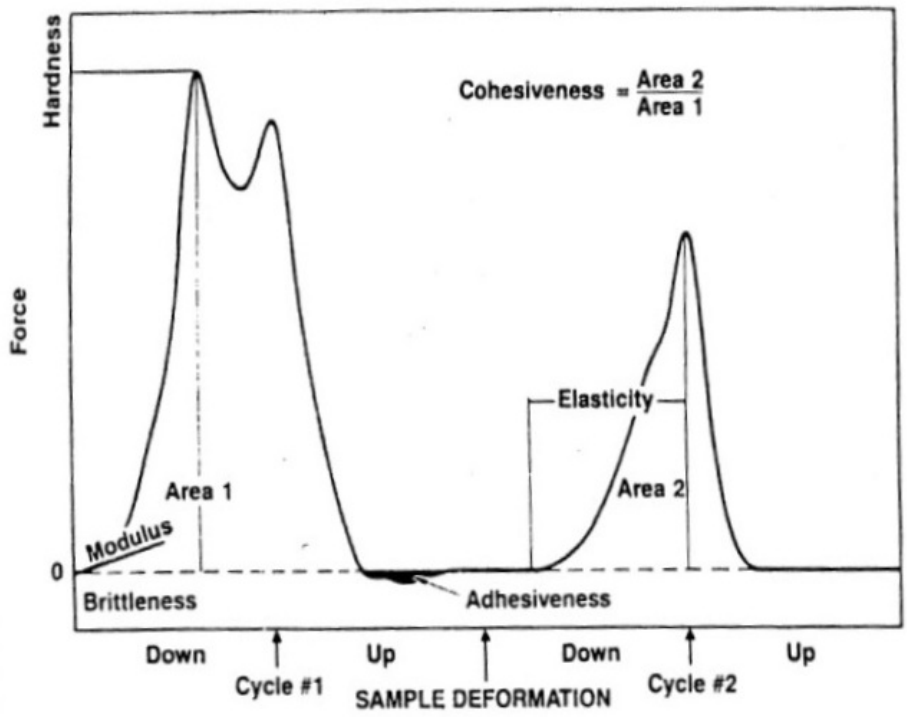

Figure 2.6 Sample of a two-cycle compression graph for texture profile analysis

Table 2.1 Parameters measured by Texture Profile Analysis (modified from Rosenthal, 1999)

Parameter	Sensorial definition	Instrumental definition
Hardness	Force required to compress a food between the molars. It is the maximum force that occurs at any time during the first cycle compression. This is correlated to the gel strength of the network and expressed in units of force (pounds or Newtons). It is worthy to note that since texture profile analysis on samples reported in literature are of various sizes and shapes, the parameter can be converted and reported in Pascals so the variation in surface area can be accounted for. This enables ease of comparison of the same material with texture experiments conducted by other authors.	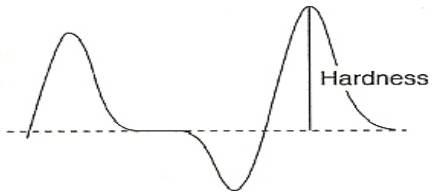
Firmness	Is the initial slope of the force-deformation curve. Also known as the modulus, is expressed in units of force per unit area (pounds per square inch or Newtons per square centimetre).	

Table 2.1 (continued)

Parameter	Sensorial definition	Instrumental definition
Elasticity	The extent to which a compressed food returns to its original size when the load is removed. It is the height of the sample in the second compression cycle relative to the original height during the first cycle of compression. Expressed as a percentage with no units, samples returning to its original height would be considered 100% elastic.	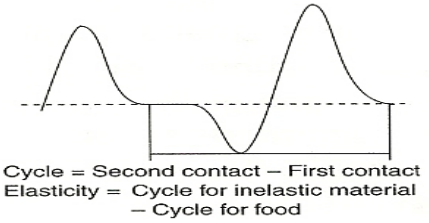
Adhesiveness	The work required to pull the food away from a surface. It is the negative force registered following the first cycle of compression when the crosshead moves back to its original position. Also known as the stickiness, there are no units for this parameter.	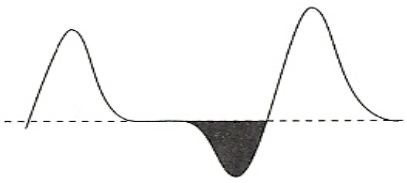
Cohesiveness	The strength of the internal bonds making up the food. It is the area under the second cycle curve divided by the area under the first cycle curve. Expressed as a percentage with no units, samples with high levels of cohesiveness are tough and difficult to break down.	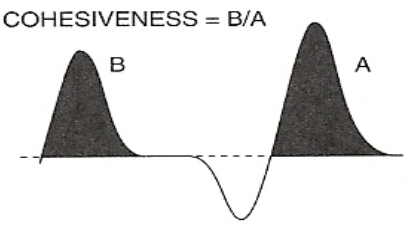

Table 2.1 (continued)

Parameter	Sensorial definition	Instrumental definition
Brittleness	The force at which the material fractures. Brittle foods are never adhesive. The first significant drop in the force/deformation curve during the first compression cycle. A sample that fractures early in the test is considered more brittle than a sample that exhibits fracture later. Expressed as the % strain required to break the gel, a low % strain indicates a more brittle sample and *vice versa*.	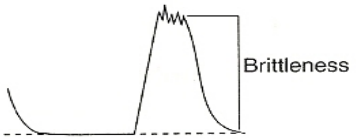
Chewiness	The energy required to chew a solid food until it is ready for swallowing.	= Hardness × Cohesiveness × Elasticity
Gumminess	The energy required to disintegrate a semisolid food so that it is ready for swallowing.	= Hardness × Cohesiveness

2.5 Scanning Electron Microscopy (SEM)

Microscopy enables the examination of the composition and surface topography of samples in much finer detail than what is possible with the unaided human eye. In the field of microscopy, the light microscopes was the initial development and since then much more complex instruments have been developed to include significantly enhanced resolving power and magnification: TEM (transmission electron microscope), SEM (scanning electron microscope), ESEM (environmental scanning electron microscope), VPSEM (variable-pressure electron microscope) and STEM (scanning transmission electron microscope). The sophistication of advances in light microscope come about by improvements in the original components of the microscope, including the addition of numerous electromagnetic lenses among other accessories. However, the significant discovery in 1920 that accelerated electrons in a vacuum behaved quite similarly to light and the interactions of electric and magnetic fields on electrons were likened to that of the interactions between glass lens and mirrors on visible light resulted in a new type of microscope: the electron microscope (FEI, 2008). As compared with light microscopes, the improved resolution of electron microscopes was largely attributed to the characteristic shorter wavelength of electrons (Davis, 2005).

In the work of this thesis, the SEM was utilised to produce two dimensional images of the surface of samples and provide details on their microstructure. Essentially the SEM consists of a lens system, electron gun, electron detector, visual and photorecording cathode ray tubes (CRTs) as shown in Figure 2.7.

The defining feature of the SEM as compared with other microscopes is that the electron beam is not static (as in TEM) and it scans in a rectangular raster over the specimen (FEI, 2008). In terms of use, it is able to examine a wide range of specimens including those with high moisture content such as low solid whey protein and starch gels (<30% w/w). The SEM can offer the convenience of examining specimens without the need for special preparations. When electrons strike (primary beam) the surface of the sample this generally results in a few possible and simultaneous scenarios. The specimen may emit photons (light), x-rays and/or absorb the electrons, this results in two main signals for imaging, namely: secondary electrons (SE) and backscattered electrons (BSE) (Goldstein *et al.*, 2003). The electrons that are generated when incident (primary) beam electrons knocks out loosely bound conduction electrons are called the SE. Their contribution to the image is that given that they have low

energy (<50 eV), they can only escape from a very shallow region at the sample surface and as a result the SE signal provides the highest resolution topographic information. The other electrons (BSE) occurs by elastically scattered electrons deflected through angles between 0° and 180° by atoms within the specimen. This causes the electrons to have high energy which will produce topographical information with lower resolution compared to SE. (Davis, 2005).

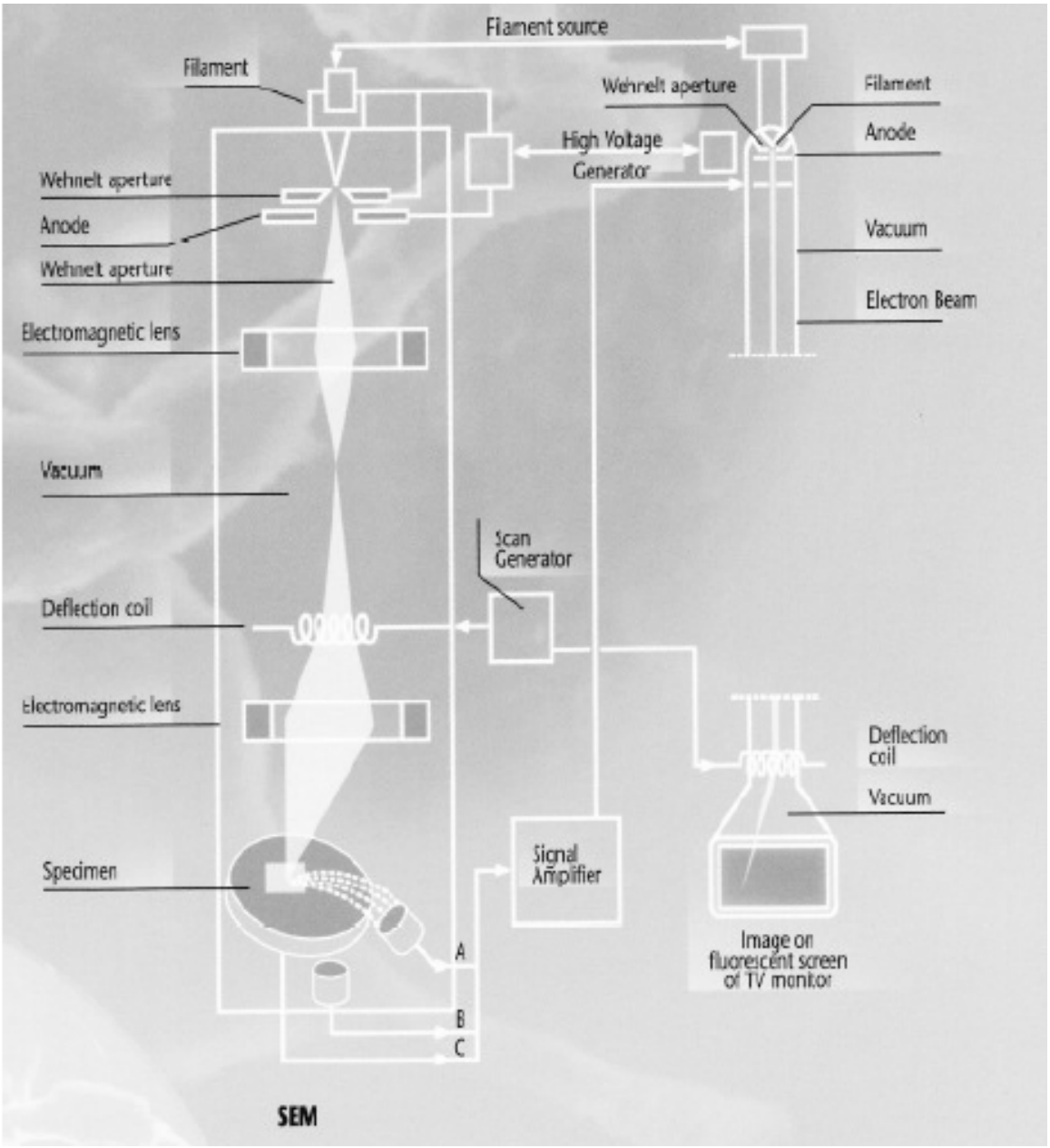

Figure 2.7 Diagram of the SEM (FEI, 2008)

Samples with relatively smooth surfaces are suitable for this imaging mode because slight topographical irregularities can cause artefacts due to shadowing (Wang & Petrova, 2012).

The basic ways of improving the resolution of a SEM image is by adjusting the accelerating voltage, spot size and working distance. Resolution, as described in the DSC section, is the smallest distance required to distinguish two particles as two separate points. The naked human eye can distinguish two points when they are at a distance of approximately 0.2mm apart. The light microscope can provide detail of particles as small as 200nm and possesses up to 1000x magnification. Meanwhile micrographs with a resolution size as small as 1nm-a millionth of a millimetre can be produced by SEM. The magnification range of the SEM is 10-10,000X. The accelerating voltage is related to the wavelength of the electrons and the working distance is the distance between the final aperture and the specimen (FEI, 2008). An increase in accelerating voltage and a decrease in working distance will improve resolution. Spot size represents the diameter of the electron beam. At high magnifications, a reduction in spot size will achieve better resolution as the diameter of the beam increases the clarity of the image decreases. At low magnifications, a reduction in spot size may not improve resolution as there is an increase in signal to noise ratio where a higher degree of SE are emitted and detected. Consequently adjustments need to be made relative to the specimen under examination as well as the aforementioned variables. Since the SEM is in the realm of electronics, the images may be digitally enhanced, i.e. to improve contrast, inversion (black becomes white) etc. using modern technology (FEI, 2008).

FEI Quanta^{TM} 200 Scanning Electron Microscope

The specific instrument used in present study was the FEI Quanta^{TM} 200 SEM (Figure 2.8 & 2.9) belonging to the RMIT Microscopy and Microanalysis Facility (RMMF). This instrument possesses three modes of operation, namely high-vacuum, low-vacuum and ESEM. The ESEM mode was the most suitable choice of operation to examine the protein and polysaccharide samples discussed in the following chapters.

Figure 2.8 FEI QuantaTM 200 in the RMIT Microscopy and Microanalysis Facility (RMMF)

Figure 2.9 Close up of the FEI QuantaTM 200 in the RMIT Microscopy and Microanalysis Facility (RMMF)

2.6 Fourier Transform Infrared Spectroscopy

Fourier Transform Infrared spectroscopy (FTIR) essentially involves passing infrared radiation through a sample. This beam of infrared energy then enters the compartment called the “interferometer” whereby computerised FTIR instrumentation performs calculations based on the well-established “Fourier transformation” analysis. The result of this analysis is a spectrum displaying the absorbance or transmittance over a specified wavelength range (Thermo Nicolet, 2001). The absorbance peaks correspond to the frequencies of vibration between the bonds of the atoms within a sample while the transmittance is the infrared radiation that has passed through the sample. While measurements conducted in absorbance and transmittance mode have both been conducted and reported in the literature, it is a matter of preference and this thesis is concerned with the former. Furthermore, the absorbance peaks can assist with identification and validation of unknown samples as well as unknown components within a sample. This comes about by the fact that each component can be associated with an absorption peak at a specific wavelength.

For example, the presence of whey protein in whey protein and starch gels can be validated by identifying spectral features occurring in the wavelength range of 1500 to 1600cm^{-1}. These features are present in the proteinaceous material by itself and are the vibrations in the amide II region resulting from stretching of the C-N bond as well as the N-H bending bonds (van der Ven et al., 2002). FTIR is also useful for the quantification of components within a compound, as the area under the absorption peak is directly proportional to the quantity present (Thermo Nicolet, 2001). Using the aforementioned example it can also be noted that the technique can help users distinguish if molecular interactions have occurred between components within the sample. For example, if there is no distortion of the whey protein spectra by the presence of starch in the amide II region, and if the spectra from the composites appear as if it is a superimposed spectra of the individual components, the absence of covalent bonds between the protein and polysaccharide can be deduced.

In comparison to older techniques, i.e. dispersive infrared spectrometers, FTIR is the preferable technique because both sample time and sensitivity have been very notably improved (Surewicz & Mantsch, 1988). After a single background correction, the user can obtain measurements within seconds rather than several minutes. Several scans that are averaged out can be conducted to increase the reproducibility of results (Thermo Nicolet,

2001). FTIR is also non-invasive. The Perkin Elmer Spectrum 100 spectrometer equipped with MIRacle ™ ZnSe single reflection ATR (attenuated total reflection) plate was utilised in this thesis and is presented in Figure 2.10.

Figure 2.10 ATR-FTIR Perkin Elmer Spectrum 100 spectrometer

2.7 *In vitro* digestion

In vitro digestion experiments are commonly carried out to analyse the structural changes and digestibility of food samples. These experiments are also used to mimic the digestive processes in the human gastrointestinal tract albeit to varying degrees. Given the complexity of the human gastrointestinal tract, such models are used with caution and understanding of the limitations, i.e. the accuracy of *in vitro* models will rarely match that of the *in vivo* model. *In vitro* models that serve to mimic *in vivo* digestion models often include the key compartments of the human gastrointestinal tract, namely the mouth, stomach and small intestines. Since most foods are absorbed in the small intestines mimicking of the large intestines is not commonly performed (Hur et al., 2011). These experiments are particularly appealing over *in vivo* experiments as they are time and cost efficient. The typical *in vitro* digestion experiment normally lasts a couple of hours in comparison to an *in vivo* experiment which may require days. In terms of cost, for *in vitro* digestion models, the apparatus and utensils required to conduct such experiments can be quite basic. While there is currently no

standard set-up for an *in vitro* digestion system the majority of experiments are conducted at 37°C which is the normal temperature of the human body. The conditions that vary considerably between *in vitro* experiments reported in literature include digestion and transit time, opting for an open or closed system, the type, source and amount of enzyme incorporated into the system and pH of the surrounding environment.

According to the review on *in vitro* human digestion models for food applications by Hur et al. (2011), a digestion of 2h was used most often in *in vitro* digestion experiments. However, Hur et al. (2011) also stressed the importance of customising parameters of the study to the food sample under investigation, especially if the aim was to closely mimic the human digestion system. For example, since it is well known lipids delay gastric emptying, the digestion time for lipid containing samples should be increased. As well as the food properties, the digestion time of foods is dependent on the individual in terms of factors such as age, sex, health status, mental state and the time of the day when the food is consumed and thus may also need to be taken into account (Hur et. al, 2011).

Open and closed systems for *in vitro* hydrolysis have both been reported in the literature. Open systems offer more convenience and provide information on the total amount of substrate being digested. Closed systems incorporate the use of semi permeable dialysis tubes. The enzyme and substrate is contained within the dialysis tubes that have ends sealed with clips and are submerged in a larger container of phosphate buffer or salt solution. The main consideration with the use of closed systems is the molecular weight cut off point of the tubes- these should be large enough to allow the end products of digestion to pass through but small enough so that the enzyme and subtrate cannot pass through. The concentration gradient from within the dialysis tube and dialysate can be measured which consequently provides information on the rate of diffusion. Since diffusion is a time dependent process, the total amount of subtrate being digested is calculated as the sum of the substrate digested within the tube and the dialysate at a specified point in time.

Many types of enzymes have been incorporated in the *in vitro* digestion models: pancreatin, pepsin, trypsin, chymotrypsin, peptidase, α-amylase and lipase (Hur et al., 2011). A mixture of enzymes present in the gastrointestinal tract are used to mimic the human gastrointestinal system while single enzymes are used to assess the digestibility of specific nutrients such as

pepsin for protein digestibility and amylase for starch digestibility. This thesis is concerned with the use of amylase to assess the digestibility of starch containing matrices and the general protocol of such experiments appears to have been widely reported and recognised in literature: Bravo et al. (1998); Evans & Thompson (2004); Koh et al.(2009); Weurding et al.(2001); Zhang et al.(1996). In terms of the source of the enzyme, enzymes of human and other animal origins have been used and currently there is not enough research to suggest use of either of them as more advantageous (Hur et al., 2011). The amount of enzyme is another important consideration as this will directly affect the enzyme activity. According to Boisen & Eggum (1991), an increase in starch intake *in vivo* corresponded to an increase in the secretion of starch degrading enzymes. If the aim is to more closely imitate the processes occurring *in vivo*, it has been suggested that an increase in the enzyme concentration should accompany the introduction of greater amounts of substrate whilst holding other parameters constant (Hur et al., 2011).

In vitro digestion may include the use of a phosphate buffer at a set pH or may use synthetic saliva (salt solutions) and gastric juices which are pH adjusted according to the GI compartments. The experimental design of the *in vitro* model with simulated compartments of the gastrointestinal tract concerned in this thesis are a modified and customised version previously published from Oomen et al., 2003 and Rabe et al., 2004. Within the mouth, stomach, duodenum, jejunum and ileum, the pH was adjusted to 6.5, 1.5, 6.4, 6.9 and 7.3 respectively. The standard error of the obtained results was calculated and error bars included appropriately in the representative graphs.

2.8 References

Boisen, S., & Eggum, B.O. (1991). Critical evaluation of *in vitro* methods for estimating digestibility in simple-stomach animals. *Nutrition Research Reviews, 4,* 141-162.

Bourne, M.C. (2002). *Food texture and Viscosity: concept and measurement* (pp. 107-128). New York: Academic Press.

Bravo, L., Siddhuraju, P., & Saura-Calixto, F. (1998). Effect of various processing methods on the *in vitro* starch digestibility and resistant starch content of Indian pulses. *Journal of Agricultural and Food Chemistry, 46,* 4667-4674.

Cakir, E., & Foegeding, E. A. (2011). Combining protein micro-phase separation and protein–polysaccharide segregative phase separation to produce gel structures. *Food Hydrocolloids, 25,* 1538–1546.

Chiu, M.H., & Prenner, E.J. (2011). Differential scanning calorimetry: an invaluable tool for a detailed thermodynamic characterisation of macromolecules and their interactions. *Journal of Pharmacy and Bioallied Sciences, 3,* 39-59.

Coleman, N. J., & Craig, D. Q. M. (1996). Modulated temperature differential scanning calorimetry: a novel approach to pharmaceutical thermal analysis. *International Journal of Pharmaceutics, 135,* 13-29.

Davis, S. (2005). Electron microscopy. In T. Cosgrove (Eds.), *Colloid science: Principles, methods and application*. Oxford: Blackwell Publishing Ltd.

Evans, A., & Thompson, D.B. (2004). Resistance to α-amylase digestion in four native high-amylose maize starches. *Cereal Chemistry, 81*, 31-37.

FEI. (2008). Electron microscopy [Booklet].

FEI.Quanta™ Scanning Electron Microscope. Retrieved 11 March 2012, <http://www.fei.com/products/scanning-electron-microscopes/quanta.aspx>

George, P. (2012). Thermal and high pressure effects on the structural properties of condensed dairy based systems, PhD thesis, RMIT University.

Gill, P. S., Sauerbrunn, S. R., & Reading, M. (1993). Modulated differential scanning calorimetry. *Journal of Thermal Analysis, 40*(3), 931-939.

Goldstein, J. I., Newbury, D. E., Echlin, P., Joy, D. C., Lyman, C. E., Lifshin, E., Sawyer, L., & Michael, J. R. (2003). Scanning electron microscopy and x-ray microanalysis (3rd ed.). New York: Springer.

Gomez- Estaca, J., Gomez-Guillen, M.C., Fernandez-Martin, F., & Montero, P. (2011). Effects of gelatin origin, bovine-hide and tuna-skin, on the properties of compound gelatin-chitosan films. *Food Hydrocolloids, 25,* 1461-1469.

Hermansson, A., & Svegmark, (1996). Developments in the understanding of starch functionality. *Trends in Food Science & Technology, 7*, 345-353.

Hou, Z., Zhang, M., Liu, B., Yan, Q., Yuan, F., Xu, D., & Gao, Y. (2012). Effect of chitosan molecular weight on the stability and rheological properties of β-carotene emulsions stabilized by soybean soluble polysaccharides. *Food Hydrocolloids, 26,* 205-211.

Huang, M., Kennedy, J. F., Li, B., Xu, X., & Xie, B. J. (2007). Characters of rice starch gel modified by gellan, carrageenan, and glucomannan: A texture profile analysis study. *Carbohydrate Polymers, 69*, 411–418.

Hur, S.J., Lim, B.O., Decker, E.A., & McClements, D.J. (2011). *In vitro* human digestion models for food applications. *Food Chemistry, 125*, 1-12.

Jones, R. (2002). Soft Condensed Matter. New York: Oxford University Press Inc.

Koh, L.W., Kasapis, S., Lim, K.M., & Foo, C.W. (2009). Structural enhancement leading to retardation of *in vitro* digestion of rice dough in the presence of alginate. *Food Hydrocolloids, 23*, 1458-1464.

Mathew, S., Brahmakumar, M., & Abraham, T.E. (2006). Microstructural imaging and characterization of the mechanical, chemical, thermal and swelling properties of starch-chitosan blend films. *Biopolymers, 82*, 176-187.

Noisuwan, A., Bronlund, J., Wilkinson, B., & Hemar, Y. (2008). Effect of milk protein products on the rheological and thermal (DSC) properties of normal rice starch and waxy rice starch. *Food Hydrocolloids, 22,* 174–183.

Oomen, A.G., Rompelberg, C.J.M., Bruil, M.A., Dobbe, C.J.G., Pereboom, D.P.K.H. & Sips, A.J.A.M (2003). Development of an *in vitro* digestion model for estimating the bioaccessibility of soil contaminants. *Archives of Environmental Contamination and Toxicology, 44,* 281-287.

Pons, M., & Fiszman, S. M. (1996). Instrumental texture profile analysis with particular reference to gelled systems. *Journal of Texture Studies, 27,* 597–624.

Rabe, S.,Krings,U., & Berger, R.G. (2004). *In vitro* study of the influence of physiological parameters on dynamic in- mouth flavor release from liquids. *Chemical Senses, 29,* 153-160.

Rabel, S. R., Jona, J. A. , & Maurin, M. B. (1999). Applications of modulated differential scanning calorimetry in performulation studies. *Journal of Pharmaceutical and Biomedical Analysis,* 21, 339-345.

Rao, M. A. (2007). *Rheology of Fluid and semi liquid foods: Principles and applications.* (2nd Ed.). New York: Springer.

Rao, M. A. (1999). Introduction. In M.A. Rao (Ed.), *Rheology of fluid and semisolid foods principles and applications* (pp. 1-24). Gaithersburg: Aspen Publishers.

Reading, M., Luget, A., & Wilson, R. (1994). Modulated differential scanning calorimetry. *Thermochimica Acta, 238,* 295-307.

Richardson, R.K & Kasapis, S. (1998) *Rheological methods in the characterisation of food biopolymers* in Instrumental methods in Food and Beverage analysis (pp. 1-48). Amsterdam: Elsevier.

Rosenthal, A. J. (1999). Relation between instrumental and sensory measures of food texture. In A. J. Rosenthal (Ed.), *Food Texture Measurement and Perception* (pp. 1-6). Maryland: Aspen publication.

Seib, P.A. (1994). Wheat starch: isolation, structure and properties. *Oyo Toshitsu Kagaku, 41,* 49-56.

Singh, N., Singh, J., Kaur, L., Sodhi, N.S., & Gill, B.S. (2003). Morphological, thermal and rheological properties of starches from different botanical sources. *Food Chemistry, 81,* 219-231.

Stading, M., Langton, M., & Hermansson, A.M. (1993). Microstructure and rheological behavior of particulate β-lactoglobulin gels. *Food Hydrocolloids, 7*, 195-212.

Stading, M., & Hermansson, A.M. (1990). Viscoelastic behavior of β-lactoglobulin gel structures. *Food Hydrocolloids, 4*, 121-135.

Sun, X.D., & Arntfield, S.D. (2010). Gelation properties of salt-extracted pea protein isolate induced by heat treatment: Effect of heating and cooling rate. *Food Chemistry, 124*, 1011-1016.

Surewicz, W.K. & Mantsch, H.H. (1988). New insight into protein secondary structure from resolution-enhanced infrared spectra. *Biochimica et Biophysica Acta, 952*, 115-130.

Texture Technologies Probes + Fixtures. Retrieved 15 May 2014, <http://www.texturetechnologies.com/texture-analysis/Probes-Fixtures.php>

Thermo Nicolet. (2001). Introduction to Fourier Transform Infrared Spectrometry. Retrieved 9 April 2012, <http://mmrc.caltech.edu/FTIR/FTIRintro.pdf>

van der Ven, C., Muresan, S., Gruppen, H., de Bont, D.B.A., Merck, K.B. & Voragen, A.G.J. (2002). FTIR spectra of whey and casein hydrolysates in relation to their functional properties. *Journal of Agricultural and Food Chemistry, 50,* 6943-6950.

Wang, Y. & Petrova, V. (2012). Scanning electron microscopy. In G. W. Padua & Q. Wang (Eds.), *Nanotechnology Research Methods for Foods and Bioproducts* (1st ed.). Iowa: John Wiley & Sons, Inc.

Weurding, R.E., Veldman, A., Veen, W.A.G., van der Aar, P.J., & Verstege, M.W.A. (2001). *In vitro* starch digestion correlates well with rate and extent of starch digestion in broiler chicken. *Journal of Nutrition, 131,* 2336-2342.

Yang, H., Irudayaraj, J., Otgonchimeg, S. & Walsh, M. (2004). Rheological study of starch and dairy ingredient-based food systems. *Food Chemistry, 86*, 571-578.

Zhang, Q., Abe, T., Takahashi, T., & Sasahara, T. (1996). Variations in *in vitro* starch digestion of glutinous rice flour. *Journal of Agricultural Food Chemistry, 44*, 2672-2674.

Chapter 3 - Phase behaviour and *in vitro* hydrolysis of wheat starch in mixture with whey protein

3.1 Abstract

Network formation of whey protein isolate (WPI) with increasing concentrations of native wheat starch (WS) has been examined. Small deformation dynamic oscillation in shear and modulated temperature differential scanning calorimetry enabled analysis of binary mixtures at the macro- and micromolecular level. Following heat induced gelation, textural hardness was measured by undertaking compression tests. Environmental scanning electron microscopy provided tangible information on network morphology of polymeric constituents. Experiments involving *in vitro* starch digestion also allowed for indirect assessment of phase topology in the binary mixture. The biochemical component of this work constitutes an attempt to utilise whey protein as a retardant to the enzymatic hydrolysis of starch in a model system with α-amylase enzyme. During heating, rheological profiles of binary mixtures exhibited dramatic increases in G' at temperatures more closely related to those observed for single whey protein rather than pure starch. Results from this multidisciplinary approach of analysis, utilising rheology, calorimetry and microscopy, argue for the occurrence of phase separation phenomena in the gelled systems. There is also evidence of whey protein forming the continuous phase with wheat starch being the discontinuous filler, an outcome that is explored in the *in vitro* study of the enzymatic hydrolysis of starch.

3.2 Introduction

In recent times, whey protein has become increasingly appreciated for its versatile functionality, superior nutritional value and significant bioactivity (Smithers, 2008). It is defined as the soluble proteins remaining in milk serum after coagulation of caseins at pH 4.6 and approximately 20 °C. The collective term mainly describes β-lactoglobulin, α-

lactalbumin and bovine serum albumin (Considine et al., 2011). Thermogelation of whey protein is an example of a functional property considered important in the food industry. This occurs by a two-step process. Firstly, proteins must surpass the critical temperature causing denaturation and partial unfolding of the globular structure. Provided that the polymer concentration is high enough, association of individual molecules subsequently follows and inevitably leads to formation of a continuous three-dimensional structure (Aguilera & Rojas, 1996).

Native wheat starch mainly consists of linear amylose and highly branched amylopectin in the ratio of 1:3, which are α(1–4) and α(1–4)/α(1–6) glucose molecules, respectively (Copeland,Blazek, Salman, & Tang, 2009). The granule has been processed for all sorts of functional utility, including thickening and pasting properties. Heating in the presence of water leads to swollen granules, disruption of amylopectin double helices and migration of amylose out into the surrounding medium (Huang, Kennedy, Li, Xu, & Xie, 2007). Most importantly, heating must occur at or above the gelatinisation temperature for the aforementioned events to occur. Upon cooling, amylose associates to form a gel, followed by aggregation (known as retrogradation) mainly due to the amylopectin component (Hermansson & Svegmark, 1996).

The complexity comes about when heating of whey protein occurs in the presence of other biopolymers in aqueous systems. Knowledge of the phase morphology in polymeric mixtures is essential, since this largely determines the techno- and biofunctionality of materials used as components of commercial products. In the presence of high levels of water molecules, serving the role of a good quality solvent, heating and subsequent cooling results in a mixed system of denatured protein and gelatinised starch. These may form interpenetrating, conformationally or electrostatically coupled, and phase separated networks, depending on physicochemical environment and concentration of the two polymers (Morris, 1986; Turgeon & Beaulieu, 2001).

Mixed preparations above the minimum critical gelling concentration, and provided no overriding drive to heterotypic binding prevails, form microphase separated networks with thermal treatment. It is then likely that one polymer will be the continuous phase, whereas the other one is contained in the form of discontinuous inclusions. In the case of globular proteins and native starch, heating followed by gelation reduces molecular mobility and the phase separated arrangement becomes permanently captured in the solid-like matrix. Phase

separation of protein and polysaccharide gels is an effective means of achieving the required structure and textural profile sought after in a wide variety of novel formulations that relate to replacement of gelatin, fat, sugar, etc. (Kasapis, 2008).

In this paper, work is carried out to establish whether whey protein and native wheat starch form phase separated networks under the current experimental protocol and, if so, to identify the structural morphology of the two polymeric networks alongside the phase topology of the binary mixture. This is also the first endeavour in using whey protein gels as a bioactive barrier to the enzymatic hydrolysis of starch in model *in vitro* studies.

3.3 Materials and methods

3.3.1 Materials

Native wheat starch (WS) was obtained from National Starch (National Starch and Chemical Co., Bangkok, Thailand), with the powder containing 94.1% starch, 0.3% ash, 0.1% fat and 5.5% moisture on a weight-per-weight basis. Whey protein isolate (WPI) was supplied from Fonterra Co-operative Group Ltd., New Zealand. The powder contained 88.71% protein, 0.93% fat, 4.83% moisture and 3.3% ash (w/w).

3.3.2 Methods

3.3.2.1 Sample preparation

Powders were dissolved in distilled water at ambient temperature and gently stirred prior to loading to prepare the following samples: 15% WS, 15% WPI, 15% WPI – 2.5% WS, 15% WPI – 5% WS, 15% WPI – 7.5% WS, 15% WPI – 10% WS, 15% WPI – 12.5% WS and 15% WPI – 15% WS. Where self-supported gels were required for compression testing and *in vitro* starch digestion, solutions were pipetted into 45 °C preheated aluminium moulds and placed into a heated water bath for 75 min. It was ensured that temperatures at the centre of the sample mass exceeded those required for the two polymers to undergo a phase transition within the first 15 min of cooking. The temperature remained at a constant 85 ± 1 °C for the remainder of the heating period.

3.3.2.2 Rheology

Low amplitude oscillatory measurements of storage modulus (G') and loss modulus (G'') were performed using a controlled strain AR-G2 rheometer with magnetic-trust bearing technology (TA Instruments, New Castle, DE). Experiments were conducted with a fixed strain of 0.1%, which is well within the linear viscoelastic region for both whey protein and wheat starch gels. The diameter of the parallel-plate measuring geometry was 40 mm and the gap distance 1 mm. Samples were loaded onto the Peltier plate and the peripheral was coated with silicon oil from BDH (50 cS) to minimise moisture loss. The entire experimental sequence utilised a scan rate of 2 °C/min whereby the system was first equilibrated at 25 °C. The solution was then heated to 85 °C, cooled from 85 to 5 °C, which was followed by a frequency sweep from 0.1 to 100 rad/s.

3.3.2.3 Modulated differential scanning calorimetry

Thermal behaviour was monitored on a Q2000 MDSC (TA Instruments, New Castle, DE). The instrument was calibrated with a traceable indium and sapphire standard. An empty pan was used as the reference. Hermetically sealed aluminium pans containing approximately 10mg of the sample were heated from 25 to 95°C and cooled from 95 to 5°C at a rate of 5°C/min. The rate of modulation was 0.53 °C for every 40 s.

3.3.2.4 Textural analysis

Gel hardness was determined by conducting single cycle compression tests on the TA-XT2 Texture Analyser (Stable Micro Systems, Godalming, UK). According to Pons and Fiszman (1996), forces registered from a probe diameter smaller than the sample diameter are often derived from puncture and shear. Thus, a 50- mm diameter cylindrical probe was chosen to compress the samples of equal diameter (50 mm) and 15 mm height. Deformation was set at 80%, on three replicates per sample, enabling fracture within the first compression cycle. The test speed was a relatively low 0.1 mm/s at ambient temperature. Textural analysis provides complimentary evidence to that of small deformation dynamic oscillation by imitating more closely the process of mastication.

3.3.2.5 Environmental scanning electron microscopy (ESEM)

Images were obtained to examine the gel microstructure and distribution of whey protein and wheat starch in single and binary preparations (FEI Quanta 200 ESEM, Hillsboro, OR). Samples were cut into cubes of about 5 × 5 × 2.5 mm whereby the internal sur- face of the original preparation was exposed to imaging. The work- ing distance, accelerating voltage, spot size and magnification were manipulated in order to obtain greater detail.

3.3.2.6 In vitro starch hydrolysis

For the enzymolysis section, semi-permeable dialysis tubes in a restricted system were the method of choice. Readings were taken from within the dialysis tube as well as the dialysate. The total amount of maltose equivalent liberated from the system was calculated as the sum of the two readings measured at any given time. Experimental protocol has been adapted from similar hydrolysis studies by Koh, Kasapis, Lim, and Foo (2009), and Jenkins et al., 1984). Fresh gels were cut into 2.4 mm diameter × 1 mm height discs. A total of 6 g of these discs was transferred into the dialysis tube (cut-off size 12–14 kDa) along with 30 ml of anhydrous monobasic sodium phosphate buffer (0.05 M) and 1 ml α-amylase (12,000 U). Currently, the use of enzymes from a human subject, as advantageous over other animal or plant sources, is inconclusive (Hur, Lim, Decker, & McClements, 2011). Therefore, the enzyme was purchased from Sigma–Aldrich (Castle Hill, Australia) being an extract of the filamentous fungus Aspergillus oryzae. Ends of the dialysis tube were sealed with clips and suspended in 800 ml of phosphate buffer.

All solutions with phosphate buffer used in this work were pH adjusted to 6.9 and preheated to 37 °C. The entire system was incubated in a constant 37 °C environment for up to 120 min. Gentle mixing occurred throughout hydrolysis. Levels of reducing sugar were estimated by taking aliquots from the dialysate and dialysis tube at constant time intervals of 30 min. Quantification was implemented colorimetrically using a 3,5-dinitrosalicylic acid (DNSA) assay. This method has previously been utilised by Koh et al. (2009) and is according to Bernfeld (1955). Specifically, upon heating to 100 °C, liberated reducing sugars from starch hydrolysis reacted with DNSA resulting in a newly coloured (reddish brown) compound (redox reaction). Absorbance was read at 540nm and data was calculated against a maltose standard curve.

3.4 Results and discussion

3.4.1 Network formation in single and co-gels of whey protein and wheat starch

The rheology experiments follow thermal transitions of the co- solutes in aqueous systems to quantify strength and physical properties. Heating profiles of the storage modulus for whey protein and wheat starch preparations under a controlled scan rate (1 °C/ min) are shown in Figure 3.1. A substantial increase in G' during heating from 25 to 85 °C, representative of phase transition, is observed. The gelatinisation of wheat starch (15% solids) in the absence of WPI begins at approximately 60 °C. A concentration of 15% (w/w) was also used in monitoring the thermal process of WPI in the absence of starch. This amount was chosen because it was above the minimum critical concentration required for thermogelation to take place. Similarly, Cakir and Foegeding, 2011 used 13% (w/v) WPI to ensure structural development in their heating experiment. The denaturation and gelation of the single 15% WPI system commences at higher temperatures of about 73–74 °C.

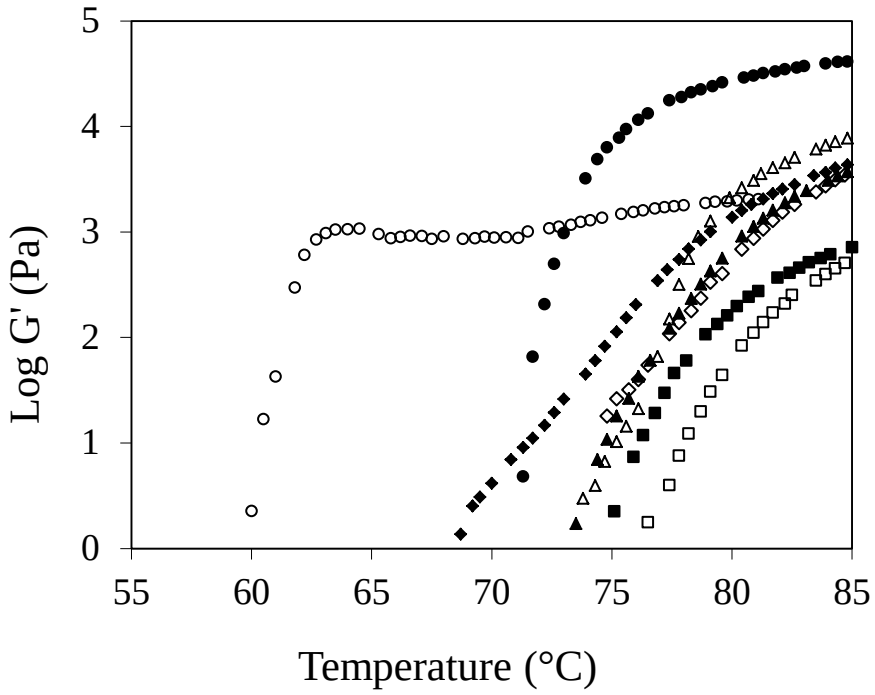

Figure 3.1 Heating profile of storage modulus for 15% whey protein with 0 (■), 2.5 (□), 5 (♦), 7.5 (◊), 10 (▲), 12.5 (Δ) and 15% wheat starch (●), and single wheat starch preparations at 15% solids (○) (scan rate: 2°C/min; frequency: 1rad/s; strain:1%).

For systems with WPI and addition of WS, gel formation occurs at higher temperatures likened to those observed in the pure WPI system. For example, the temperature at which 15% WPI with 2.5% WS transforms from solution to gel is, within variation of repeated experimental runs, similar to that recorded for the pure 15% WPI. At the highest concentration of starch addition, a sharp increase in G' occurs at roughly 70 °C. Thus the 15% WPI – 15% WS sample remains closer to the physical gelation temperature of the pure WPI than the single WS system.

The G' of pure starch increases rather slowly over the cooling period from 85 to 5 °C (results not shown here). Qualitatively, this is in agreement with the observations made by Yang, Irudayaraj, Otgonchimeg, and Walsh (2004). According to their experiments on pure wheat starch, gel strength increases as cooling progresses. Corn and rice starches were noted as showing a similar trend (Tsia, Li, & Lii, 1997; Yang et al., 2004). One reason that may reduce the extent of G' increase upon cooling is that while hydrogen bonds in the gel matrix increase, the contraction of the gel volume compensates for any visible increases in the storage modulus (Tsia et al., 1997; Yang et al., 2004). The final elastic modulus of the pure starch is much lower than the pure WPI and composite systems following identical cooling routines to 5 °C.

As the temperature decreases, WPI stores energy in the system, due to a final balance of hydrophilic and hydrophobic bonds contributing to structure formation. The mixtures also show gradual increases in G' similar to that observed in the pure WPI sample. For example, G' for the mixture with the least amount of starch (2.5%) is higher than the single WS system but comparable to that of the pure WPI system. At the end of the cooling regime there is a distinct difference in the G' value of the 15% WPI – 15% WS sample compared to single starch preparations. The 15% WPI - 15% WS sample holds the highest G' value of all samples examined.

Following the controlled cooling run, three-decade frequency sweeps were conducted at 5 °C in the vicinity of 0.1–100 rad/s (results not shown here). The G' and G'' of all samples exhibited minimal dependence over the increasing frequency rate for a given deformation within the linear viscoelastic region. There was no clear difference in the slopes of storage and loss modulus spectra as a function of frequency of oscillation for the various singles systems of WPI or WS and their binary mixtures.

Overall, no systematic changes in the cooling and frequency sweeps were observed following the heating procedure. In both the heating and cooling regime, the pattern of the binary system indicates that whey protein remains dominant in the overall properties of the macromolecular network. Since single thermal- transition peaks are observed in these mixtures, it is unlikely that whey protein and wheat starch formed bicontinuous networks. Instead, it is likely that micro-phase separated particulate structures were formed with heating. Given that single starch preparations form structures (gelatinise) earlier than the denaturation temperatures of whey protein upon heating (Figure 3.1), and the absence of an early wave of structure formation with starch parentage in composite gels, results argue that whey protein forms the suspending matrix through which starch is dispersed.

3.4.2 Differential scanning calorimetry

DSC studies were carried out to identify endothermic processes occurring over similar temperature regimes conducted in the mechanical studies. The analytical tool was therefore useful in pro- viding comparison and validation of thermal trends in physicochemical observations.

Figure 3.2 shows the DSC heating curves (5 °C/min) for single starch, whey protein and selected mixtures of the two polymers. Phase transition of the 15% WS occurred at the lowest temperature in comparison to 15% WPI and the blends. The sample showed a distinct single endothermic peak, which was relatively sharp. The on- set temperature of the WS was observed at approximately 54 °C. The peak at 60 °C coincides with the phase transition temperature measured in the rheological experiments of the preceding section. Furthermore, similar gelatinisation temperatures of wheat starch have been noted by various authors (Jane et al., 1999; Jenkins & Donald, 1998; Sasaki, Yasui, & Matsuki, 2000).

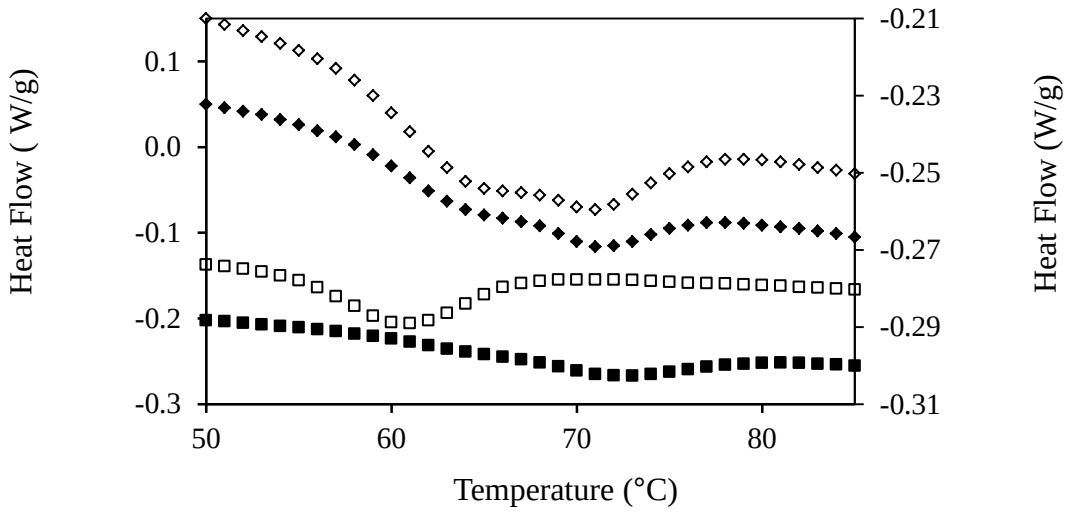

Figure 3.2 DSC endotherms for 15% whey protein (■), 15% wheat starch (□), 15% whey protein with 3% wheat starch (♦) and 15% whey protein with 6% wheat starch (◊) (scan rate: 5°C/min).

The onset and peak temperature observed from the 15% WPI sample occurred at about 67 and 72 °C, respectively. In comparison, 15% WPI has a broad denaturation peak which reflects a more gradual network development. As explained by Fitzsimons, Mulvihill, and Morris (2008), this may be due to masking of endothermic transitions by individual whey protein fractions, in particular that of α-lactalbumin followed by β-lactoglobulin. Aguilera and Rojas (1996) note that the denaturation temperature of α-lactalbumin is 61–61.5 °C, and for β-lactoglobulin and bovine serum albumin is 75.9–81.2 °C and 71.9–74 °C, respectively.

Noisuwan, Bronlund, Wilkinson, and Hemar (2008) investigated the thermal properties of milk proteins with normal and waxy rice starch. For their 10% pure WPI solution, the onset and peak temperatures recorded were 72 and 75°C, respectively. Similarly, Aguilera and Rojas (1996) measured the thermal transitions of whey protein and cassava starch. The onset and peak temperatures recorded for the single protein systems were 66 and 74.5°C, respectively. Results from the literature are in broad agreement with current experimentation, with some variability being expected, due to experimental protocol and source of materials. For example, Noisuwan et al. (2008) used a scan rate of 2 °C/min while in the current context the scan rate was set at 5 °C/min. Furthermore, Aguilera and Rojas (1996) note a pH of 5.75 for the pure WPI solution, whereas the pH of WPI solution in the present work is ~6.8. It is

known that pH and heating rate have an impact on re- corded whey protein denaturation temperature (Bernal & Jelen, 1985).

Onset and peak temperature of whey protein with wheat starch mixtures are congruent with those of the pure systems (Figure 3.2). For example, DSC peaks attributable to the two polymeric components are visible in the 15% WPI – 3% WS and 15% WPI – 6% WS samples. The observation proves that both solutes have undergone transition from solution to gel. Further, the absence of any other thermal event indicates that there are no direct physicochemical interactions between constituents in the mixture; for example, those of heterotypic junctions. There is a slight shift in the onset and peak temperatures attributable to WS gelatinisation. Kasapis and Al-Marhoobi (2005) conducted DSC experiments which also saw a shift in the peak attributed to 1.5% j-carageenan when mixed with 10% gelatin. Consequently, a potential explanation was sought from Van de Velde et al. (2005) who pinpointed such behaviour as an integral feature of phase separation phenomena, resulting in increased actual concentrations of the two components in the blend.

3.4.3 Hardness

Uniaxial compression tests were conducted and the hardness of WPI/WS gels recorded (Figure 3.3). The pure WPI system appeared opaque, which is a feature described by Turgeon and Beaulieu (2001), associated with the formation of a particulate as opposed to a fine stranded structure. Micro-phase separation is more likely to occur with a particulate rather than fine stranded WPI gel, which is the phase morphology argued for the binary mixture in this work. The maximum force encountered by the 15% WPI sample during the single-cycle compression was much greater than the translucent WS gel of the same concentration. Mixing WPI with 2.5– 7.5% (w/w) WS did not enhance gel strength, producing hardness values comparable to the single 15% WPI matrix. However, an associated increase in the large deformation properties can be seen with further addition of WS from 10% onwards.

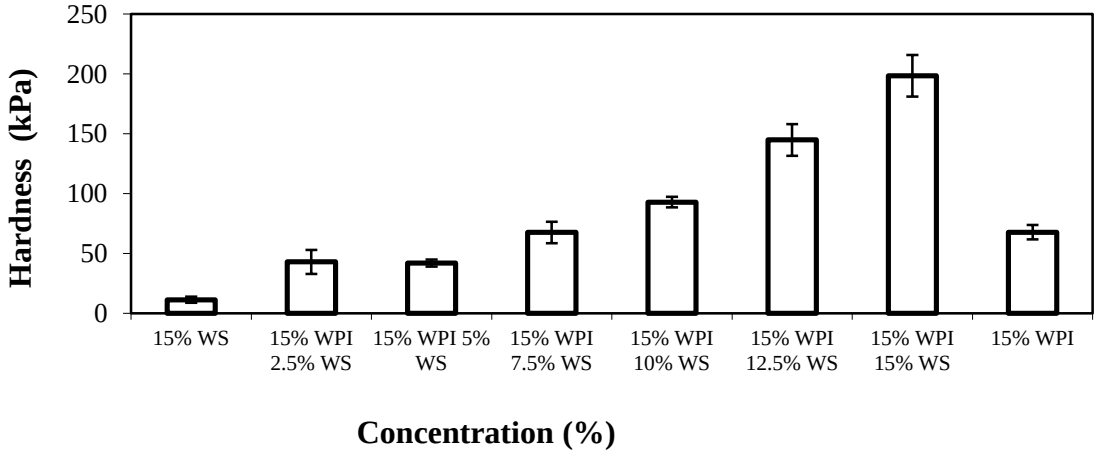

Figure 3.3 Measured hardness of whey protein and wheat starch gels at different concentrations using a compression rate of 0.1 mm/s.

The 15% WPI – 15% WS sample exhibits the greatest hardness, with its value being much higher than the sum of individual components. Mleko, Li-Chan, and Pikus (1997) also observed a synergistic effect in co-gels of WPI and j-carrageenan, arguing that this is the outcome of the protein forming a continuous phase. It appears, therefore, that binary mixtures at high levels of starch create phase separated systems where the overall level of water available in each polymeric phase decreases. This leads to an effective (final) whey protein concentration in its phase that is higher than the original amount added to the mixture (15%) leading to stronger networks, as seen from the values of hardness in Figure 3.3.

3.4.4 Microstructure

Microstructure imaging provides tangible evidence of phase morphology in polymeric mixtures. This valuable resource is utilised in the current context to monitor any changes in the distribution of whey protein and wheat starch as a function of composition.

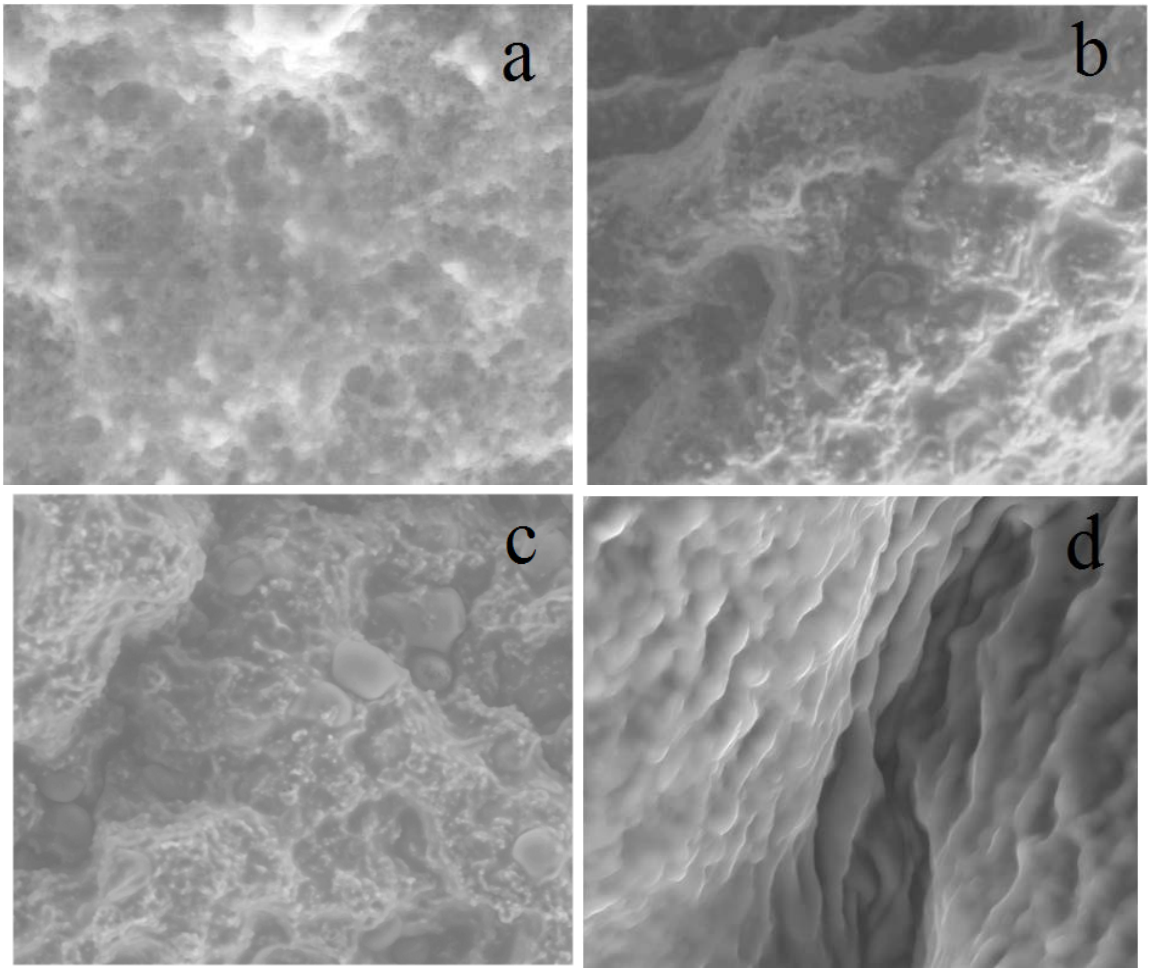

Figure 3.4 ESEM images for 15% whey protein (a), 15% whey protein with 5% wheat starch (b), 15% whey protein with 12.5% wheat starch (c), and 15% wheat starch (d).

The microstructure of WPI/WS gels are shown in Figure 3.4. WPI in the absence of starch formed aggregated and homogenous gels (Figure 3.4a). In contrast, WS in the absence of WPI (Figure 3.4d) forms regularly oriented and aggregated structures characteristic of a polymeric network following gelatinisation of the starch granule. Composite networks were highly compact and coherent, with changes in microstructure could be seen by increasing WS in the WPI base (Figure 3.4b and c). A greater amount of starch agglomerates are apparent in the 15% WPI – 12.5% WS than the 15% WPI – 5% WS sample. It is confirmed by eye that samples are not bulk phase separated, as opposed to the micro-phase separation images recorded presently. In particular, Figure 3.4c provides further support of segregative interactions and the tendency of “self-association” between like molecules. The image depicts intense clusters of starch aggregates distributed against a featureless backdrop of the continuous WPI matrix.

3.4.5 *In vitro* starch digestion

To date, there is a lack of agreement on a standard *in vitro* starch hydrolysis procedure (Germaine et al., 2008; Goni, Garcia-Alonso, & Saura-Calixto, 1997). Consequently, a restricted system was employed to mimic a simplified version of the human gastrointestinal tract, as opposed to an open system that does not include a semi- permeable membrane. Aliquots were taken from inside the dialysis tube and dialysate. The extent and rate of starch hydrolysis among whey protein and wheat starch gels of various concentrations was measured. Analysing the rate of hydrolysis of the polysaccharide in mixture with whey protein was particularly important since it is fundamental to the concept of glycaemic index.

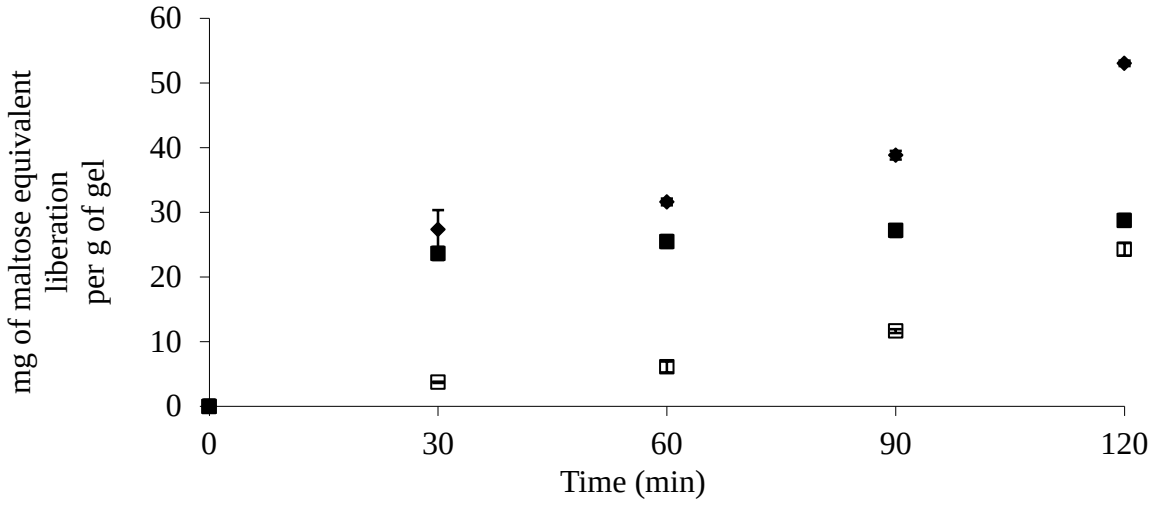

.

Figure 3.5 Amount of reducing sugars (maltose equivalent) liberated during *in vitro* α-amylase digestion of 15% whey protein and 7.5% wheat starch gel in dialysis tube (■), dialysate (□) and total (♦).

The focus of Figure 3.5 is on amylolysis of the 15% WPI – 7.5% WS gel over a period of 120 min of observation. During the first 30 min, a substantial increase of liberated maltose is observed within the dialysis tube. It appears, therefore, that enzyme-substrate activity is the highest during the initial period of sampling. Since diffusion is often a time-dependent process, such process may account for the comparatively lower levels of disaccharide equivalent detected in the dialysate. Extension of the timeframe to 120 min sees a plateau in

the level of liberated sugars from inside the dialysis tube and a gradual increase from the dialysate

This pattern is reflected in the rate of starch hydrolysis where there is an overall decrease from the 30 min mark and thereafter for the preparation of 15% WPI with 7.5% WS (Figure 3.6). Although a closed system has been employed, the end products of starch digestion may still impose on the activity of digestive enzymes to a considerable extent and thus provide an explanation of the examined trends (Singh, Dartois, & Kaur, 2010). Overall, there is an increase in the total amount of maltose equivalent liberated from the gel. At 120 min the total maltose liberated is 53.03 mg for each gram of the 15% WPI – 7.5% WS gel (Figure 3.5). This is in comparison to an average of 24.28 mg from the dialysate. Differences in the total and dialysate values were similarly observed in binary gels of other concentrations (results not shown here). The disparity serves to emphasise the existence and magnitude of a time lag accompanying the diffusion process, with the true total of maltose liberated from the system being the sum of the amounts within the dialysis tube and dialysate.

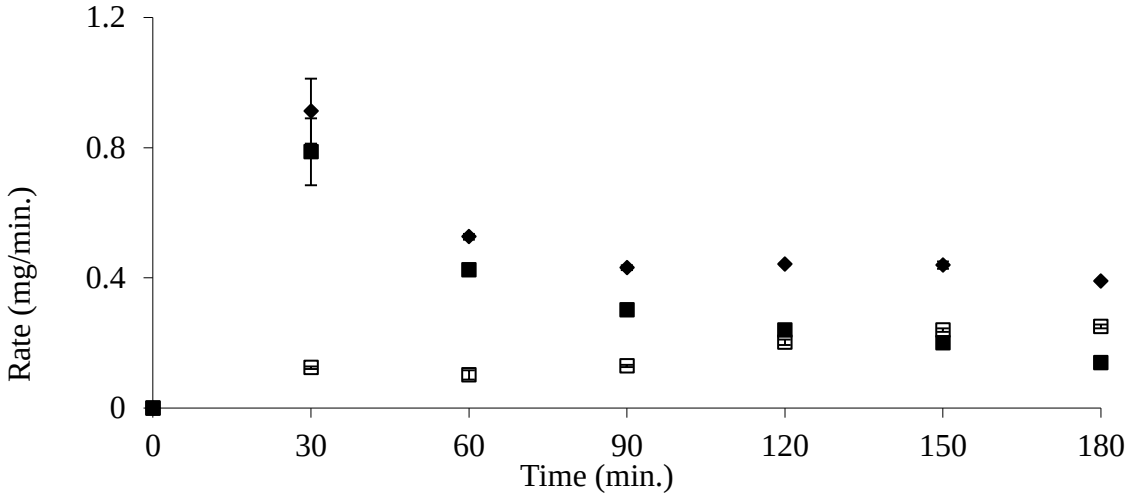

Figure 3.6 Rate of reducing sugars (maltose equivalent) liberated during *in vitro* α-amylase digestion of 15% whey protein and 7.5% wheat starch gel in dialysis tube (■), dialysate (□) and total (♦).

Total amount of sugars liberated from whey protein and wheat starch gels over various concentrations and timescales of observation are shown in Figure 3.7. As expected, liberation from the single WS sample was the highest and for the pure WPI gel, the lowest. The latter readings can serve as the sensitivity threshold of the present protocol of analysis. At all time

scales measured, the greater the addition of WS, the higher the total maltose liberated. This was also the case in regards to starch-hydrolysis rate recorded in Figure 3.8, where greater incorporation of WS results in more sugar being liberated per unit of time.

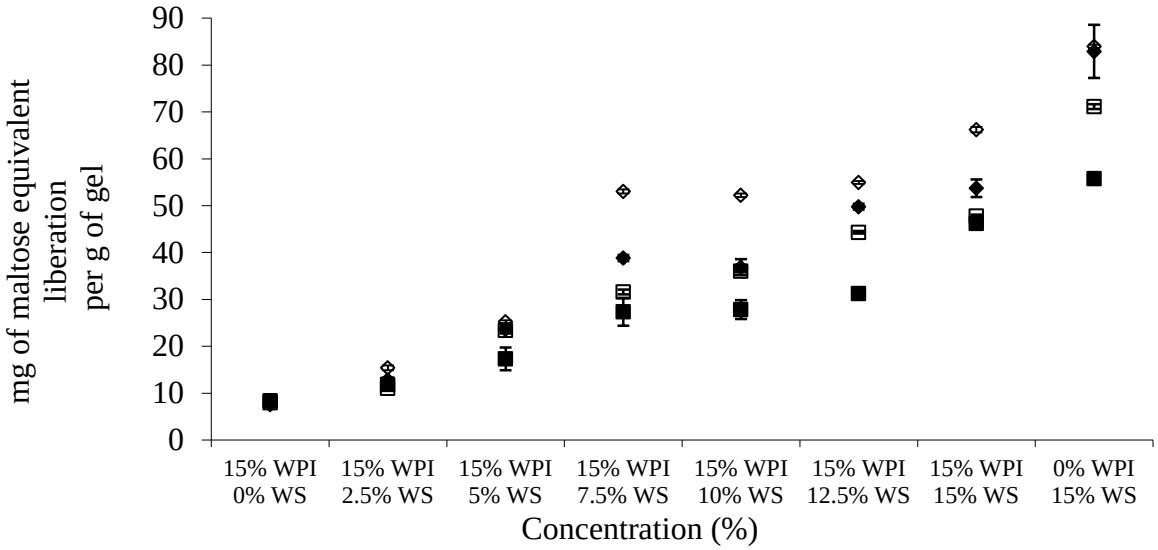

Figure 3.7 Total amount of reducing sugars (maltose equivalent) liberated during *in vitro* α-amylase digestion of whey protein and wheat starch gels at 30 (■), 60 (□), 90 (♦) and 120 (◊) min.

Specifically, 15.42 mg of maltose was detected at 120 min as compared to 12.83 mg at 90 min for the 15% WPI – 2.5% WS concentration in Figure 3.7. Similarly with the 15% WPI – 12.5% WS gel, where at 120 min, a higher amount of maltose was detected in comparison to the amount measured at 90min (54.9 and 49.78 mg, respectively). In contrast to the amount of starch hydrolysed, the rate of which it occurred decreased over time. For all WPI/WS combinations, the rate of hydrolysis at the 30 min mark was by far the highest in Figure 3.8. By 120 min, the rate of hydrolysis was reduced to half if not less than that measured at 30 min.

The presence of WPI has an effect on starch digestibility. For example, the amount of maltose yielded from each gram of 15% WPI – 15% WS sample at the end of the experiment was 66.23mg, which was lower than the pure WS form with a corresponding value of 84 mg (Figure 3.7). Regarding work in Figure 3.8, a reduced rate of starch hydrolysis is observed from the 15% WPI – 15% WS sample, as compared to the 15% pure WS gel. The presence of proteins can interfere with nutritional characteristics to pro- mote starch malabsorption

through disulfide-bonds and blocking of enzyme binding sites (Goni et al., 1997; Oates, 1997; Singh et al., 2010). As evident from the results in the previous sections, phase separation of WPI/WS gels appears to have occurred. Phase distribution whereby the continuous protein matrix is dispersed with discontinuous starch inclusions may also help to explain the difference in maltose liberated from the pure starch and WPI/WS gels.

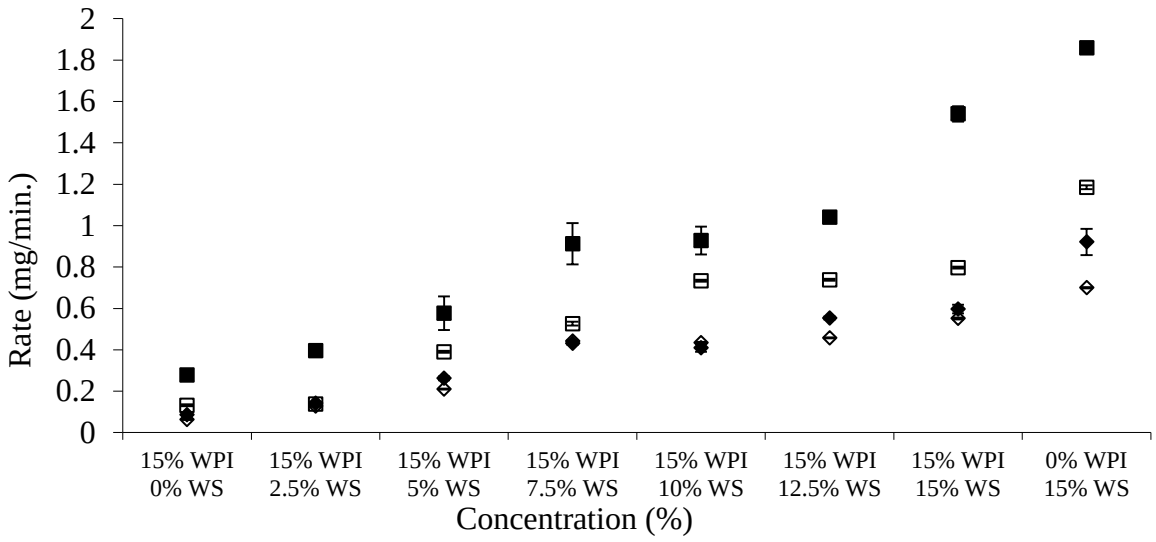

Figure 3.8 Rate of total amount of reducing sugars (maltose equivalent) liberated during *in vitro* α-amylase digestion of whey protein and wheat starch gels at 30 (■), 60 (□), 90 (♦) and 120 (◊) min.

While whey protein may serve to entrap starch, the effect is downplayed by the cutting of gels into smaller pieces during the preparation stage leading to an increased surface area and exposure for enzymatic attack. This was carried out in an effort to imitate the structure and mechanics of food upon consumption (Englyst, Englyst, Hudson, Cole, & Cummings, 1999). It has also been noted that minor levels of protein may be found within the polysaccharide inclusions in co-gels (Fitzsimons, Mulvihill, & Morris, 2008). A slower release of sugar into the dialysate could be likened to a reduced spike in blood sugar levels, with incorporation of WPI in a WS based system ultimately reducing the glycaemic index of this product.

3.5 Conclusions

The present study follows the thermal transformation of globular whey proteins and wheat starch from aqueous colloidal systems to self-supporting gels. Evidence of micro phase separation phenomena is imminent. For polymer concentration ratios examined, a continuous distribution of whey protein interspersed with discontinuous starch inclusions is proposed. This phase morphology shows *in vitro* reduction in α-amylase digestion of the polysaccharide in the presence of whey protein. There is also an associated fall in the rate of hydrolysis for these co-gels. Findings are therefore encouraging with respect to a reduction of glycaemic load in starch/whey protein based formulations. Results suggest further ventures in the manipulation of phase morphology *via* polymeric interactions and physicochemical environment. Future work will consider reinforcing the effect of WPI to retard starch hydrolysis. An enhanced *in vitro* digestion model mimicking the human gastrointestinal tract procedure will also be used to ascertain trends.

3.6 Acknowledgements

This research was fully supported under Australian Research Council's Linkage Projects funding scheme (Project number LP100200617).

3.7 References

Aguilera, J. M., & Rojas, E. (1996). Rheological, thermal and microstructural properties of whey protein–cassava starch gels. *Journal of Food Science*, 61, 962–966.

Bernfeld, P. (1955). Amylases, α and β. In S. P. Colowick & N. O. Kaplan (Eds.), *Methods in enzymology* (pp. 149–158). New York: Academic Press.

Bernal, V., & Jelen, P. (1985). Thermal stability of whey proteins – A calorimetric study. *Journal of Dairy Science*, 68, 2847–2852.

Cakir, E., & Foegeding, E. A. (2011). Combining protein micro-phase separation and protein–polysaccharide segregative phase separation to produce gel structures. *Food Hydrocolloids*, 25, 1538–1546.

Considine, T., Noisuwan, A., Hemar, Y., Wilkinson, B., Bronlund, J., & Kasapis, S. (2011). Rheological investigations of the interactions between starch and milk proteins in model dairy systems: A review. *Food Hydrocolloids*, 25, 2008–2017.

Copeland, L., Blazek, J., Salman, H., & Tang, M. C. (2009). Form and functionality of starch. *Food Hydrocolloids*, 23, 1527–1534.

Englyst, K. N., Englyst, H. N., Hudson, G. J., Cole, T. J., & Cummings, J. H. (1999). Rapidly available glucose in foods: An *in vitro* measurement that reflects the glycemic response. *The American Journal of Clinical Nutrition*, 69, 448–454.

Fitzsimons, S. M., Mulvihill, D. M., & Morris, E. R. (2008). Co-gels of whey protein isolate with crosslinked waxy maize starch: Analysis of solvent partition and phase structure by polymer blending laws. *Food Hydrocolloids*, 22, 468–484.

Germaine, K. A., Samman, S., Fryirs, C. G., Griffiths, P. J., Johnson, S. K., & Quail, K. J. (2008). Comparison of *in vitro* starch digestibility methods for predicting the glycaemic index of grain foods. *Journal of the Science of Food and Agriculture*, 88, 652–658.

Goni, I., Garcia-Alonso, A., & Saura-Calixto, F. (1997). A starch hydrolysis procedure to estimate glycemic index. *Nutrition Research*, 17, 427–437.

Hermansson, A., & Svegmark, K. (1996). Developments in the understanding of starch functionality. *Trends in Food Science & Technology*, 7, 345–353.

Huang, M., Kennedy, J. F., Li, B., Xu, X., & Xie, B. J. (2007). Characters of rice starch gel modified by gellan, carrageenan, and glucomannan: A texture profile analysis study. *Carbohydrate Polymers*, 69, 411–418.

Hur, S. J., Lim, B. O., Decker, E. A., & McClements, D. J. (2011). *In vitro* human digestion models for food applications. *Food Chemistry*, 125, 1–12.

Jane, J., Chen, Y. Y., Lee, L. F., McPherson, A. E., Wong, K. S., Radosavljevic, M., et al. (1999). Effects of amylopectin branch chain length and amylose content on the gelatinisation and pasting properties of starch. *Cereal Chemistry*, 76, 629–637.

Jenkins, D. J. A., Wolever, T. M. S., Thorne, M. J., Jenkins, A. L., Wong, G. S., Josse, R. G., et al. (1984). The relationship between glycemic response, digestibility, and factors influencing the dietary habits of diabetics. *The American Journal of Clinical Nutrion*, 40, 1175–1191.

Jenkins, P. J., & Donald, A. M. (1998). Gelatinisation of starch: A combined SAXS/ WAXS/DSC and SANS study. *Carbohydrate Research*, 308, 133–147.

Kasapis, S., & Al-Marhoobi, I. M. (2005). Bridging the divide between the high- and low-solid analyses in the gelatin/j-carrageenan mixture. *Biomacromolecules*, 6, 14–23.

Kasapis, S. (2008). Phase separation in biopolymer gels: A low- to high-solid exploration of structural morphology and functionality. *Critical Reviews in Food Science and Nutrition*, 48, 341–359.

Koh, L. W., Kasapis, S., Lim, K. M., & Foo, C. W. (2009). Structural enhancement leading to retardation of *in vitro* digestion of rice dough in the presence of alginate. *Food Hydrocolloids*, 23, 1458–1464.

Mleko, S., Li-Chan, E. C. Y., & Pikus, S. (1997). Interactions of j-carrageenan with whey proteins in gels formed at different pH. *Food Research International*, 30, 427–433.

Morris, V. J. (1986). Multicomponent gels. In G. O. Philips, D. J. Wedlock, & P. A. Williams (Eds.), *Gums and stabilisers for the food industry 3* (pp. 87–99). London: Elsevier.

Noisuwan, A., Bronlund, J., Wilkinson, B., & Hemar, Y. (2008). Effect of milk protein products on the rheological and thermal (DSC) properties of normal rice starch and waxy rice starch. *Food Hydrocolloids*, 22, 174–183.

Oates, C. G. (1997). Towards an understanding of starch granule structure and hydrolysis. *Trends in Food Science & Technology*, 8, 375–382.

Pons, M., & Fiszman, S. M. (1996). Instrumental texture profile analysis with particular reference to gelled systems. *Journal of Texture Studies*, 27, 597–624.

Sasaki, T., Yasui, T., & Matsuki, J. (2000). Effect of amylose content on gelatinisation, retrogradation and pasting properties of starches from waxy and non-waxy wheat and their F1 seeds. *Cereal Chemistry*, 77, 58–63.

Singh, J., Dartois, A., & Kaur, L. (2010). Starch digestibility in food matrix: A review. *Trends in Food Science & Technology*, 21, 168–180.

Smithers, G. W. (2008). Whey and whey proteins – from gutter-to-gold. *International Dairy Journal*, 18, 695–704.

Tsia, M. L., Li, C. F., & Lii, C. Y. (1997). Effects of granular structures on the pasting behaviours of starches. *Cereal Chemistry*, 74, 750–757.

Turgeon, S. L., & Beaulieu, M. (2001). Improvement and modification of whey protein gel texture using polysaccharides. *Food Hydrocolloids*, 15, 583–591.

Van de Velde, F., Antipova, A. S., Rollema, H. S., Burova, T. V., Grinberg, N. V., Pereira, L., et al. (2005). The structure of j/i-hybrid carrageenans II. Coil–helix transition as a function of chain composition. *Carbohydrate Research*, 340, 1113–1129.

Yang, H., Irudayaraj, J., Otgonchimeg, S., & Walsh, M. (2004). Rheological study of starch and dairy ingredient-based food systems. *Food Chemistry*, 86, 571–578.

Chapter 4 - Effect of calcium chloride on the structure and *in vitro* hydrolysis of heat induced whey protein and wheat starch composite gels

4.1 Abstract

The formation of heat induced whey protein isolate (WPI) and wheat starch (WS) gels in the presence of added calcium chloride (5-192mM) has been examined. Thermal properties, including the onset temperature of starch gelatinisation and protein denaturation, are defined by low amplitude oscillation on shear and modulated temperature differential scanning calorimetry. Upon heating and subsequent cooling, comparison of the storage modulus values bear information on the enhancement of protein aggregation by the electrolyte and the occurrence of phase separation phenomena between the two polymeric constituents in the mixture. Further confirmation of observed trends has been provided by measurements on textural hardness of gels in single cycle compression tests. Porous and aggregated microstructures are identified upon visual examination by environmental scanning electron microscopy. The gels were subjected to *in vitro* enzymatic hydrolysis and the role of calcium in reducing the extent of starch degradation by α-amylase has been established. It is evident from the results that ionic strength in the form of added calcium ions largely influences gelation kinetics of whey protein leading to significant variability in the hydrolytic potential of α-amylase on wheat starch.

4.2 Introduction

The superior nutritional value, granted GRAS status, and versatile functionality of whey proteins are a part of the appeal in utilizing the additive in many food formulations (Smithers, 2008). Manufacturers most commonly take advantage of its gelation mechanism and

emulsification properties to manipulate bulk and interfacial features thus affecting organoleptic properties in end products (Doi, 1993).

Effective incorporation of whey protein is achievable by developing products on a sound technological basis and could directly benefit consumers by providing a healthy alternative to a range of popular convenience foods (Hongsprabhas & Barbut, 1996). This is particularly important as it has been estimated that in excess of a million Australians have obesity and Type 2 diabetes, and about half of those are not aware that they have the condition (Health Insite, 2008). The current society is suffering from 'diseases of choice' where few seem inclined to change their nutritional habits. Food directly influences blood glucose concentrations and response. However, this response is influenced by many factors such as the food form (whole or ground), cooking and processing, particle size and structure.

Heat induced protein gelation primarily occurs *via* partial unfolding of the corpuscular molecule and exposure of non-polar and sulfhydryl groups (Lupano & Gonzalez, 1999; Matsudomi, Rector & Kinsella, 1991; Steventon, Gladden & Fryer, 1991; Verheul & Roefs, 1998). Aggregation subsequently follows, involving disulphide and non-covalent interactions, i.e. electrostatic and van der Waals forces, hydrogen and/or hydrophobic bonds (Britten & Giroux, 2001; Damodaran, Parkin & Fennema, 2008; Hoffman & Van Mil, 1997; Kinsella & Whitehead, 1989; Shimada & Cheftel, 1988; Verheul & Roefs, 1998). The characteristics of the heat set protein gel depends on a multitude of factors including heating rate, holding time and temperature, pH, ionic strength, mineral content and presence of other hydrocolloids forming a rather complex physicochemical environment (Barbut, 1995; Damodaran, Parkin & Fennema, 2008; Ju & Kilara, 1998; Kuhn, Cavallieri & Cunha, 2010; Mulvihill, Rector & Kinsella, 1990; Verheul & Roefs, 1998). Calcium salts are known to be especially effective at enhancing thermal stability and increasing protein aggregation (Kuhn, Cavallieri & Cunha, 2010).

Added calcium influences the degree of network formation through electrostatic shielding of the negatively charged molecules (Baumy & Brule, 1988). Furthermore, the divalent ion binds to the free carboxylic groups of aspartic and glutamic acids to form salt bridges that induce extensive cross-links. This type of behaviour has been of much interest in the structural properties and molecular demixing phenomena of globular protein-polysaccharide mixtures (Kinekawa, Fuyuki & Kitabatake, 1998). Several developments of this have now emerged, and mixtures of whey protein with hydrolysed starch or dietary fibre have been

engineered in an attempt to create novel product concepts for weight management and pleasant mouthfeel (Yang, Liu, Ashton, Gorczyca & Kasapis, 2013). Due to thermodynamic incompatibility, heated mixtures of protein with polysaccharides, above ~4% total solids in preparations, result in phase separated networks, and texture can be manipulated based on the polymeric constituent that forms the continuous matrix in the gel (Damodaran, Parkin & Fennema, 2008).

The present investigation is a fundamental study on the effect of added calcium chloride to heat induced whey protein and wheat starch composite gels. The main focus is on the role of calcium as a potential enhancer of structural behaviour in whey protein against the enzymatic degradation of starch in mixtures. The work is based on the hypothesis that understanding the molecular aspects of segregative phase separation between proteins and polysaccharides allows the manipulation of phase behaviour that in turn controls textural profile and sugar release in food materials.

4.3 Materials and methods

4.3.1 Materials

Native wheat starch was obtained from National Starch and Chemical Co., Bangkok, Thailand, with the powder containing 94.1% starch, 0.3% ash, 0.1% fat and 5.5% moisture on a weight-per-weight basis. Whey protein isolate was supplied by Fonterra Co-operative Group Ltd., Palmerston North, New Zealand. The powder contained 88.71% protein, 0.93% fat, 4.83% moisture and 3.3% ash (w/w). Calcium chloride dehydrate was AnalaR grade and was purchased by Sigma Chemicals, Castle Hill, Australia.

4.3.2 Methods

4.3.2.1 Sample preparation

Calcium chloride solutions of 5 to 192mM were added to single and mixed dispersions of whey protein and wheat starch. These preparations were as follows (% w/v): 3WS, 6WS, 9WS, 12WS, 15WS, 15WPI, 15WPI – 3WS, 15WPI – 6WS, 15WPI – 9WS, 15 WPI – 12WS and 15WPI-15 WS. Since incubation time can significantly influence protein aggregation and subsequent gel microstructure, powders were dissolved, gently stirred and then immediately

used for experimentation (Ju & Kilara, 1998). The above was the preparation of samples used for rheology experiments. For the preparation of samples for texture analysis, microscopy and *in vitro* hydrolysis, gels were prepared by pipetting solutions into 45°C preheated aluminium moulds that were placed into a heated waterbath for 75 min. The temperature for the gelatinisation of wheat starch and denaturation of whey protein begins at ~60°C and ~73°C respectively (Yang, Liu, Ashton, Gorczyca & Kasapis, 2013). The temperature at the centre of each sample was set to exceed that required for starch and protein to undergo phase transition (~60°C and ~73°C respectively) within the first 15 min, after which a constant temperature of 85±1°C was maintained for the remainder of the heating period.

4.3.2.2 Rheology

Small deformation dynamic oscillation measurements of elastic modulus (G') and viscous modulus (G'') were performed on shear using a controlled strain AR-G2 rheometer with magnetic-trust bearing technology (TA Instruments, New Castle, DE). Experiments were conducted with a fixed strain of 0.1%, which is well within the linear viscoelastic region of single and mixed preparations of these materials. Parallel-plate measuring geometry was 40 mm in diameter with a gap of 1 mm. Samples were loaded onto the Peltier plate and covered with silicon oil from BDH (50 cS) to minimise evaporation. The entire experimental sequence utilised a scan rate of 2°C/min, for which the system was first equilibrated at 25°C for 2 min. The solution was then heated to 85°C, cooled from 85 to 5°C, followed by a frequency sweep from 0.1 to 100 rad/s.

4.3.2.3 Modulated differential scanning calorimetry

The thermal pattern was monitored on a Q2000 MDSC (TA Instruments, New Castle, DE) calibrated with a traceable indium and sapphire standard. An empty pan was used as the reference. Hermetically sealed aluminium pans containing 10 ±1 mg of the sample were heated from 25 to 95°C and cooled from 95 to 5°C at a rate of 5°C/min. The rate of modulation was 0.53°C for every 40 seconds. The instrument interfaced a refrigerated cooling unit to achieve temperatures down to 0°C and a nitrogen purge cell with a flow rate of 25 mL/min.

4.3.2.4 Textural analysis

Single cycle compression tests using the TA-XT2 Texture Analyser (Stable Micro Systems, Surrey, England) were performed to determine gel hardness. According to Pons & Fiszman (1996), forces registered from a probe diameter smaller than the sample diameter are often derived from puncture and shear. Thus, a 50 mm diameter cylindrical probe was chosen to compress the samples of equal diameter (50 mm) and 15 mm height. Deformation was set at 80% enabling fracture within the first compression cycle. The compression rate employed throughout the experimentation was 0.1 mm/s at ambient temperature. Data was collected in triplicate for each WPI-WS-$CaCl_2$ combination tested and the results presented are an average ± S.E. of n=3.

4.3.2.5 Environmental scanning electron calorimetry

Micrographs were taken to examine the microstructure of single and binary mixtures of whey protein and wheat starch with varying levels of added $CaCl_2$ using an ESEM system (Fei Quanta 200, Hillsboro, Oregon, USA). Samples were cut into cubes of about 5 x 5 x 2.5 mm dimension whereby the internal surface of the original preparation was exposed to imaging. Observing the microstructure of these high moisture gels requires exposure to a gaseous secondary electron detector (GSED) at an accelerating voltage of 20 kV and pressure of 5.75 torr.

4.3.2.6 In vitro starch hydrolysis

Enzymolysis was conducted with a closed system utilizing semi permeable dialysis tubes (MW cut off 12-14 kDa). Aliquots were taken within the dialysis tube as well as the dialysate for reading at the end of the 180 min length digestion. Total sugar reduction was calculated as the sum of the two readings measured. The experimental procedure has been adapted from hydrolysis studies by Koh, Kasapis, Lim, & Foo (2009) and Jenkins et al. (1984). In further detail, freshly prepared gels were cut into 2.4 mm diameter x 1 mm height discs. A total of 6g of these discs were transferred into the dialysis tube along with anhydrous monobasic sodium phosphate buffer (30 mL, 0.05 M) and 1 mL α-amylase (12000 U). The enzyme utilised in this experiment was an extract from porcine pancreas, purchased from Sigma-Aldrich (Castle Hill, Australia).

The dialysis tube ends were sealed with clips and suspended in 800 ml of sodium phosphate buffer (0.05 M). All phosphate buffer utilised within the experiment was adjusted to pH 6.9 and preheated to 37°C. Incubated samples were subject to gentle agitation and a 37± 1°C thermal environment. Reduced sugars were quantified colorimetrically using the 3, 5-dinitrosalicylic acid (DNSA) assay. This method has previously been utilised by Koh, Kasapis, Lim, & Foo (2009) and Bernfeld (1955). Upon heating to 100°C for 5 min, liberated reducing sugars react with DNSA resulting in a newly colored (reddish brown) compound (redox reaction). Absorbance was read at 540 nm and data was calculated against a maltose standard curve producing reducing sugars in maltose equivalents. After summing the data from the dialysis tube and the dialysate, the results were presented are an average ± S.E. of n=3.

4.4 Results and discussion

4.4.1 Rheological characterisation of single and mixed wheat starch and whey protein systems

During heating the two hydrocolloids undergo a first order thermodynamic transition. Starch gelatinisation begins with the swelling of B-type and A-type granules and migration of amylose out of the granule to form a continuous phase (Hermansson & Svegmark, 1996; Singh, Singh, Kaur, Sodhi & Gill, 2003). In the case of whey proteins, hydrophobic regions and sulfhydryl groups are exposed, and a network is consequently formed through covalent and non-covalent interactions (Bottomley, Evans, & Parkinson, 1990; Bryant & McClements, 1998; Kuhn, Cavallieri, & Cunha, 2010).

As indicated in Table 4.1, a positive storage modulus could not be measured by the end of the cooling regime (following heating) for an aqueous starch solution of 3% (w/v) solids, with the gel strength being negligible. It is well known that a concentration threshold exists in the gelation of polymers and the WS solution with total solids of 3% appears to fall below this level (Ferry, 1948; Ring, 1985). Gel strength of this preparation, however, becomes measurable with addition of $CaCl_2$. For higher concentrations of starch, significant increases in storage modulus could be monitored (Figure 4.1a). The onset temperature of phase transition during heating for 15% starch with 30 and 64mM $CaCl_2$ occurs at about 67 and

73°C respectively (Figure 4.1a). Tester and Sommerville (2000) record wheat starch gelatinisation temperatures of 61°C but note that this depends on starch to water ratio.

Table 4.1. Rheology of whey protein and wheat starch systems in the presence of calcium chloride.

Calcium chloride (mM)	0		30		64		120	
	Log G' cooling endpoint	δ°	Log G' cooling endpoint	δ°	Log G' cooling endpoint	δ°	Log G' cooling endpoint	δ°
3 WS	NA	53.47	1.44	2.86	1.33	3.43	1.25	9.65
6 WS	1.56	14.57	1.19	4.00	2.59	2.29	3.16	3.43
9 WS	3.35	1.15	3.17	0.57	3.44	1.72	3.78	2.29
12 WS	3.79	1.15	3.83	1.72	3.78	1.72	3.88	2.29
15 WS	3.66	3.43	3.77	1.15	3.81	4.57	4.19	1.15
15 WPI	4.65	9.65	4.41	10.76	3.91	12.95	4.55	17.74
15 WPI 3 WS	4.44	9.65	4.28	9.65	4.59	10.20	4.81	14.04
15 WPI 6 WS	4.81	9.09	4.91	9.65	4.93	10.76	5.02	13.50
15 WPI 9 WS	4.99	9.09	5.21	10.76	5.00	10.76	5.24	14.04
15 WPI 12 WS	5.24	9.09	5.47	10.20	5.60	9.65	5.35	12.41
15 WPI 15 WS	5.45	9.09	6.00	10.20	5.43	11.31	5.53	13.50

NA – values too low to measure

Previous authors have also noted the significant impact salts may have on the thermal properties of starch systems (Ahmad & Williams, 1999; Ciacco & Fernandes, 1979; Damodaran, Parkin & Fennema, 2008; Jane, 1993; Katsuta, 1998; Russell & Oliver 1989). In the case of sago starch, 6% (w/v) preparations exhibited increase in gel strength with added calcium chloride. The outcome was thought to arise from a positive drive related to $CaCl_2$ interactions with water molecules (Riou, Havea, McCarthy, Watkinson & Singh, 2001) and a negative contribution due to $CaCl_2$ interactions with starch hydroxyl groups (Ahmad & Williams, 1999). The latter results in the formation of starch-ion complexes that promotes the gelation process of associating linear chains of amylose. The maximum log G' values at the cooling endpoint for single WS systems in the present work (6 % to 15% WS) are associated with those containing 120mM $CaCl_2$ (Table 4.1).

Figure 4.1a also reproduces an upward slope in the traces of the elastic modulus for 15% WPI at 30 and 64 mM $CaCl_2$, which occurs at ~63°C and is in line with experience (Kuhn, Cavallieri & Cunha, 2010; Ramasubramanian, D'Arcy & Deeth, 2012). Literature reports greater aggregation of β-lactoglobulin in the presence of $CaCl_2$ (Pappas & Rothwell, 1991).

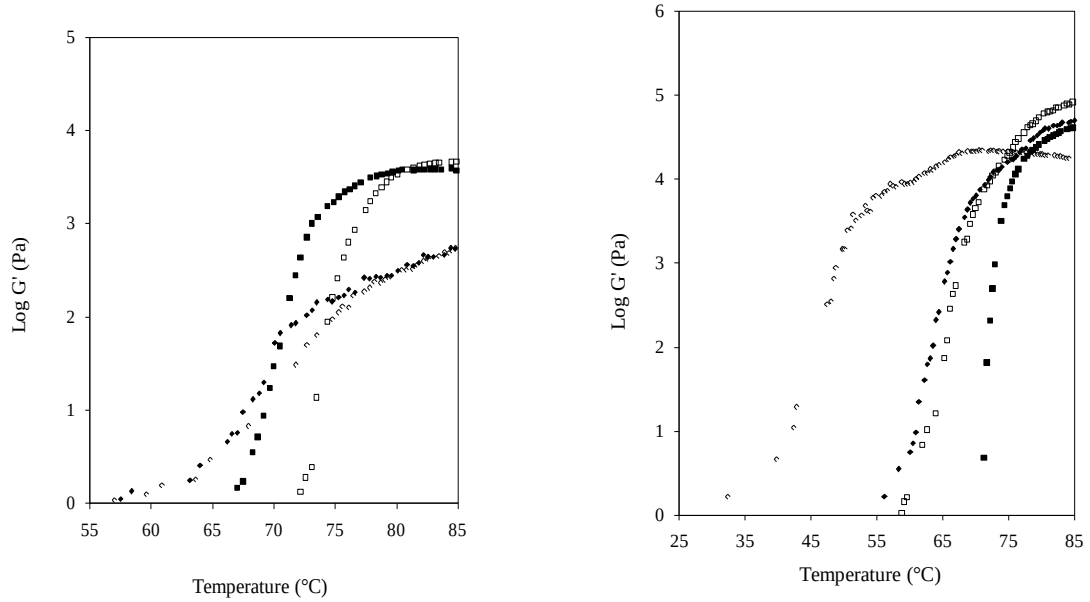

(a) (b)

Figure 4.1 (a) Heating profile of storage modulus for 15% wheat starch with 30mM (■), 64mM (□) and 15% whey protein with 30mM (♦), 64mM (◊) of calcium chloride, and (b) heating profile of storage modulus for 15% whey protein plus 15% wheat starch mixtures with 0mM (■), 30mM (□), 64mM (♦), 120mM (◊) of calcium chloride (scan rate: 2°C/min; frequency: 1rad/s; strain:1%).

In the present study an earlier temperature at which a significant increase in the 15% WPI storage modulus was observed with increasing $CaCl_2$ addition (data not shown). That is, phase transition temperature monitored for 15% WPI samples with 0, 30, 64 and 120mM $CaCl_2$ was ~73°C, 63°C, 63°C and 53°C, respectively. While there was an insignificant difference in the temperature detected for phase transition between 30 and 64mM $CaCl_2$ addition, the overall trend suggests the presence of an aggregated protein network occurring at earlier temperatures due to the increased availability of the salt to form intermolecular calcium cross-bridges (Jeyarajah & Allen, 1994).

At the end of the heating period, storage modulus of 15% WS systems is higher than the WPI counterparts in Figure 4.1a. During cooling the G' of WS continues to increase but the result of hydrogen bonding is partially offset by the contraction of the gel volume (Tsia, Li & Lii, 1997; Yang, Irudayaraj, Otgonchimeg & Walsh, 2004). The storage modulus which gives an indication of gel strength also continues to rise during the cooling phase of examined protein

samples and the trend appears to be more obvious. During cooling there is further development of the gel structure by non-covalent interactions, between denatured protein molecules (Harrington, Foegeding, Mulvihill & Morris, 2009). Besides hydrophobic interactions and hydrogen bonding, disulfide bonds may also be forming intramolecularly. This is according to Sun & Arntfield (2011) who noted that globular protein networks are still forming when a fast cooling rate is applied i.e. (2°C/min). According to George, Lundin & Kasapis (2013), the 15% WPI randomly aggregates to form a network depicted as clusters. In fact, storage modulus values for whey protein measured at the end of cooling were greater than that for starch at every level of added $CaCl_2$ (Table 4.1).

Storage modulus at the cooling endpoint of mixed WPI-WS systems rises as the total concentration of WS increases from 3% to 15% as shown in Table 4.1. The increase in gel strength can be explained by an increased local concentration of WPI with the increasing addition of WS in the phase separated gel (Cakir & Foegeding, 2011; Yang, Liu, Ashton, Gorczyca & Kasapis, 2013). This observation is also generally observed with added calcium. For example at the end of the cooling period, mixtures with 120mM $CaCl_2$ correspond to a high gel strength (log G' 5.53), when compared to single starch (log G' 4.19) and whey protein (log G' 4.55) gels. In Figure 4.1b, the storage modulus of 15% WPI 15% WS at various levels of added $CaCl_2$ during heating to 85°C is shown. The trend observed with single WPI, is also seen with the 15% WPI 15% WS system – that is, there is a decrease in the temperature at which an aggregated network is formed with increasing addition of $CaCl_2$ (Figure 4.1b). While the values of the storage modulus at the end of this heating stage remain below log G' 5.0, at the cooling endpoint in Table 4.1, corresponding values range from log G' 5.43 to 6.0 indicating modulus development patterns in the mixture as for the single protein systems. Since WPI has shown to dominate in the overall properties of the mixed WPI-WS gel, it is an indication that WPI forms the continuous phase.

4.4.2 Thermal analysis of wheat starch and whey protein preparations

The starch and protein DSC endotherms are reproduced in Figures 4.2(a-b). There is a shift in the gelatinisation temperatures of 15% starch in the presence of $CaCl_2$ from 69°C to 72°C that has been reported earlier (Biliaderis, 1990), but not for 15% whey protein at these levels of polyelectrolyte (30 and 64 mM). In the case of mixtures with a total level of solids of 30%, phase changes occur early (67°C) in comparison to when 30 and 64mM $CaCl_2$ have been

incorporated (about 72°C in Figure 4.2b). Results are summarised in Table 4.2, where peak gelatinisation temperatures of 3 to 15% starch occur between 60°C and 72°C and the peak denaturation temperatures for whey protein occur between 67.5°C and 74.3°C with calcium chloride addition. The variation in gelatinisation temperature can be explained by the impact of different concentrations of WS and $CaCl_2$ present in the system. As noted by Biliaderis, Maurice & Vose (1980), the ratio of starch to water influences the endothermic transition. Furthermore, the interactions of cations with the –OH groups of starch generate heat which enables destabilisation of starch granules and a consequential decrease in the gelatinisation temperature (Ahmad & Williams, 1999). On the other hand, calcium has strong electrostatic interactions with water molecules which increases the viscosity of the salt solution (Jane, 1993). The increased viscosity of the salt solution impedes the rate of diffusion into the starch granule and consequently increases the energy required for gelatinisation to take place (Jane, 1993). Similarly for proteins, it is well known that varying concentration will influence the extent of protein-protein and protein-solvent interactions and thus affect the thermal stability of the macromolecule (Totosaus, Montejano, Salazar & Guerrero, 2002). In the experiments conducted by Glibowski, Mleko & Wesolowska-Trojanowska (2006), the concentration of $CaCl_2$ incorporated into WPI solutions provided marked differences in the occurrence of a phase transition during heat treatment.

In mixed systems without calcium ions, two distinct peaks are observed in dispersions with 3 to 9% WS, with the first peak centering at 65°C and the second peak appearing at about 71°C (Table 4.2). It is reasonable to assume that peaks reflect starch gelatinisation followed by protein denaturation. The observed shift in peak gelatinisation temperatures is believed to be due the presence of WPI occupying a share of the total water volume. Consequently, a reduction of water is available for starch gelatinisation thus delaying the process as indicated by a higher phase transition temperature. Two separate DSC peaks were also observed by Lupano & Gonzalez (1999) in whey protein with cassava starch and it was stated that the availability of water is a key influence in gelatinisation (Damodaran, Parkin & Fennema, 2008). The present results point to the absence of associative interactions between WPI and WS as independent thermal transitions and the absence of any new thermal events were recorded in DSC heating scans. At higher starch concentrations (12 to 15%) in the absence of calcium ions and in the remaining mixtures with the electrolyte, systems did not display two thermal events, since the gelatinisation process becomes progressively masked by protein denaturation.

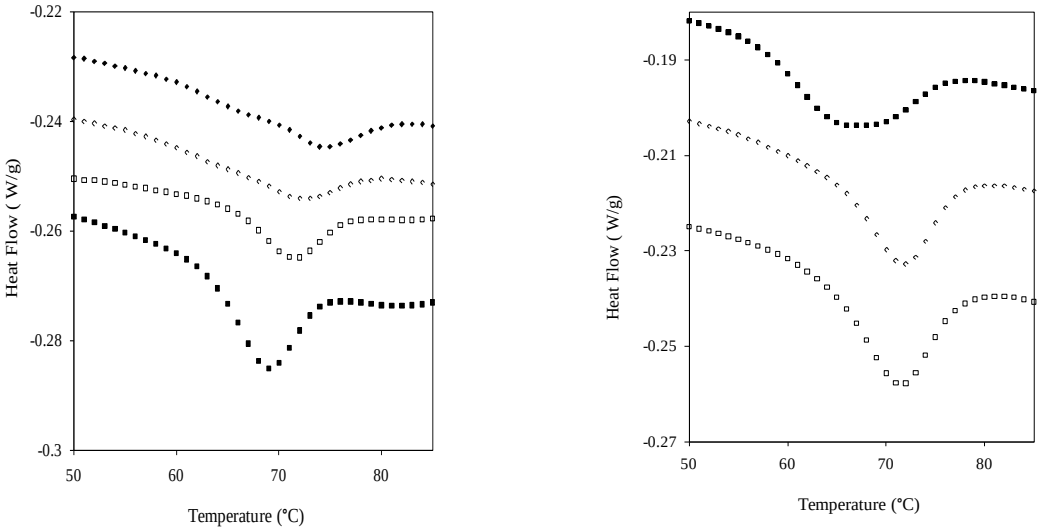

(a) (b)

Figure 4.2 (a) DSC endotherms for 15% wheat starch with 30mM (■), 64mM (□) and 15% whey protein with 30mM (♦), 64mM (◊)of calcium chloride, and (b) DSC endotherms for 15% whey protein plus 15% wheat starch with 0mM (■), 30mM (□), 64mM (◊) of calcium chloride (scan rate: 5°C/min).

Table 4.2 DSC peak temperatures (T_{peak}) of whey protein and wheat starch systems in the presence of calcium chloride.

Calcium chloride (mM)	**0**	**30**	**64**	**120**
	T_{peak} (°C)	T_{peak} (°C)	T_{peak} (°C)	T_{peak} (°C)
3 WS	61.5	68.5	71.5	71.0
6 WS	60.5	69.0	71.0	69.0
9 WS	61.0	69.0	71.0	67.5
12 WS	60.5	69.0	71.0	69.0
15 WS	60.0	69.0	72.0	67.5
15 WPI	72.0	74.3	72.5	67.5
15 WPI 3 WS	65, 71	72.5	73.0	67.0
15 WPI 6 WS	65,71	72.0	72.0	66.5
15 WPI 9 WS	65,70	72.0	72.0	66.0
15 WPI 12 WS	67.5	71.0	72.0	65.0
15 WPI 15 WS	67.0	72.0	71.5	64.0

4.4.3 Large deformation properties of wheat starch and whey protein gels

Figure 4.3 provides a snapshot of the variability in the values of hardness measured for 15% WPI 6% WS, and 15% WPI 12% WS gels in the absence and presence of added $CaCl_2$. As evident, the 15% WPI 12% WS gel presented greater hardness than the 15% WPI 6% WS gel. This remained consistent when comparisons were made at 30, 64 and 120mM addition of $CaCl_2$ (Figure 4.3). For example, the 15% WPI 12% WS 120mM $CaCl_2$ gel is significantly harder than the 15% WPI 6% WS 120mM $CaCl_2$ gel (Figure 4.3). This observation as a function of total solids was previously argued for in the rheology work and provides further evidence of a protein continuous, starch discontinuous phase separated gel.

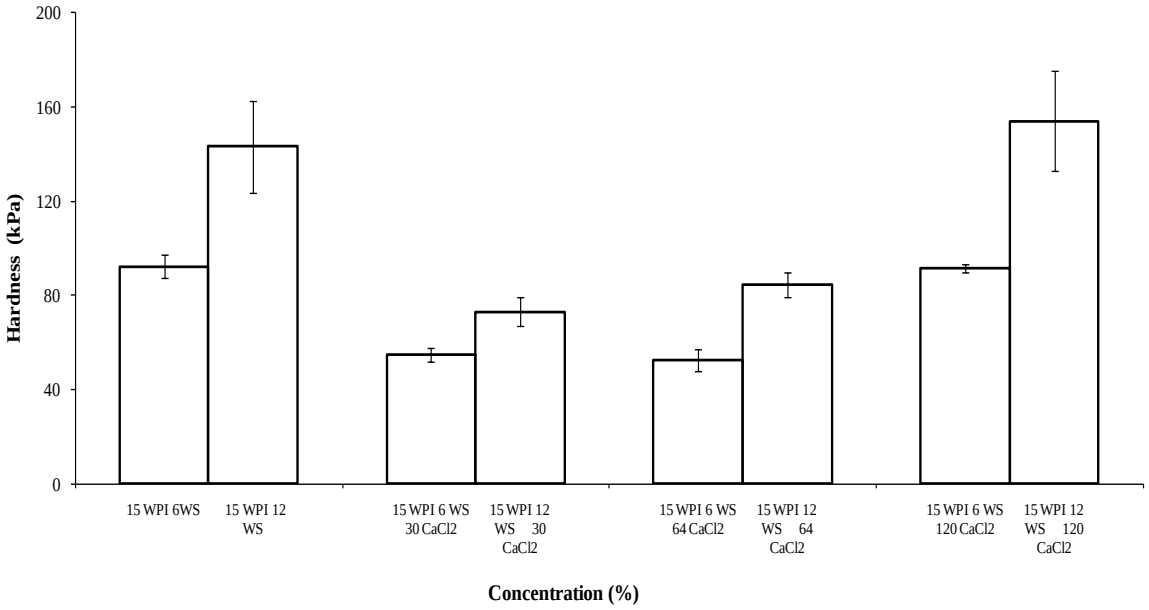

Figure 4.3 Compressive hardness for gels of 15% whey protein with 6% wheat starch, and 15% whey protein with 12% wheat starch at various levels of calcium chloride addition (compression rate: 0.1 mm/s).

An initial drop followed by a recovery in hardness measurements was observed for both systems, with the hardest gel being at 120 mM $CaCl_2$ with respect to addition of $CaCl_2$. At low levels of $CaCl_2$ addition there is an initial drop in measured hardness as the influence of calcium interactions with starch are more obvious. That is, the interactions of calcium with water molecules suppresses onset starch granule swelling and subsequent crosslinking of amylose chains (Jane, 1993). At higher additions of $CaCl_2$, gels exhibit greater hardness as the effect of calcium interacting with protein is heightened. Furthermore, calcium interactions

with water means there is an effective increase in the concentration of the WPI further enhancing gel hardness. An additional effect of calcium – water interaction is the suppression of gelatinisation of the WS.

Overall, a great deal of variability exists in regards to the impact of calcium ion levels on the measured hardness of WPI-WS gels. This is the outcome of a heterogeneous phase distribution in demixed systems (Damodaran, Parkin, & Fennema, 2008; Matsudomi, Rector & Kinsella, 1991; On-Nom, Grandison & Lewis, 2012), which can provide diversity in textural profiles of end products based on distinct formulations of polymeric constituents in the presence of a specific counterion (Damodaran, Parkin & Fennema, 2008).

The effect of the thermal regime on WPI and WS samples can be evaluated by the phase angle values; those below 45° signify formation of more elastic networks. Although the phase angle was below 45° for all samples except 3 WS as listed in Table 4.1, the starch solutions below 12% (w/v) solids did not form self-supportive gels sufficient for large deformation tests. The measured hardness of WPI and WS samples from large deformation tests are summarised in Table 4.3. However, as more of the cation is added, lower starch concentrations are required to produce firm enough gels for analysis. For example, in the absence of calcium ions, compressible WS gels were only apparent at the 15% solids mark, but with the addition of 30mM $CaCl_2$, gels with a total of 12% starch were measurable. Furthermore, polysaccharide gels with 120mM $CaCl_2$ could be tested at 9% solids. Hardness of single WS systems was much lower than 15% (w/v) WPI samples across all levels of added electrolyte. Thus, the force required to break 15% WS and 15% WPI matrices of varying ionic strength ranged from 11.30 to 25.23 kPa and 63.95 to 89.42 kPa, respectively.

Addition of 3% WS to 15% WPI did not induce significant changes on hardness, with fracture forces in both preparations measuring about 64kPain Table 4.3. Gel strength tends to progressively increase thereafter with addition of starch, and forces required to fracture gels were the highest in samples of 15% WPI with15% WS. Verheul & Roefs (1998) state that the porosity of gels decreases with increasing solids that fill spaces, and compression of densely packed, as opposed to largely porous structures, would promote hardness. For 15% WPI with 15% WS gels at 120mM $CaCl_2$, this is 188.68 kPa (Table 4.3), i.e. much higher than the sum of their individual components (80.08 kPa) hence denoting phase separation phenomena in the mixture.

Table 4.3 Maximum hardness of whey protein and wheat starch (%) gels with various concentrations of calcium chloride.

Calcium chloride (mM)	0		30		64		120	
	Hardness* (kPa)	S.E	Hardness* (kPa)	S.E	Hardness* (kPa)	S.E	Hardness* (kPa)	S.E
3 WS	NA		NA		NA		NA	
6 WS	NA		NA		NA		NA	
9 WS	NA		NA		NA		9.08	2.43
12 WS	NA		13.60	1.63	10.03	0.77	14.60	1.93
15 WS	11.30	2.47	15.43	1.52	25.23	1.96	19.31	3.15
15 WPI	63.95	5.82	85.71	6.94	89.42	17.15	60.77	9.63
15 WPI 3 WS	63.48	1.45	86.57	11.93	56.67	5.28	70.37	5.13
15 WPI 6 WS	92.38	5.02	55.06	3.05	52.72	4.80	91.67	1.99
15 WPI 9 WS	93.16	5.43	126.71	4.88	65.49	1.17	103.56	13.78
15 WPI 12 WS	143.39	19.48	73.25	5.90	84.69	5.40	154.09	21.25
15 WPI 15 WS	221.77	10.40	113.79	4.77	215.41	6.69	188.68	6.16

NA – values too low to measure

*Data was collected in triplicate for each WPI-WS-CaCl2 combination tested and the results presented are an average ± S.E. of n=3.

4.4.4 Tangible evidence of phase separation in wheat starch and whey protein composite gels

The microstructures of single and mixed polymer gels are shown in Figures 4.4(a-f). It is evident that increasing the level of calcium ions from 5 to 192mM results in more aggregated protein gels at 15% solids. This rather aggressive type of structure formation creates polymer rich domains in a network of high porosity, e.g. in Figure 4.4c. The extent of protein aggregation is maintained in mixtures of WPI and WS with a total level of solids of 30% in the presence of added calcium chloride. Besides the corpuscular structures of the protein, however, addition of starch exhibits well-developed and elongated strands in the micrographs, e.g. in Figure 4.4d. Phase separated matrices are evident in Figure 4.4e where discontinuous elevations of polysaccharide ridges are surrounded by a flat protein background. These rather dense microassemblies maintain structural parentage of the individual components and argue for a whey protein continuous phase suspending starch inclusions in the composite gel.

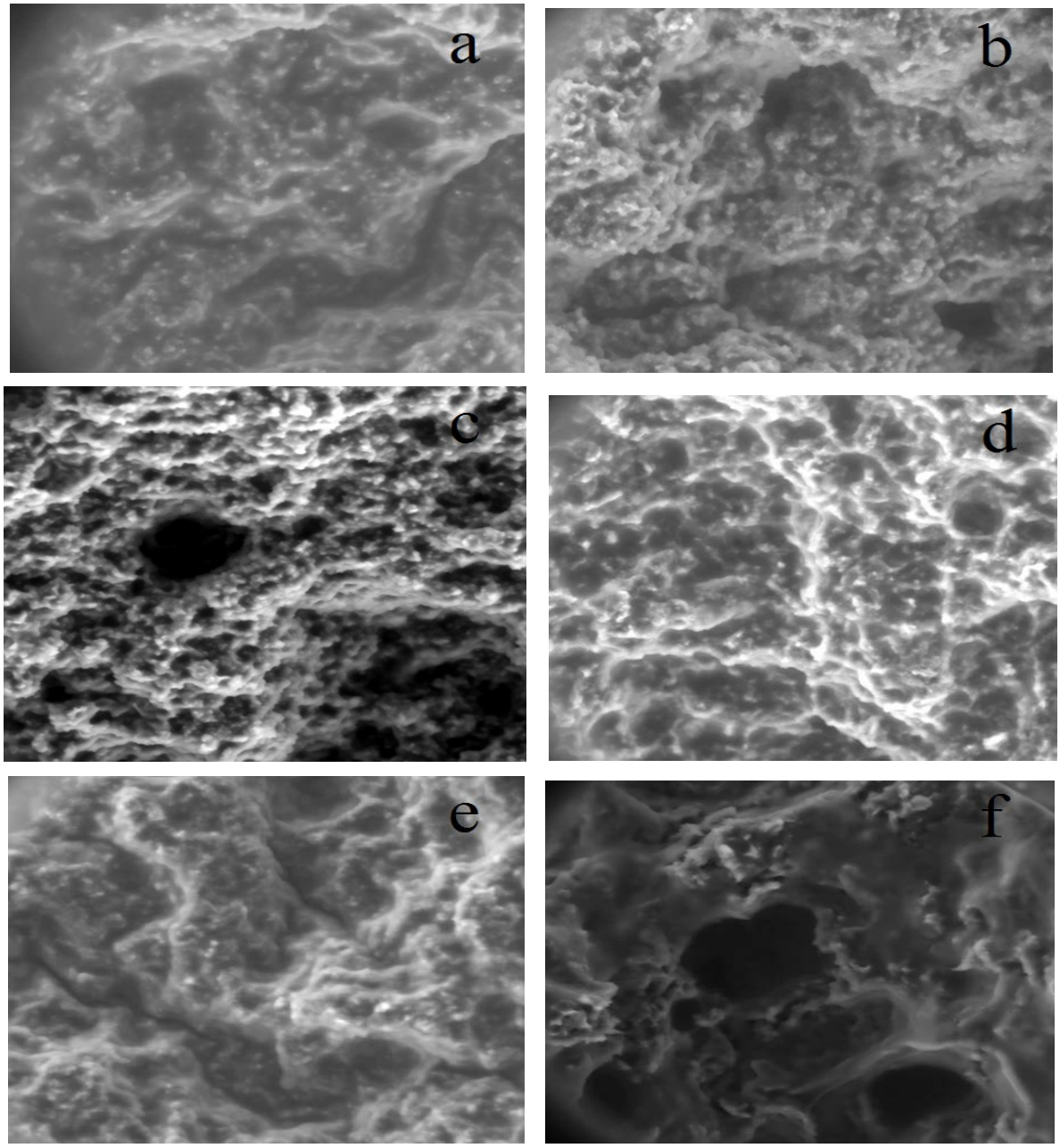

Figure 4.4 ESEM images for 15% whey protein with 5mM (a), 64mM (b), 192mM (c), and 15% whey protein plus 15% wheat starch with 5mM (d), 64mM (e) and 192mM (f) of added calcium chloride.

4.4.5 In vitro starch digestion in the presence of a calcium induced whey protein gel

In this part of the study, amylolysis of whey protein and wheat starch gels containing up to 192mM $CaCl_2$ was conducted and the total amount of reducing sugars liberated from the systems is presented in Figure 4.5. The action of α-amylase involves catalysing the endohydrolysis of α-1,4 glucosidic bonds in amylose and amylopectin molecules to produce

maltose (Samborska, Guiavarch, Van Loey & Hendrickx, 2006; Singh, Dartois & Kaur, 2010). The products from the hydrolytic action of α-amylase also include maltotriose, maltotetraose, dextrins and branched oligosaccharides (Singh et al. 2010). The amount of maltose in whey protein preparations is considered to be the background "noise" of the working protocol. This remains relatively consistent across the different levels of calcium chloride featured presently and provides a baseline of comparison with mixed systems. Starch addition at 5, 10 and 15% solids to a 15% whey protein sample increases the amount of substrate for the hydrolytic action of α-amylase leading to higher levels of polysaccharide digestion. Upon analysis of the samples at a constant level of WPI and WS a significant variation in the sugar liberated between different concentrations of incorporated $CaCl_2$ was evident. Two factors are important here, namely: according to Tester & Sommerville (2000), a decreased availability of water largely limits the extent of gelatinisation and the observation of Blazek & Gilbert (2010) who noted that starch granules in their native form possess limited digestibility. Given the above statements one may expect that with increased total solids by increasing levels of $CaCl_2$ there would be a consistent decrease in the amount of maltose liberated from the gel. While this may occur, one must also acknowledge the interactions of $CaCl_2$ with water, WPI and WS as discussed in the previous sections. The relationship between total maltose liberated from the gel with increasing levels of added polyelectrolyte takes the shape of a parabola (with a minimum vertex). Gels with intermediate levels of calcium chloride addition (about 48 mM) appear to be the most robust against starch degradation.

As depicted in Figure 4.5, low or high additions of the polyelectrolyte in the composite gels are prone to enzymatic attack. Research in structural properties of the two materials reported in the preceding sections assist in the elucidation of hydrolytic trends. Thus, we have stated presently and in an earlier investigation on composite gels of whey protein and starch without added counterions that polymer incompatibility determines three dimensional phase morphology (Yang, Liu, Ashton, Gorczyca & Kasapis, 2013). In the large deformation tests, composite gels prepared without $CaCl_2$ and those with salt at 120mM presented the greatest hardness (Figure 4.3). These combinations corresponded well to those found to exhibit the highest levels of sugar liberation during starch hydrolysis i.e. mixed gels containing 5mM and 120mM $CaCl_2$. However it is not argued that the hardness of the gel is an indicator of starch protection or lack thereof. While the outcome of starch hydrolysis is the same for both gel combinations, the reasoning is different; i.e. the basis of the increased firmness is not the

same as the basis of the increased enzymatic hydrolysis. The rheological data (measured storage modulus values) supports the difference in gel firmness, protein aggregation and as a result enzymatic hydrolysis. $CaCl_2$ addition of up to 120mM addition actively promoted continued aggregation of protein. This is due to calcium reducing the electrostatic repulsion between proteins and assisting protein cross-linking by the formation of salt bridges (Baumy & Brule 1988). As supported by tangible evidence in Section 3.4, low levels of calcium addition resulted in lightly cross-linked whey protein networks, whereas excessive aggregation featured at high inclusions of the counterion.

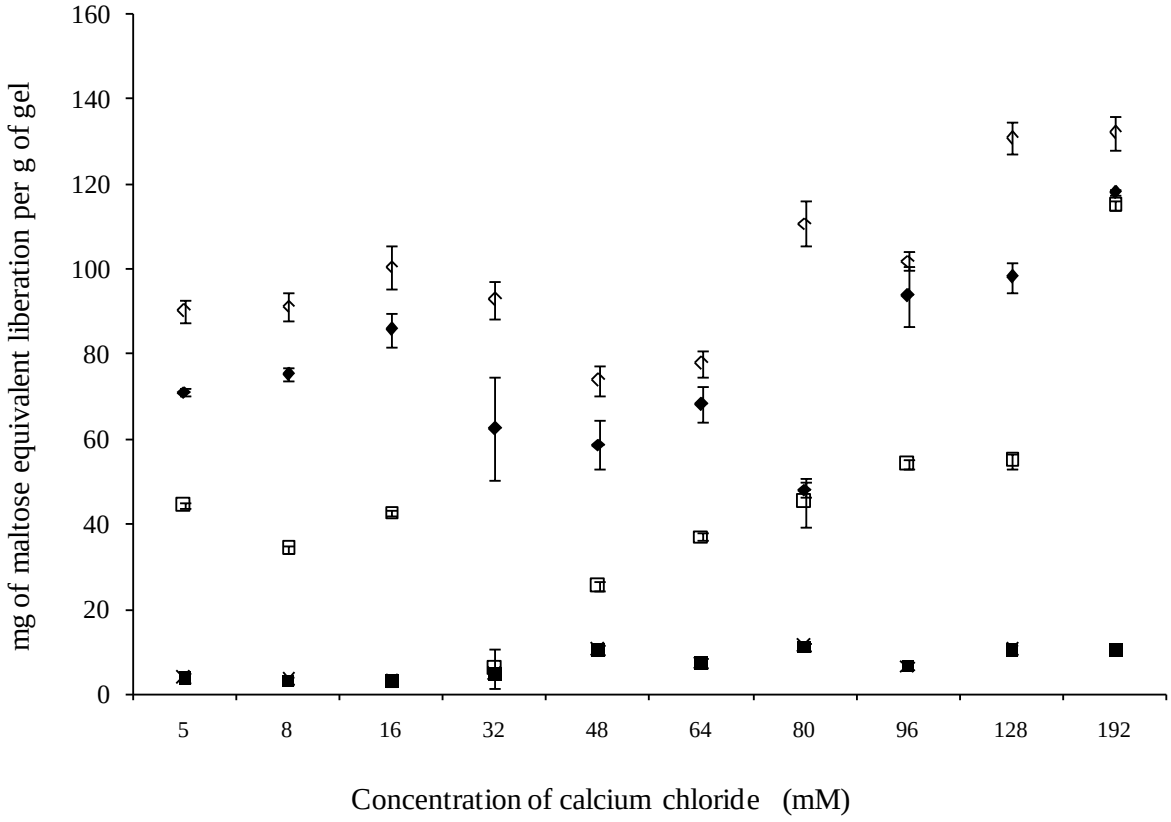

Figure 4.5 Total amount of reducing sugars in maltose equivalents 180 min liberated from *in vitro* α-amylase digestion of 15% whey protein (■), 15% whey protein plus 5% wheat starch (□), 15% whey protein plus 10% wheat starch (♦), and 15% whey protein plus 15% wheat starch (◊) at various levels of calcium chloride addition.

In the case of low levels of $CaCl_2$ addition, there is a reduced barrier effect to enzymatic activity due to space voids in low crosslinked networks. As for addition of 120mM $CaCl_2$,

highly aggregated protein chains form large-pore matrices of reduced intermolecular functionality. Pores at high levels of calcium chloride increase the surface area and entry point for α-amylase attack making systems susceptible to starch degradation. Intermediate levels of $CaCl_2$ appear to provide the optimum amount of network crosslinks for shielding against starch hydrolysis.

4.5 Conclusions

Calcium chloride has been incorporated into heat induced whey protein and wheat starch gels, which were then brought to ambient temperatures. The work recorded the interaction of calcium ions with both polymers in single and composite preparations and reported a range of structure-function relationships leading to variable functionalities in these systems. Cooling of denatured whey protein was found to form a continuous matrix suspending filler inclusions of gelatinised starch. Structural understanding achieved was utilised effectively to follow patterns of enzymatic (α-amylase) hydrolysis of the polysaccharide. It was proposed that informed manipulation of polyelectrolyte addition is critical in order to provide the optimum spatial structure for maximum protection of starch against enzymatic degradation. The present work forms the foundation for a better understanding of the structural morphology in whey protein/starch mixtures, which is essential for further exploration in the development of model systems with a low glycemic index. In future work the rate of sugar release and assessment of the structural changes during starch digestion will be measured for a range of WPI: WS: $CaCl_2$ combinations (15 WPI: 3-15 WS: 40-70mM $CaCl_2$).

4.6 Acknowledgements

This research was fully supported under Australian Research Council's *Linkage Projects* funding scheme (project number LP100200617).

4.7 References

Ahmad, F.B., & Williams, P.A. (1999). Effects of salts on the gelatinisation and rheological properties of sago starch. *Journal of Agricultural and Food Chemistry*, *47*, 3359-3366.

Barbut, S. (1995). Effects of calcium level on the structure of pre-heated whey protein isolate gels. *LWT- Food Science and Technology*, *28*, 598-603.

Baumy, J.J., & Brule, G. (1988). Binding of bivalent cations to α-lactalbumin and β-lactoglobulin: effects of pH and ionic strength. *Le Lait*, *68*, 33-48.

Bernfeld, P. (1955). Amylases, α and β. In S.P. Colowick, & N.O. Kaplan (Eds.), *Methods in enzymology* (pp. 149-158). New York: Academic Press.

Blazek, J., & Gilbert, E.P. (2010). Effect of enzymatic hydrolysis on native starch granule structure. *Biomacromolecules*, *11*, 3275-3289.

Bottomley, R.C., Evans, M.T.A., & Parkinson, D.J. (1990). Whey proteins. In P. Harris (Ed.) *Food Gels*, (pp. 435-466). London/New York: Elsevier Applied Science.

Biliaderis, C.G. (1990). Thermal analysis of food carbohydrates. In V. R. Harwalkar, & C. Y. Ma (Eds.), *Thermal Analysis of Foods* (pp. 168-219). Cambridge, U.K.: Elsevier Applied Science.

Biliaderis, C.G., Maurice, T.J., &Vose, J.R. (1980). Starch gelatinisation phenomena studied by differential scanning calorimetry. *Journal of Food Science, 45*, 1669-1674.

Britten, M., & Giroux, H.J. (2001). Acid-induced gelation of whey protein polymers: effects of pH and calcium concentration during polymerisation. *Food Hydrocolloids*, *15*, 609-617.

Bryant, C.M., & McClements, D.J. (1998). Molecular basis of protein functionality with special consideration of cold-set gels derived from heat-denatured whey. *Trends in Food Science and Technology, 9*, 143-151.

Ciacco, C. F., &Fernandes, J. L. A. (1979). Effect of various ions on the kinetics of retrogradation of concentrated wheat starch gels. *Starch,31*, 51-53.

Damodaran, S., Parkin, K.L., & Fennema, O.R. (2008). *Fennema's food chemistry:* Boca Raton, CRC Press/Taylor & Francis.

Doi, E. (1993). Gels and gelling of globular proteins. *Trends in Food Science & Technology, 4,* 1-5.

Ferry, J.D. (1948). Protein gels. *Advances in Protein Science, 4,* 1-76.

Fitzsimons, S.M., Mulvihill, D.M., & Morris, E.R. (2008). Co-gels of whey protein isolate with crosslinked waxy maize starch: Analysis of solvent partition and phase structure by polymer blending laws. *Food Hydrocolloids, 22,* 468-484.

George, P., Lundin, L., &Kasapis, S. (2013). Fundamental studies on the structural functionality of whey protein isolate in the presence of small polyhydroxyl compounds as co-solute. *Food Chemistry, 139,* 420-425.

Glibowski, P., Mleko, S., &Wesolowska-Trojanowska, M. (2006). Gelation of single heated vs. double heated whey protein isolate. *International Dairy Journal, 16,* 1113-1118.

Harrington, J.C., Foegeding, E.A., Mulvihill, D.M. & Morris, E.R. (2009). Segregative interactions and competitive binding of Ca^{2+} in gelling mixtures of whey protein isolate with Na^{+} κ-carrageenan. *Food Hydrocolloids, 23,* 468-489.

Health Insite - An Australian Government Initiative, Reviewed September 2008. "Diabetes Facts", Publisher: Nutrition Australia, <http://www.healthinsite.gov.au/topics/Diabetes_Statistics>

Hermansson, A., &Svegmark, (1996). Developments in the understanding of starch functionality. *Trends in Food Science & Technology, 7,* 345-353.

Hoffmann, M.A.M., & Van Mil, P.J.J.M. (1997). Heat-induced aggregation of β-lactoglobulin: role of the free thiol group and disulphide bonds. *Journal of Agriculture and Food Chemistry, 45,* 2942-2948.

Hongsprabhas, P., &Barbut, S. (1996). Ca^{2+}-induced gelation of whey protein isolate: effects of pre-heating. *Food Research International, 29,* 135-139.

Jane, J.-L.(1993). Mechanism of starch gelatinisation in neutral salt solutions. *Starch, 45,* 161-166.

Jeyarah, J., & Allen, J.C. (1994). Calcium binding and salt-induced structural changes of native and preheated β-lactoglobulin. *Journal of Agricultural and Food Chemistry, 42*, 80-85.

Jenkins, D.J.A., Wolever, T.M.S., Thorne, M.J., Jenkins, A.L., Wong, G.S., Josse, R.G., &Csima, A. (1984). The relationship between glycemic response, digestibility, and factors influencing the dietary habits of diabetics. *The American Journal of Clinical Nutrition, 40*, 1175-1191.

Ju, Z.Y., &Kilara, A. (1998). Aggregation induced by calcium chloride and subsequent thermal gelation of whey protein isolate. *Journal of Dairy Science, 81*, 925-931.

Katsuta, K. (1998). Effects of salts and saccharides on the rheological properties and pulsed NMR of rice starch during the gelatinisation and retrogradation processes. In P. A. Williams, & G. O. Phillips (Eds.), *Gums and Stabilisers for the Food Industry 9* (pp. 59-68), Cambridge, U.K.: Royal Society of Chemistry.

Kinekawa, Y., Fuyuki, T., &Kitabatake, N. (1998). Effects of salts on the properties of sols and gels prepared from whey protein isolate and process whey protein. *Journal of Dairy Science, 81*, 1532-1544.

Kinsella, J.E., & Whitehead, D.M. (1989). Proteins in whey: chemical, physical and functional properties. *Advances in Food and Nutrition Research, 33*, 343-438.

Koh, L.W., Kasapis, S., Lim, K.M., & Foo, C.W. (2009). Structural enhancement leading to retardation of *in vitro* digestion of rice dough in the presence of alginate. *Food Hydrocolloids, 23*, 1458-1464.

Kuhn, K.R., Cavallieri, A.L.F., & Cunha, R.L. (2010). Cold-set whey protein gels induced by calcium or sodium salt addition. *International Journal of Food Science & Technology, 45*, 348-357.

Lupano, C.E., & Gonzalez, S. (1999). Gelation of whey protein concentrate-cassava starch in acidic conditions. *Journal of Agricultural and Food Chemistry, 47*, 918-923.

Matsudomi, N., Rector, D., & Kinsella, J.E. (1991). Gelation of bovine serum albumin and β-lactoglobulin; effects of pH, salts and thiol reagents. *Food Chemistry, 40*, 55-69.

Mulvihill, D.M., Rector, D., & Kinsella, J.E. (1990). Effects of structuring and destructuring anionic ions on the rheological properties of thermally induced beta-lactoglobulin gels. *Food Hydrocolloids, 4*, 267-276.

On-Nom, N., Grandison, A.S., & Lewis, M.J. (2012). Heat stability of milk supplemented with calcium chloride. *Journal of Dairy Science, 95,* 1623-1631.

Pappas, C.P., &Rothwell, J. (1991). The effects of heating, alone or in the presence of calcium or lactose, on calcium binding to milk proteins. *Food Chemistry, 42*, 183-201.

Pons, M., &Fiszman, S.M. (1996). Instrumental texture profile analysis with particular reference to gelled systems. *Journal of Texture Studies, 27*, 597-624.

Ramasubramanian, L., D'Arcy, B., &Deeth, H.C. (2012). Heat-induced coagulation of whole milk by high levels of calcium chloride. *International Journal of Dairy Technology, 65*, 183-190.

Ring, S.G. (1985). Some studies on starch gelation. *Starch, 37*, 80-83.

Riou, E., Havea, P., McCarthy, O., Watkinson, P., & Singh, H. (2001). Behavior of protein in the presence of calcium during heating of whey protein concentrate solutions. *Journal of Agricultural and Food Chemistry, 59,* 13156-13164.

Russell, P. L. & Oliver, G. (1989). The effect of pH and NaCl content on starch gel aging. A study by DSC and rheology. *Journal of Cereal Science, 10*, 123-138.

Samborska, K., Guiavarch, Y., Van Loey, A., & Hendrickx, M. (2006). *Journal of Food Process Engineering, 29,* 287-303.

Shimada, K., &Cheftel, J.C. (1988). Texture characteristics, protein solubility, and sulphydryl group/ disulfide bond contents of heat-induced gels of whey protein isolate. *Journal of Agricultural and Food Chemistry, 36*, 1018-1025.

Singh, J., Dartois, A., &Kaur, L. (2010). Starch digestibility in food matrix: a review. *Trends in Food Science & Technology, 21*, 168-180.

Singh, N., Singh, J., Kaur, L., Sodhi, N.S., & Gill, B.S. (2003). Morphological, thermal and rheological properties of starches from different botanical sources. *Food Chemistry, 81*, 219-231.

Smithers, G.W. (2008). Whey and whey proteins - from “gutter-to-gold”. *International Dairy Journal, 18,* 695-704.

Steventon, A.J., Gladden, L.F., & Fryer, P.J. (1991). A percolation analysis of the concentration dependence of the gelation of whey protein concentrates. *Journal of Texture Studies, 22,* 201-218.

Sun, X.D., &Arntfield, S.D. (2010). Gelation properties of salt-extracted pea protein isolate induced by heat treatment: Effect of heating and cooling rate. *Food Chemistry, 124,* 1011-1016.

Tester, R.F., &Sommerville, M.D. (2000). Swelling and enzymatic hydrolysis of starch in low water systems. *Journal of Cereal Science, 33,* 193-203.

Totosaus, A., Montejano, J.G., Salazar, J.A., & Guerrero, I. (2002). *International Journal of Food Science and Technology, 37,* 589-601.

Tsia, M. L., Li, C. F., &Lii, C.Y. (1997). Effects of granular structures on the pasting behaviours of starches. *Cereal Chemistry, 74,* 750-757.

Verheul, M., &Roefs, S.P.F.M. (1998). Structure of whey protein gels, studied by permeability, scanning electron microscopy and rheology. *Food Hydrocolloids, 12,* 17-24.

Yang, N., Liu, Y., Ashton, J., Gorczyca, E., &Kasapis, S. (2013). Phase behavior and *in vitro* hydrolysis of wheat starch in mixture with whey protein, *Food Chemistry, 137,* 76-82.

Yang, H., Irudayaraj, J., Otgonchimeg, S., & Walsh, M. (2004). Rheological study of starch and dairy ingredient-based food systems. *Food Chemistry, 86,* 571-578.

Chapter 5 - The influence of chitosan on the physicochemical properties of whey protein and wheat starch composite systems

5.1 Abstract

The physicochemical properties of medium molecular weight chitosan (CHT), whey protein isolate (WPI) and native wheat starch (WS) as low-to intermediate-solid single systems and composite preparations were investigated. The analysis involved monitoring the thermal behaviour of these biopolymers during heating from 25 up to 95°C and subsequent cooling to 5°C under small deformation dynamic oscillation in-shear and micro differential scanning calorimetry experiments. Further information regarding the microstructure and network morphology of the systems was revealed through subjecting thermally developed gels to large deformation compression testing, scanning electron microscopy and infrared spectroscopy. The study found a significant change in the mechanical strength of WPI networks upon incorporation of CHT due to the electrostatic interactions between the two polymeric constituents in the mixture. In the tertiary system, the presence of low levels of starch contributed to a reduction in the firmness of the gel matrix. However, at higher additions of the polysaccharide, a recovery in the stored energy of systems was apparent, as recorded by the present experimental techniques.

5.2 Introduction

Chitin is a non starch organic material, which has a similar structure to cellulose (Chen, Wang, Lai & Lin, 2003). It is the second most abundant biopolymer in nature, sourced from the shells of crustaceans, shellfish and cell walls of fungi (Alishahi & Aider, 2012; Chang, Lin & Chen, 2003; Chen, Wang, Lai & Lin, 2003; Cho, Heuzey, Begin & Carreau, 2006; Knorr, 1984). The partial alkaline deacetylation of chitin gives rise to the cationic polysaccharide named chitosan (CHT) (Hong & McClements, 2007; Miralles, Martinez-Rodriguez, Santiago, van de Lagemaat & Heras, 2007). Characteristics of this molecule involve solubility in organic acids such as formic, acetic and lactic acid at pH levels below

~6.3 (Chen, Wang, Lai & Lin, 2003; Hong & McClements, 2007). The linear biopolymer is made up of two monosaccharides, namely N-acetyl-glucosamine and D-glucosamine, which are linked by β-(1→4) glycosidic bonds (Alishahi & Aider, 2012). Varying degrees of deacetylation (DDA) exist depending on the amount of glucosamine in the molecule. To be classified as CHT however, the DDA must be at a minimum of 70% but normally ranges from 75 to 95%.

In aqueous solutions, the DDA, molecular weight, pH and ionic strength play a significant role in determining the functionality of CHT. It is the presence of reactive hydroxyl and amino groups which enable chemical modifications to structure resulting in versatile functional properties (Wang et al., 2006). The solubility of CHT is a result of the protonation of the free amine groups (below pH ~6.3). Apparently, the higher the DDA, the greater the amount of amino groups ($-NH_3^+$) available for reactions (Chen, Wang, Lai & Lin, 2003). As well as a flexible structure, the non-toxicity, biodegradability and biocompatibility of CHT make it the "material of choice" for various applications in the food and pharmaceutical industry. The hydrophilic polyelectrolyte has been used in downstream processes to purify wastewater by coagulating and binding proteins and lipids (Chang, Lin & Chen, 2003; Shahidi, Arachchi & Jeon, 1999).

Tests also prove CHT possesses antimicrobial, antibacterial and antifungal properties (Chang, Lin & Chen, 2003; Shahidi, Arachchi, & Jeon, 1999). Consequently, it has been used as coating on fresh fruits and vegetables to preserve and extend shelf life (Chang, Lin & Chen, 2003; El Ghaouth, Arul, Ponnampalam & Boulet, 1991; El Ghaouth, Ponnampalam, Castaigne & Arul, 1992). The use of CHT as an encapsulating agent is also particularly interesting. In one instance CHT served as a nanocarrier for ascorbic acid, with the molecule providing a barrier against degradation of vitamers in the harsh conditions of the gastrointestinal tract of rainbow trout (Alishahi & Aider, 2012).It has also been suggested that the formation of hydrogel particles from β-lactoglobulinand CHT may be useful for the encapsulation of functional food ingredients (Hong & McClements, 2007). Between the pH of 5 and 7, an opportunity exists for electrostatic attraction between WPI and CHT molecules, where CHT is positively charged while anionic patches exist on the WPI surface (Hong & McClements, 2007).

The thermodynamic incompatibility of protein-polysaccharides in aqueous solutions is the driving force for a micro-phase separated arrangement captured in the thermally developed

matrix of globular proteins. Previous work provides evidence of whey protein forming a continuous network, with the discontinuous starch inclusions acting as a filler in the soft solid phase (Yang, Liu, Ashton, Gorzyca & Kasapis, 2013). Several developments on the ability of whey protein to encapsulate wheat starch in a bid to reduce the glycemic index of preparations during enzymatic hydrolysis have also been reported (Yang, Luan, Ashton, Gorzyca & Kasapis, 2013). The current work communicates the findings on the influence of chitosan in whey protein and wheat starch mixtures. The aim is to characterise the physical and chemical properties of chitosan, whey protein and wheat starch systems at varying polymer concentrations and pH conditions. This is the first of a two component work of which the focus is on network microstructure with regards to enhanced retardation of the enzymatic hydrolysis of starch.

5.3 Materials and methods

5.3.1 Materials

Soluble medium molecular weight chitosan powder was purchased from Sigma-Aldrich, Co. (St. Louis, MO, USA). According to the manufacturer, the degree of deacetylation was ≥ 75%. Whey protein isolate was supplied from Fonterra Co-operative Group Ltd., New Zealand. The powder contained 88.71% protein, 0.93% fat, 4.83% moisture and 3.3% ash (w/w). Unmodified starch from wheat was obtained from National Starch (National Starch and Chemical Co., Thailand), with the powder containing 94.1% starch, 0.3% ash, 0.1% fat and 5.5% moisture on a weight-per-weight basis. All other chemicals utilised were of analytical grade or higher.

5.3.2 Methods

5.3.2.1 Sample preparation

Required quantities of CHT/WPI/WS powder were weighed. While WPI and WS powders were directly dissolved in the water, the CHT powder was dissolved in a 1% (v/v) acetic acid solution consisting of acetic acid in Milli-pore water. Single WPI and WS dispersions were prepared at concentrations of 5, 10, 15 and 20% (w/v) while the pH was adjusted to 5.5. Single CHT was prepared at concentrations of 1, 1.5 and 2% (w/v) while the pH was adjusted

to 5.5, 6 and 6.5. Mixed systems (%, w/v) were also prepared at pH 5.5:2CHT-15WPI, 2CHT-15WPI-5WS, 2CHT-15WPI-10WS, 2CHT-15WPI-15WS. After preparation, mixtures were left to rest and degas for three hours prior to loading onto equipment or thermal development of a gel. The cooking of the gel consisted of pipetting solutions into 45°C preheated aluminium moulds covered with aluminium foil and immersed in a heated waterbath for 75 minutes set at 85 ± 1°C.

5.3.2.2 Rheology

Measurements of small deformation dynamic oscillation in-shear were performed using a controlled strain AR-G2 rheometer with magnetic-trust bearing technology (TA Instruments, New Castle, DE). Experiments were conducted with a fixed strain of 0.1%, which is well within the linear viscoelastic region of these materials. The parallel-plate measuring geometry was 40 mm in diameter with a gap distance of 1 mm. Samples were loaded onto the Peltier plate and the periphery was sealed with silicon oil from BDH (50 cS) to prevent evaporation. The entire experimental sequence utilised a scan rate of 2°C/min whereby the system was first equilibrated at 25°C. The solution was then heated to 85°C, cooled from 85 to 5°C, followed by a three decade frequency sweep (0.1 to 100 rad/s). Standard rheological parameters including tan δ, storage (G') and loss (G'') modulus were measured as functions of temperature and frequency.

5.3.2.3 Differential scanning calorimetry

This was conducted using the Setaram Micro-DSC VII (Setu-rau, Caluire, France). The material was filled in the 850 mg cell at an equal weight to the reference sample consisting of Milli-pore water. Cells were stabilised for 1 hour at 25°C (isothermal), heated from 25 to 95°C and cooled from 95 to 5°C at a rate of 1°C/min. The proprietary software, Calisto, was used to further monitor thermal behaviour including the determination of endothermic or exothermic peaks and changes in heat enthalpy.

5.3.2.4 Textural analysis

Single cycle compression tests using the TA-XT2 Texture Analyser (Stable Micro Systems, Surrey, England) were performed to determine gel hardness. A 50 mm diameter cylindrical probe was chosen to compress the samples of equal diameter (50 mm) and 15 mm height. Deformation was set at 75%, on three replicates per sample, enabling fracture within the first compression cycle. The test speed employed was 0.1 mm/s at ambient temperature.

5.3.2.5 Scanning electron microscopy

Gels were broken apart and the internal surface was placed upward facing for exposure to scanning by the beam of high energy electrons. Images were collected from various physical locations of the sample. The Environmental mode is suitable for imaging of samples in the hydrated state and thus, in a bid for greater resolution, was the choice for operation. Micrographs of single and composite systems of chitosan, whey protein and wheat starch were taken at x500 and x1000 magnification (FEI Quanta 200 ESEM, Hillsboro, Oregon, USA).

5.3.2.6 Infrared spectroscopy

Spectra pertaining to whey protein, chitosan and wheat starch samples were obtained using the Perkin Elmer Spectrum 100 FTIR spectrometer equipped with MIRacle ™ ZnSe single reflection ATR plate (Perkin-Elmer, Norwalk, CT, USA). The spectrum was recorded as the absorbance values derived from an average of 8 scans in the range of 650-4000 cm^{-1} with a resolution of 4 cm^{-1}. This was corrected against the background spectrum of the solvent at ambient temperature. The Spectrum Version 6.0.2 software was used to deconvolute spectra within the range of 1600-1500 cm^{-1}. The area of the peaks was then calculated to provide further inquest on the nature of molecular interactions between the polymeric constituents in the system.

5.4 Results and discussion

5.4.1 Small-strain rheological properties of single polymeric networks

The rheological behaviour during bidirectional shear of temperature and frequency sweeps on CHT, WPI and WS at different concentrations and pH conditions were studied. During heating, single CHT systems were solubilised but no obvious increase in the values of G' was sighted (results not shown here). The observation was valid across all concentrations and pH levels tested on the heteropolysaccharide. During the cooling period, the G' of CHT systems, set at pH 5.5 and varying concentrations (1, 1.5 and 2%), reflected the same trend, i.e. an increased storage of energy in the structure occurring in a rather monotonic fashion (Figure 5.1a). The polysaccharide concentration appears to be a significant determinant in the resulting strength of the system. More specifically, 2% CHT content provided a higher G' by the end of the cooling run than the 1.5% concentration and the latter was stronger than the 1% counterpart.

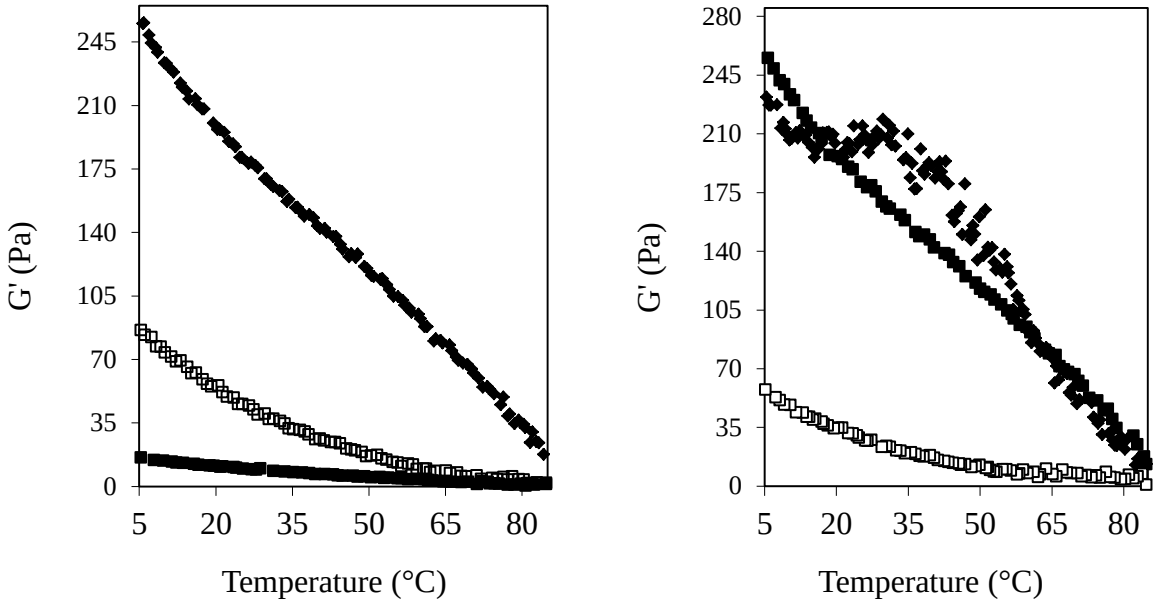

Figure 5.1 (a) Cooling profile of storage modulus for 1 (■), 1.5 (□) and 2% (♦) chitosan at pH 5.5 and (b) Cooling profile of storage modulus for 2% chitosan at pH 5.5 (■), 6 (□) and 6.5 (♦) (scan rate: 1°C/min; frequency: 1rad/s; strain: 1%).

Increase in concentration enables a higher degree of intermolecular interactions to occur and more energy to be stored in the system. The effect of concentration on the viscoelastic properties of CHT systems has previously been noted (Cho, Heuzey, Begin & Carreau, 2006; Martinez, Chornet & Rodrigue, 2004). The concentration of CHT also appeared to be related to higher G' values for complex-coacervate forming systems of CHT with WPI (Bastos et al., 2010). Since the tan δ at the cooling endpoint of all CHT concentrations investigated is well below 1 (results not shown here), the systems are said to possess solid-like properties. The maximum concentration of CHT used in the present study is 2% and is chosen for further experiments examining the effect of pH.

According to literature, CHT is positively charged and soluble in acid solutions at pH levels under ~6.3 (Hong & McClements, 2007). More specifically, at this pH range, the amine groups of CHT are protonated to $–NH_3^+$ and there is strong electrostatic repulsion between chitosan molecules (Hong & McClements, 2007)-the lower the pH, the greater the solubility of chitosan. As the pH is raised towards the basic range, however, CHT progressively loses the positive charge due to deprotonation of the amino groups. At this point, the CHT may precipitate from solution (Hong & McClements, 2007). For this reason, the three pH levels chosen for testing (5.5, 6.0 and 6.5) fell within or near the domain where CHT retained a predominantly cationic character.

During the cooling sweep, the storage modulus of 2% CHT at the three experimental values of pH gradually increases as the temperature decreases (Figure 5.1b). It is important to note a plateau in the elastic component of the 2% CHT sample adjusted to pH 6.5, which occurs within the temperature range of 15 to 35°C. It is known that the addition of alkali to raise the pH of the CHT solution takes place instantly and locally (Chenite, Gori, Shive, Desrosiers & Buschmann, 2006). When the CHT solutions were pH adjusted in this work, addition of HCl or NaOH occurred under continuous stirring in order to minimise localised pH effects. Nevertheless, some non-uniformity may not be avoided in the case of CHT at pH 6.5. Adjustment of the aqueous solutions above the stable threshold (i.e. above the pKa value) forms hydrated gel-like precipitates (Chenite, Gori, Shive, Desrosiers & Buschmann, 2006), which may be the case in our sample at the highest pH resulting in a relatively heterogeneous matrix.

Storage modulus values of CHT at pH 6.5 gradually rise again with further cooling. By the end of the cooling sweep, the corresponding values of the sample at pH 6.0 were much lower

than for the higher pH counterpart (Figure 5.1b). This could also be related to the fact that the pH of 6 is also quite close to the pKa value of chitosan. The highest G' value corresponds to the 2% CHT sample adjusted to pH 5.5, and it was decided to consider this smooth development of network strength for further analysis by incorporating WPI and WS.

The rheological behaviour of single systems of WPI at pH 5.5 and various concentrations during heating and cooling are presented in Figure 5.2. The loss of the protein secondary structure for 10, 15 and 20% WPI appeared at about 76.3, 77.0 and 69°C, respectively. In contrast to the onset of structure formation for 10 and 15% WPI, the highest WPI concentration exhibited a much earlier gelation temperature. Results are in broad agreement with literature where the phase transition of 10% β-lactoglobulin was 73°C (Rafe, Rasazi & Farhooshm, 2013). The three-degree difference from our 10% WPIshould be attributed to the presence of α-lactalbumin, bovine serum albumin and immunoglobulins that exhibit different phase transition temperatures; α-lactalbumin possesses twice the quantity of disulphide bonds than β-lactoglobulin yielding a more temperature resistant structure.

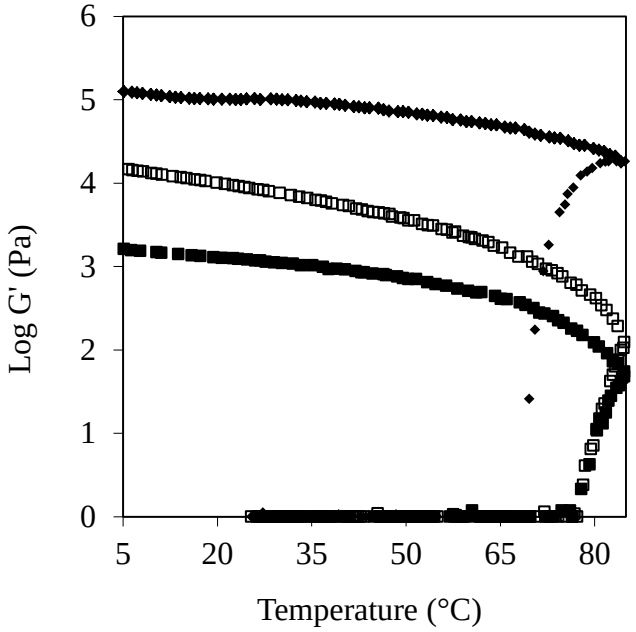

Figure 5.2 Heating and cooling profile of storage modulus for 10 (■), 15 (□) and 20% (♦) whey protein at pH 5.5 (scan rate: 1°C/min; frequency: 1rad/s; strain: 1%).

The onset of gelatinisation for 5, 10 and 15% WS at pH 5.5 was recorded at 80, 65and 62.3°C, respectively (Figure 5.3). It is interesting that an upward slope in G'values could be

seen for 5 WS despite the low concentration. Similar to WPI, the highest WS concentration exhibited a sharp transition at an earlier temperature than the remaining starch preparations. To compare the molecular forces behind structure formation in our materials, the increase in strength of WPI is a result of accumulating energy from disulphide interactions during heating and non-covalent forces including electrostatic and van der Waals forces, hydrogen and hydrophobic bonds, which contribute to the linear increase in gel strength with cooling (Chronakis & Kasapis, 1993; Cooney, Rosenberg & Shoemaker, 1993; Manoj, Kasapis, & Hember, 1997; Rafe, Rasazi & Farhoosh, 2013; Yang, Liu, Ashton, Gorczyca & Kasapis, 2013). In the WS samples, the increase in G' throughout the cooling run is less dramatic than WPI.

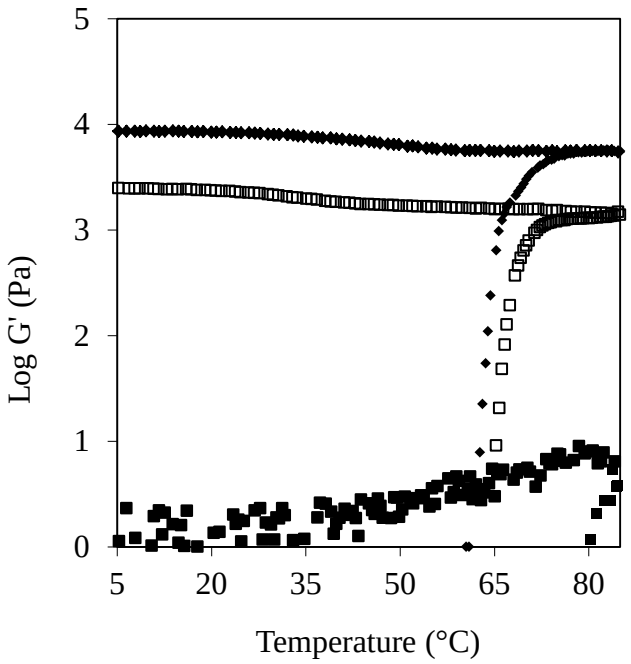

Figure 5.3 Heating and cooling profile of storage modulus for 5 (■), 10 (□) and 15% (♦) wheat starch at pH 5.5 (scan rate: 1°C/min; frequency: 1rad/s; strain: 1%).

A possible explanation for the latter is the absence of covalent interactions, and the formation of hydrogen bonds leading to contraction of gel volume as it has been reported previously for starch matrices (Tsia, Li & Lii, 1997; Yang, Irudayaraj, Otgonchimeg & Walsh, 2004; Yang, Liu, Ashton, Gorzyca & Kasapis, 2013). In the case of 5 WS, the G' values fluctuate with an overall decline in Figure 5.3, which should be attributed to the low level of solids being insufficient to form a stable three dimensional network. Besides the 5% WS, the concentration

effect is applicable to both protein and starch systems whereby higher concentrations result in cohesive structures. Thus, the cooling endpoint log G' value of 20% WPI is 5.1, while at 15 and 10% WPI values are 4.1 and 3.2, respectively. The cooling endpoint log G' value of 15% WS is 3.9 while for 10 and 5%WS itis 3.4 and 0.05, respectively. At the end of the cooling regime, WPI preparations possess a higher network strength than WS gels at equal concentrations.

5.4.2 Mechanical properties of the polymeric mixtures

Following characterisation of the rheological behaviour in single systems, blends were examined, with their storage modulus values during controlled heating and cooling being plotted in Figure 5.4. It can be immediately seen that the significant increase in G' during heating of the single WPI and WS components did not prevail in their mixtures. Heating of the 15WPI-2CHT sample does not reproduce the increase in G' occurring at 77.0°C, which is apparent in the corresponding WPI gel in Figure 5.2. It appears that the presence of CHT has interfered with the thermal gelation of our systems, as discussed for salt soluble proteins (Chen, Wang, Lai & Lin, 2003), and the inhibition of protein-protein aggregation for β-lactoglobulin (Mounsey, O'Kennedy, Fenelon & Brodkorb, 2008). These authors also reported on the pH dependent ability of chitosan to either promote or inhibit denaturation of whey proteins.

Incorporation of up to 10% WSin the mixture of WPI and CHT (Figure 5.4) also did not show an abrupt increase in G', as is apparent for the single WS gels in Figure 5.3. It appears that at low and intermediate levels of starch addition, trends recorded during heating of single WPI and WS systems are not evidenced in the mixed systems indicating distinct molecular processes. However, addition of 15% starch in the 15 WPI 2 CHT 15 WS sample, produces an increase in G' during heating with a wave of structure formation at around 65°C, which is close to the phase transition temperature of 15 WS (62.3°C). Gelation in the mixture occurred at slightly higher temperatures than the single starch preparation due to the presence of WPI with a structuring temperature of 77.0°C (Figure 5.2).

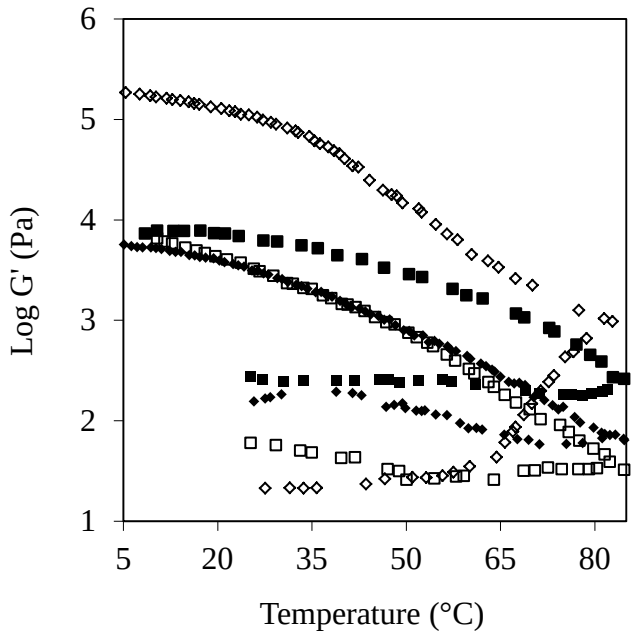

Figure 5.4 Heating and cooling profile of storage modulus for 2% chitosan with 15% whey protein and 0 (■), 5 (□), 10 (♦) and 15% (◊) wheat starch at pH 5.5 (scan rate: 1°C/min; frequency: 1rad/s; strain: 1%).

During cooling, mixtures increase gradually in network strength to the very end, with the log G' of 2CHT-15 WPI, for example, being 3.8. The cooling endpoint log G' of 15 WPI without CHT is 4.2, indicating a considerable decrease in the network strength of the binary gel. Clearly, CHT interferes with the process of whey protein agglomeration for network formation. Further, the presence of low levels of WS (5 and 10%) in 2CHT-15WPI yields a lower cooling log G' endpoint than the binary gel of chitosan and whey protein. Incorporation of 15 WS in 2CHT-15WPI, however, results in a higher cooling log G' endpointthan all mixtures under investigation in Figure 5.4. Three-decade frequency sweeps conducted from 0.1 to 100 rad/s for the composite systems record tan δ values well below 1 and minimal dependence of G' and G'' traces on frequency as pertains to self supporting gels (data not shown here).

5.4.3 Textural analysis

These tests were conducted for the purpose of understanding the long deformation structural properties of our materials that are closely related to sensory evaluation during the act of

mastication (Montejano, Hamann & Lanier, 1985; van den Berg, van Vliet, van der Linden, van Boekel & van de Velde, 2007). Heat-set biopolymer gels were formed and the texture was investigated by measuring the maximum force required to compress samples to 75% of their initial height. Hardness values from triplicate measurements of single and mixed gels of CHT, WPI and WS can be seen in Figure 5.5. Two percent CHT remained a relatively soft gel after cooking and consequently possessed very low hardness values. At about 47.4 kPa, measured hardness was the highest in single 15% WPI gel samples, whereas the corresponding starch concentration gave a value of 18.8 kPa in qualitative agreement with the small deformation oscillatory results discussed earlier in Figures 5.1 to 5.3. In regards to mixed gels, addition of CHT to the 15% WPI gel appeared to reduce the maximum force required for uniaxial compression about 10.0 kPa. Further, incorporation of low levels of starch (5%) into the binary system sees a dramatic reduction in hardness down to 5.7 kPa. At 10 and 15% WS addition, the tertiary gels recover considerably as for the small deformation counterparts in Figure 5.4, further supporting the argument for a distinct molecular mechanism in network formation amongst the three polymeric constituents.

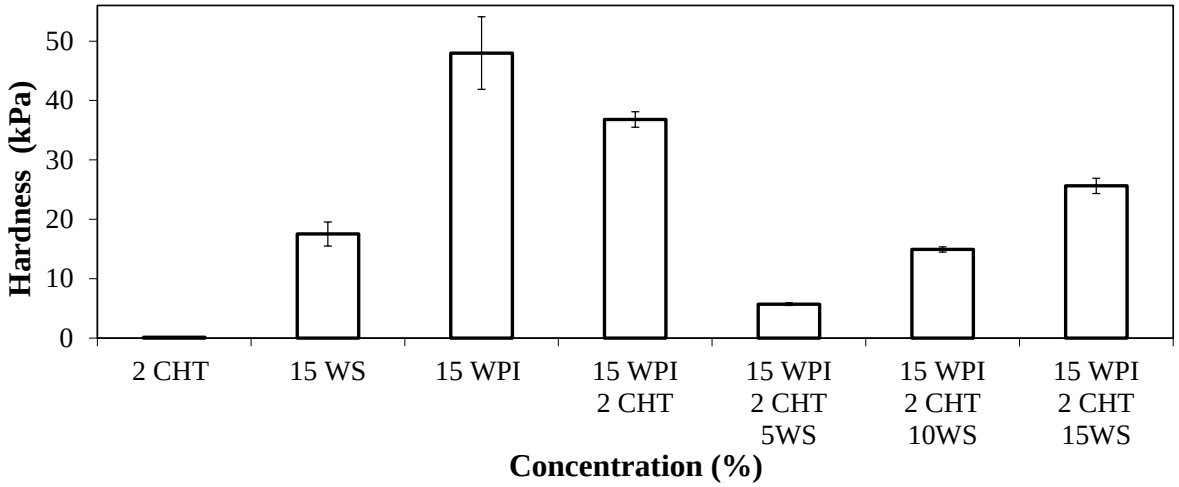

Figure 5.5 Measured hardness of pH 5.5 chitosan, whey protein and wheat starch gels at various concentrations using a compression rate of 0.1 mm/s.

5.4.4 Differential scanning calorimetry

To offer complimentary perspectives, to rheological studies discussed thus far, of molecular interactions in our materials adjusted to pH 5.5, thermal properties were examined by micro-

calorimetry, with resulting thermographs being displayed in Figure 5.6. In regards to single component systems, endothermic peaks are evident for both WPI and WS. Thus the onset and midpoint temperatures for 15WPI and 15WS are 78.9, 81.5°C and 59.7, 65°C, respectively. The onset of thermal transitions are at temperatures close to those measured earlier using rheology (Figures 5.2 and 5.3), where an abrupt increase in G' for these concentrations of WPI and WS occurred during heating at 77 and 62.3°C, respectively.

The peak arising from WS is sharp while it is much broader in the case witnessed for WPI (Figure 5.6). The latter is related to a more progressive network development due to the overlapping of thermal events in various proteinaceous fractions of WPI possessing distinct phase-transition temperatures. Aguilera & Rojas (1999) report that the denaturation temperature for α-lactalbumin ranges from 61-61.5°C while for β-lactoglobulin and BSA range from75.9-81.2°C and 71.9-74°C, respectively. No exothermic or endothermic reactions could be detected for the single 2% chitosan sample within the sensitivity limits of our microcalorimeter.

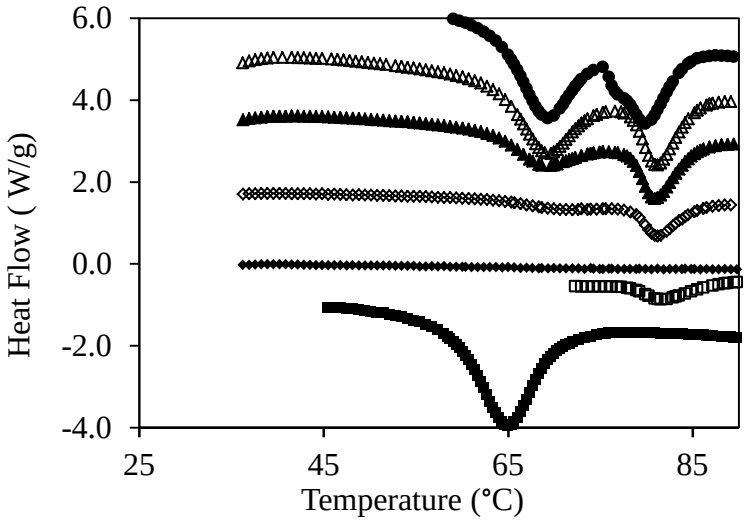

Figure 5.6 DSC endotherms for 15% wheat starch (■), 15% whey protein (□), 2% chitosan (♦), 15% whey protein with 2% chitosan (◊), 15% whey protein with 2% chitosan and 5% wheat starch (▲), 15% whey protein with 2% chitosan and 10% wheat starch (Δ) and 15% whey protein with 2% chitosan and 15% wheat starch (●) at pH 5.5 (scan rate: 1°C/min).

In the thermogram of 15WPI-2CHT, a single endothermic peak was apparent in Figure 5.6. The onset temperature of the peak occurred at 78.5°C and possessed a midpoint value of 81.2°C. Since the thermal transition appeared at very similar temperatures to the single WPI thermograph, data suggests CHT did not significantly change the thermal stability of WPI. Lee and Hong (2009) conducted DSC experiments with the single whey protein fractions of α-lactalbumin and β-lactoglobulin in conjunction with chitosan. They found that the presence of CHT served to delay the endothermic reaction to higher temperatures, which for pure α-lactalbumin was 83°C and was shifted to 92°C in α-lactalbumin/CHT mixtures. In the case of β-lactoglobulin, midpoint temperatures were shifted in the opposite direction from 91°C in the single system to 82°C in the protein/chitosan mixture. The DSC peak value of 81.2°C found for the whey protein/chitosan mixture in the present study is close to that reported in literature for the β-lactoglobulin/chitosan mixture, since the molecular fraction is the main component of WPI largely influencing its thermal behaviour.

For tertiary systems incorporating WS, two DSC peaks were witnessed in Figure 5.6. Judging from the temperature at which the peaks occurred, the first peak is attributed to starch gelatinisation while the second peak is due to protein denaturation. This outcome indicates the absence of direct chemical or electrostatic interactions between starch and whey protein in mixtures under our experimental conditions. The midpoint value of the first and second DSC peaks occurs in the temperature range of 68.9-69.3°C and 79.8-81.2°C, respectively. Peaks attributed to WS in the mixture are shifted higher about four degrees in comparison to temperatures for single WS samples indicating a certain degree of delay in gelatinisation. The reason behind this observation is that starch in the mixture must now share the water available for hydration with whey protein, thus requiring higher temperatures for granule swelling.

This type of peak alteration in terms of size and temperature band is known for phase separated biopolymer mixtures, and Kasapis and Al-Marhoobi (2005) reported it for the melting point temperatures of 1.5% κ-carageenan when mixed with 10% gelatin. Prasanth, Kittur and Tharannathan (2002) demonstrated that CHT in distinct physicochemical environments exhibits variation in endotherm peak area and position that was associated with the water-holding capacity and strength of water-chitosan interactions. According to Rahman, Machado-Velasco, Sosa-Morales and Velez-Ruiz (2009), the area under the CHT peak is proportional to the heat energy released or absorbed by the sample during thermal treatment. Furthermore, Simi and Abraham (2010) noted that the sharpness of the DSC peak in

xyloglucan/chitosan systems was associated with their gel strength, as measured in corresponding rheological experiments on the mixture. The more starch is added in the preparations of our work, the DSC endotherm peak becomes sharper and more pronounced in Figure 5.6, an outcome that correlates well with the increase in hardness values of mixed preparations in the presence of 10 and 15% starch (Figure 5.5).

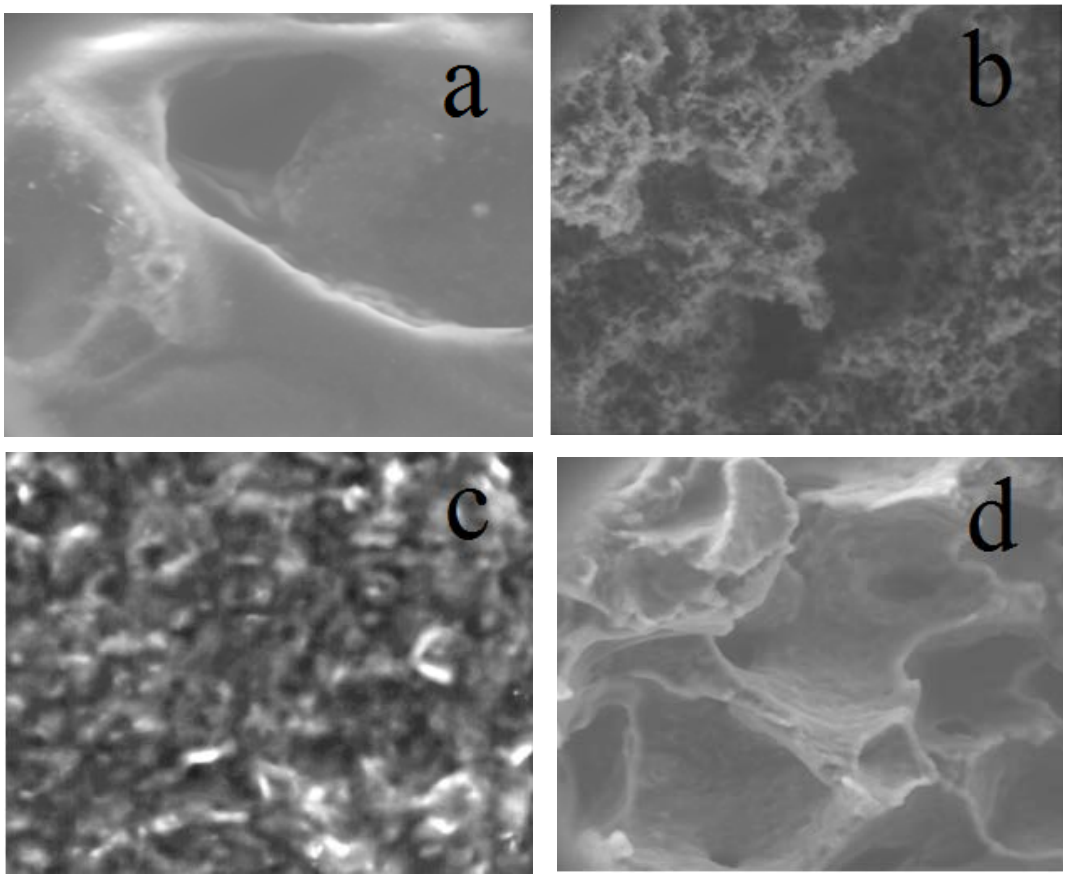

Figure 5.7 ESEM images for pH 5.5 gels of 2% chitosan (a), 15% whey protein (b) 15% wheat starch (c) and 2% chitosan 15% whey protein 10% wheat starch (d).

5.4.5 Microstructure as visualised from microscopy images

Tangible evidence of the surface topology in single and composite systems of protein and polysaccharides was afforded using scanning electron microscopy in environmental imaging mode. The images of single and mixed gel samples at x500 magnification are presented in Figures 5.7(a-d). Single CHT networks are distinct and appear to produce a slimy, mucilaginous appearance (Figure 5.7a). The single system of WPI in Figure 5.7b can be

distinguished as a matrix consisting of globular aggregates, hence appearing to be particulate rather than fine stranded in nature. Particulate gels are known to be thermally developed by β-lactoglobulin in conditions of lowered electrostatic repulsion such as when the pH is close to the isoelectric point. The whey protein micrograph is similar to the spherical particles observed by Bromley, Krebs and Donald (2006) when imaged β-lactoglobulin gels at pH 5.3. Clearly, the micrograph of WPI is distinct from that of single starch preparations, which show remnants of a granular and highly refractive-index structure, hence forming a heterogeneous matrix in Figure 5.7c. Finally, the micrograph of the macroscopic gel containing 15 WPI 2 CHT10 WSappears to generatea distinct feature that may be construed as the outcome of combining the chitosan and whey protein networks in close proximity to each other (Figure 5.7d).

5.4.6 FT-IR spectroscopy on single and mixed preparations

This is a highly sensitive, non-destructive technique which was used to examine thermally developed protein and polysaccharide gel preparations followed by cooling to ambient temperature. The frequencies of vibration between bonds of atoms in the sample are reflected as absorption peaks in Figure 5.8. Clearly WPI, CHT and WS spectra were distinct from each other as related to their physicochemical features. No new bands attributed to addition of CHT or WS to WPI could be seen, an outcome which indicates the absence of covalent bonding between the three polymeric ingredients in the mixture. Composites appear as superimposed but augmented spectra of the individual components in the binary and tertiary systems.

Vibrations in the amide II region of the proteinaceous material is related to C-N stretching combined with N-H bending bonds (van der Ven et al., 2002). These spectral features within the wavelength of 1500 to 1600 cm^{-1} predominate in the pure WPI system and are further intensified with the addition of CHT in the binary system or the addition of WS to produce the tertiary mixture in Figure 5.8. Consequently, the area under the peak in amide II region was quantitatively measured to further validate the qualitative spectral observations, and the outcome of these calculations is shown in Figure 5.9. Clearly, integration of the spectral peaks argues that addition of chitosan alters to a good extent the secondary conformation of whey protein in the binary gel, which is indicative of direct electrostatic interactions between the two polymeric components. This volume of molecular interactions is further increased in the presence of starch that is sterically excluded from the phase of whey protein with chitosan,

thus further encouraging close proximity and electrostatic association of the two oppositely charged components at pH 5.5 of the tertiary mixture.

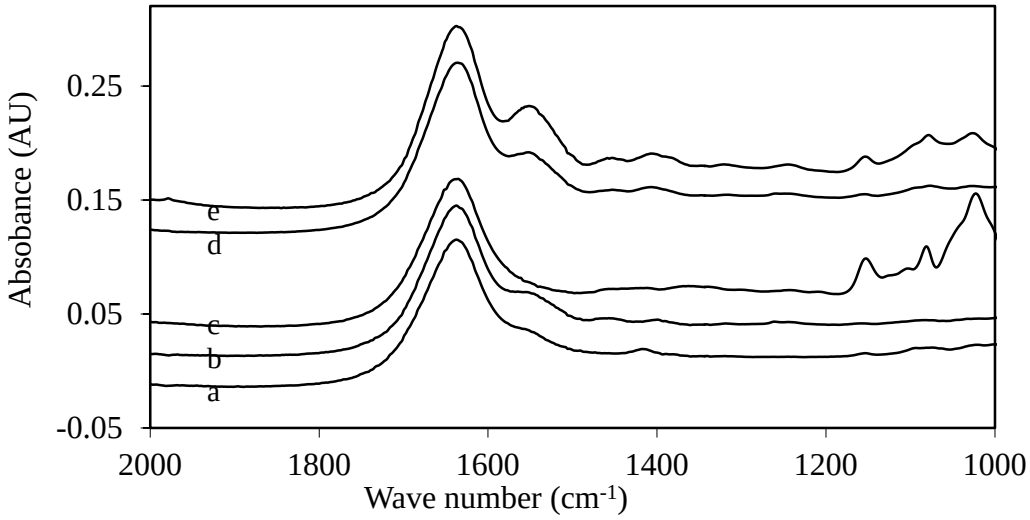

Figure 5.8 FTIR spectra corresponding to pH 5.5 gels of 2% chitosan (a), 15% whey protein (b), 15% wheat starch (c), 15% whey protein with 2% chitosan (d), and 15% whey protein with 2% chitosan and 10% wheat starch (e).

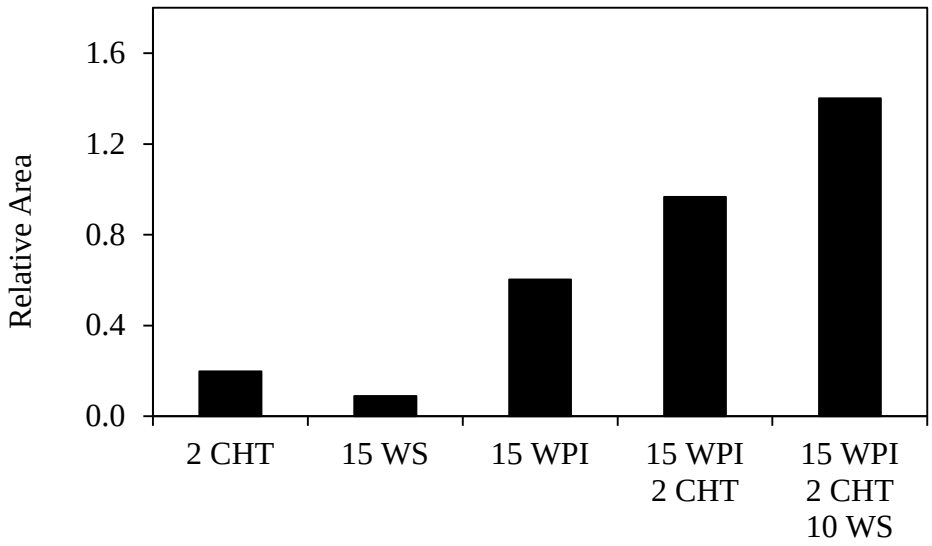

Figure 5.9 Relative area of absorbance between the wavelength range of 1500-1600 cm^{-1} for FTIR spectra corresponding to single and mixed systems of chitosan, whey protein and wheat starch gels at pH 5.5.

5.5 Conclusions

Mixtures of whey protein and starch have been examined earlier in terms of their phase separation behaviour and its effect on structural properties and physiological property in retarding *in-vitro* starch hydrolysis. The present work introduces chitosan in whey protein and starch preparations in an effort to further understand the molecular properties of binary and tertiary mixtures. It is clear from small and large-deformation thermomechanical measurements in this work that chitosan interferes with whey protein denaturation and subsequent agglomeration of globular particles to form a three dimensional structure. This is also evidenced in microscopy images that show an altered network arrangement of the protein in the presence of the polysaccharide. Infra-red spectra indicate that the distinct pattern of macromolecular assembly is based on direct electrostatic interactions between the oppositely charged chain segments of whey protein and chitosan at the experimental pH. The effectiveness of this barrier to molecular mobility will be examined next in relation to the *in-vitro* retardation of enzymatic hydrolysis of gelatinised starch embedded within the whey protein/chitosan matrix.

5.6 Acknowledgements

This research was fully supported under Australian Research Council's *Linkage Projects* funding scheme (project number LP100200617).

5.7 References

Aguilera, J.M., &Rojas, E. (1996). Rheological, thermal and microstructural properties of whey protein-cassava starch gels. *Journal of Food Science, 61,* 962-966.

Alishahi, A., &Aider,M. (2012). Applications of chitosan in the seafood industry and aquaculture: A review. *Food and Bioprocess Technology,* 5, 817-830.

Bastos, D.S., Barreto, B.N., Souza, H.K.S., Bastos, M., Rocha-Leao, M.H.M., Andrade, C.T., &Goncalves, M.P. (2010). Characterisation of a chitosan sample extracted from Brazillian shrimps and its application to obtain insoluble complexes with a commercial whey protein isolate. *Food Hydrocolloids, 24,* 709-718.

Bromley, E.H.C., Krebs, M.R.H., & Donald, A.M. (2006). Mechanisms of structure formation in particulate gels of β-lactoglobulin formed near the isoelectric point. *European Physical Journal E, 21,* 145-152.

Chang, K.L.B., Lin, Y.S. & Chen, R.H. (2003). The effect of chitosan on the gel properties of tofu (soybean curd). *Journal of Food Engineering, 57,* 315-319.

Chenite, A., Gori, S., Shive, M., Desrosiers, E., &Buschmann, M.D. (2006). Monolithic gelation of chitosan solutions *via* enzymatic hydrolysis of urea. *CarbohydratePolymers, 64,* 419-424.

Chen, Y.C., Wang, C.H., Lai, L.S., & Lin, K.W. (2003). Rheological properties of chitosan and its interaction with porcine myofibrillar proteins as influenced by chitosan's degree of deacetylation and concentration. *Journal of Food Science, 68,* 826-831.

Cho, J., Heuzey, M., Begin, A., &Carreau, P.J. (2006). Viscoelastic properties of chitosan solutions: Effect of concentration and ionic strength. *Journal of Food Engineering, 74,* 500-515.

Chronakis, I. S., & Kasapis, S. (1993). Structural properties of single and mixed milk/soya protein systems. *Food Hydrocolloids, 7,* 459-478.

Cooney, M. J., Rosenberg, M., & Shoemaker, C. F. (1993). Rheological properties of whey protein concentrate gels. *Journal of Texture Studies, 24,* 325-334.

El Ghaouth, A., Arul, J., Ponnampalam, R., &Boulet, M. (1991). Chitosan coating effect on storability and quality of fresh strawberries. *Journal of Food Science, 56,* 1618-1620

El Ghaouth, A., Ponnampalam, R., Castaigne, F. & Arul, J. (1992). Chitosan coating to extend the storage life of tomatoes. *HortScience, 27,* 1016-1018.

Guzey, D., &McClements, D.J. (2006). Characterisation of β-lactoglobulin-chitosan interactions in aqueous solutions: A calorimetry, light scattering, electrophoretic mobility and solubility study. *Food Hydrocolloids, 20,* 124-131.

Hong, Y., &McClements, D.J. (2007). Formation of hydrogel particles by thermal treatment of β-lactoglobulin-chitosan complexes. *Journal of Agricultural and Food Chemistry, 55,* 5653-5660.

Kachanechai, T. Jantawat, P.,& Pichyangkura R. (2008). The influence of chitosan on physicochemical properties of chicken salt-soluble protein gel. *Food Hydrocolloids, 22,* 74-83.

Kasapis, S., & Al-Marhoobi, I.M. (2005). Bridging the divide between the high- and low-solid analyses in the gelatin/κ-carrageenan mixture. *Biomacromolecules, 6,* 14-23.

Knorr, D. (1984). Use of chitinous polymers in food- a challenge for food research and development. *Food Technology, 38,* 85-89, 92-97.

Lee, A., & Hong, Y. (2009). Coacervate formation of α-lactalbumin-chitosan and β-lactoglobulin-chitosan complexes. *Food Research International, 42,* 733-738.

Martinez, A., Chornet, E., &Rodrigue, D. (2004). Steady-shear rheology of concentrated chitosan solutions. *Journal of Texture Studies, 35,* 53-74.

Manoj, P., Kasapis, S., &Hember, M. W. N. (1997). Sequence-dependent kinetictrapping of biphasic structures in maltodextrin- whey protein gels. *Carbohydrate Polymers, 32,* 141-153.

Miralles, B., Martinez- Rodriguez, A., Santiago A., van de Lagemaat, J., & Heras, A. (2007). The occurrence of a Maillard-type protein-polysaccharide reaction between β-lactoglobulin and chitosan. *Food Chemistry, 100,* 1071-1075.

Montejano, J. C., Hamann, D. D., & Lanier, T. C. (1985). Comparison of two instrumental methods with sensory texture of protein gels. *Journal of Texture Studies, 16,* 403–424.

Mounsey, J.S., O'Kennedy, B.T., Fenelon, M.A. & Brodkorb, A. (2008). The effect of heating on β-lactoglobulin-chitosan mixtures as influenced by pH and ionic strength. *Food Hydrocolloids, 22,* 65-73.

Nicolai, T., Britten, M., & Schmitt, C. (2011). β-Lactoglobulin and WPI aggregates: Formation, structure and applications. *Food Hydrocolloids, 25,* 1945-1962.

Prasanth, K.V.H., Kittur, F.S., &Tharannathan, R.N. (2002). Solid state structure of chitosan prepared under different N-deacetylating conditions. *Carbohydrate Polymers, 50,* 27-33.

Rafe, A., Razavi, S.M.A., &Farhoosh, R. (2013). Rheology and microstructure of basil seed gum and β-lactoglobulin mixed gels. *Food Hydrocolloids, 30,* 134-142.

Rahman, M. S., Machado-Velasco, K. M., Sosa-Morales, M. E. and Velez-Ruiz, J. F. (2009). Freezing Point: Measurement, Data, and Prediction. In M. S. Rahman (Ed.), *Food Properties Handbook* (2nd ed., pp. 153-192). Boca Raton: CRC.

Shahidi, F., Arachchi, J. K. V., & Jeon, Y. J. (1999). Food applications of chitin and chitosans. *Trends in Food Science and Technology, 10,* 37–51.

Simi, C.K., & Abraham, T.E. (2010). Transparent xyloglucan-chitosan complex hydrogels for different applications. *Food Hydrocolloids, 24,* 72-80.

Torres, M.A., Beppu, M.M., Santana, C.C., &Arruda, E.J. (2006). Viscous and viscoelastic properties of chitosan solutions and gels. *Brazilian Journal of Food Technology, 9,* 101-108.

Tsia, M. L., Li, C. F., &Lii, C.Y. (1997). Effects of granular structures on the pasting behaviours of starches. *Cereal Chemistry, 74,* 750-757.

van den Berg, L., van Vliet, T., van der Linden, E., van Boekel, M.A.J.S, & van de Velde, F (2007). Breakdown properties and sensory perception of whey proteins/polysaccharide mixed gels as a function of microstructure. *Food Hydrocolloids, 21,* 961-976.

van der Ven, C., Muresan, S., Gruppen, H., de Bont, D.B.A., Merck, K.B & Voragen, A.G.J. (2002). FTIR spectra of whey and casein hydrolysates in relation to their functional properties. *Journal of Agricultural and Food Chemistry, 50,* 6943-6950.

Wang, Q.Z., Chen, X.G., Liu, N., Wang, S.X., Liu, C.S., Meng, X.H., & Liu, C.G. (2006). Protonation constants of chitosan with different molecular weight and degree of deacetylation. *Carbohydrate Polymers, 65*, 194-201.

Yang, H., Irudayaraj, J., Otgonchimeg, S., & Walsh, M. (2004). Rheological study of starch and dairy ingredient-based food systems. *Food Chemistry, 86*, 571-578.

Yang, N., Liu, Y.T., Ashton, J., Gorczyca, E., &Kasapis, S. (2013). Phase behaviour and *in vitro* hydrolysis of wheat starch in mixture with whey protein. *Food Chemistry, 137*, 76-82.

Yang, N., Luan, J., Ashton, J., Gorczyca, E., & Kasapis, S. (2013). Effect of calcium chloride on the structure and *in vitro* hydrolysis of heat induced whey protein and wheat starch composite gels. *Food Hydrocolloids*, in press.

Yuan, Y., Wan, Z., Yin, S., Yang, X., Qi, J., Liu, G., & Zhang, Y. (2013). Characterisation of complexes of soy protein and chitosan heated at low pH. *Food Science and Technology, 50*, 657-664.

Chapter 6 - *In vitro* starch hydrolysis of chitosan incorporated whey protein and wheat starch composite gels

6.1 Abstract

The study examined the influence of low and medium molecular weight chitosan incorporated into whey protein isolate and wheat starch thermo gels on the *in vitro* hydrolysis of starch. Gels were subjected to the following external conditions containing α-amylase at constant incubation temperature of 37℃. In the first procedure, they were immersed in phosphate buffer (0.05M) and maintained at pH 6.9 throughout the entire digestion. In the second instance, they were introduced into a salt solution, with pH and total volume adjusted at times in sync with the human gastrointestinal tract. The amount of maltose equivalent liberated from the gel was determined using DNSA and measuring absorbance at 540nm against a maltose standard curve. Results indicate that low and medium molecular weight chitosan, in combination with whey protein isolate, was effective at enhancing the protective barrier against starch degradation. The trend was more apparent when gels were subjected to benign systems than in a dissolution medium with adjusted pH. Overall, less maltose was liberated from gels containing medium molecular weight chitosan, as opposed to the low molecular weight counterpart, and results compare favorably with the outcome of the *in vitro* digestion of binary whey protein isolate and wheat starch composites.

6.2 Introduction

Chitosan is a linear polysaccharide derived from partial alkaline N-deacetylation of chitin (Kong, Chen, Xing & Park, 2010). The molecule is comprised of glucosamine (2-amino-2-deoxy-β-D-glucopyranose) and N-acetylglucosamine [β-(1-4)-2-acetamido-2-deoxy-β-D-glucopyranose] polymers (Helgason et al., 2008; Huang, Sun, Xiao & Yang, 2012). In acidic aqueous solutions below the pKa value (~6.3), chitosan (CHT) is soluble due to protonation

of amine groups (Thongngam & McClements, 2004). The dissociated form adopts an extended conformation as a result of electrostatic repulsion and stabilisation by inter and intra molecular hydrogen bonds (Franca, Freitas & Lins, 2011).

A great deal of research has been fuelled towards the use of chitosan in many food and pharmaceutical applications based on the ability to interact with anionic components *via* electrostatic forces (Wang, Assaad, Ispas-Szabo, Mateescu& Zhu, 2011; Yuan et al., 2013). Chitosan was used successfully to precipitate β-lactoglobulin from cheese whey through complex formation with pH manipulation (Casal, Montilla, Moreno, Olano& Corzo, 2006). It exhibits antibacterial activity by direct interaction with lipopolysaccharides on the surface of Gram-negative bacteria (Kong, Chen, Xing & Park, 2010). Microencapsulation of drugs and lipids using chitosan in polymer blends has also been investigated, with a study by Honary, Maleki & Karami (2009) examining the *in vitro* release of prednisolone from CHT-alginate systems with varying CHT molecular weight. Helgason et al. (2008) aimed to enhance the understanding of CHT interactions with oil-in-water emulsion droplets. The research methodology involved simulating the conditions of the human gastrointestinal tract to provide a realistic perspective of the influence of CHT on the bioavailability of lipids.

The subject of interest in this study is starch hydrolysis and digestion, i.e. a complex physical and chemical process involving three key organs: mouth (pH ~6.5), stomach (pH ~1.5) and small intestines (pH ~6-7) (Oomen et al., 2003). The pH, food retention time, peristaltic motion and external environment, i.e. digestive enzymes, secretion of bile salts and total volume, vary vastly between and within these compartments. Each system plays a distinct role, but it is the site of the small intestine that facilitates absorption of most nutrients across the mucosa into the bloodstream (Kong & Singh, 2008).

CHT has been used extensively in the development of food products that reduce fat absorption in the gastrointestinal tract in response to pressing global concerns of obesity (Helgason et al., 2008). This is associated with Type 2 diabetes, the prevalence of which is also on a dramatic rise (Zimmet, Alberti & Shaw, 2001). Statistics estimate that in excess of a million Australians suffer from obesity and Type 2 diabetes (Health Insite, 2008). The prevention and management of the latter involves adhering to a low GI diet where carbohydrate consumption sees glucose release and absorption in a slow and steady manner (Jenkins et al., 2002; Jenkins et al., 1982; Miller 1994). In our previous work, heated whey protein isolate (WPI) and wheat starch (WS) dispersions were found to form micro phase

separated gels with a continuous protein phase supporting discontinuous polysaccharide inclusions (Yang, Liu, Ashton, Gorczyca & Kasapis, 2013). When subject to *in vitro* starch hydrolysis, the rate and degree of reducing sugar liberated from the co-gels of WPI and WS were noticeably lower than single WS systems of equal concentration. It was concluded that the binary gel matrix provided a promising basis for further development of low GI foods.

In a separate forum, it was noted that WPI was capable of stimulating the release of insulin, which is beneficial in the control of glycemic index (Belobrajdic, McIntosh & Owens, 2009; Luhovyy, Akhavan & Anderson, 2007). Since the chitosan molecule is non-toxic and biodegradable (Tan et al., 2013),there is opportunity for its inclusion in a whey protein based system. Therefore, chitosan was incorporated into WPI-WS gels and the protective effect of CHT-WPI interactions during *in vitro* starch hydrolysis was assessed. While chitosan is currently utilised as a food additive, preservative and encapsulant for drugs and lipids, to the authors' knowledge the protective effect of CHT with WPI on the hydrolysis of gelatinised starch has not been rationalised on fundamental grounds.

6.3 Materials and methods

6.3.1 Materials

Whey protein isolate (WPI) was purchased from Fonterra Co-operative Group Ltd., New Zealand. The powder consisted of 88.71% protein, 0.93% fat, 4.83% moisture and 3.3% ash (w/w). Native wheat starch (WS) was supplied from National Starch (National Starch and Chemical Co., Thailand), with the powder containing 94.1% starch, 0.3% ash, 0.1% fat and 5.5% moisture (w/w). Low molecular weight chitosan (LMW CHT), medium molecular weight chitosan (MMW CHT) and α-amylase from *Aspergillus oryzae* was supplied from Sigma-Aldrich, Co. (Castle Hill, Australia). As specified by the manufacturer, the degree of deacetylation (DDA) for both low and medium molecular weight chitosan was about 80% and the viscosity was 20-300 cP and 300-800 cP, respectively. All other chemicals utilised were of analytical grade.

6.3.2 Methods

6.3.2.1 Sample preparation

Required amounts of WPI and WS were weighed and dissolved in deionised water to produce single or binary mixtures. Both chitosans were solubilised in 1% (v/v) acetic acid prior to incorporating with the WPI-WS dispersions. The focus was on low and intermediate solid preparations, which included the following concentrations (%, w/w): 15 WPI, 7.5 WS, 15 WS, 2 LMWCHT, 2 MMWCHT, 15 WPI-7.5 WS, 15 WPI-15 WS, 15 WPI-2 LMWCHT, 15 WPI-2 MMWCHT, 7.5 WS-2 LMWCHT, 7.5 WS-2 MMWCHT, 15 WS-2 LMWCHT, 15 WS-2 MMWCHT, 15 WPI-7.5 WS-2 LMW CHT, 15 WPI-7.5 WS-2 MMWCHT, 15 WPI-15 WS-2 LMWCHT and 15 WPI-15 WS-2 MMWCHT. The fixed amounts of 15% WPI, 7.5% WS, 15% WS and 2% CHT were chosen based on the physicochemical and structural characterisation of these systems in Yang, Liu, Ashton, Gorczyca & Kasapis (2013), and it is the intention presently to build on these research efforts that produced a level of understanding. All samples were adjusted to pH 5.5 by the addition of HCl or NaOH;at pH 5.5,WPI is above its pI of ~5.1 and CHT, below its pKa value of ~6.3. Adjusting the pH to 5.5 targeted maximum electrostatic bonding between predominantly negatively charged WPI and cationic CHT.

Since the storage length of chitosan solutions has shown to significantly impact the functional properties (Tan et al., 2013), all dispersions in the present study were freshly prepared. They were subsequently cooked in an 85 ± 1°C waterbath for 75 min to form thermogels ready for use in the hydrolysis experiments. Huang, Xiao & Yang (2012) highlighted that temperature affects the complexation of protein with polysaccharides and found reduced levels of soy protein isolate and chitosan coacervation at high temperature (55°C). In the present study, all samples were subjected to the same temperature and time cooking regime to eliminate such effect on electrostatic interactions, hydrogen bonding and hydrophobic associations leading to experimental variation in the hydrolysis results. Gelatinised starch is contained in most foods hence we tried to mimic real food systems where possible by heat application to transform polymer dispersions into viscosity enhancing gels.

6.3.2.2 In vitro starch hydrolysis

Thermogels were pushed through a screen sieve (opening size of 1.0 mm) and 3g of the sample was subjected to α-amylase hydrolysis in two set-up conditions. In the first set up, gels were hydrolysed in benign systems with an external medium consisting of anhydrous monobasic sodium phosphate buffer (0.05M) adjusted to pH 6.9. The pH remained consistent throughout the entire period of experimentation. The second layout of amylolysis proved slightly more complex by factoring in time and pH adjustment of the external medium to reflect to a certain extent that of the human gastrointestinal tract. In this scenario, gels were immersed in a salt solution adapted from the work of Rabe, Krings, & Berger (2004). The medium was adjusted to pH 6.5 for 5 min followed by a decrease to pH 1.5 for 30 min. Subsequently, the pH was raised to 6.4 for 1h, pH 6.9 for 1h and pH 7.3 for 1h.

All enzyme hydrolysis experiments were conducted at 37±1°C for 215 min. The total volumes were also taken into account to reflect those likely to be found in the human digestive tract for both set-up protocols. Aliquots were taken at the initial 5 min mark and then for every 30 min until the end of experimentation. The enzyme was deactivated by heat and samples were centrifuged at 4,000 rpm for 15 min. Hydrolytic activity was measured by quantifying the liberated maltose equivalent from the supernatant using a 3,5-dinitrosalicyclic acid (DNSA) assay according to Bernfeld (1955). The absorbance was measured at 540 nm and compared against a good quality maltose standard curve (r^2= 0.99). All samples were replicated three times and the mean with standard error were calculated and reported.

6.4 Results and discussion

6.4.1 The effect of chitosan on the retardation of starch hydrolysis in benign systems

Previous work examined the microstructure of gels formed by whey protein and wheat starch in concentrations applicable to the current study (Yang, Liu, Ashton, Gorczyca & Kasapis, 2013). The multidisciplinary approach of analysis pointed to the formation of a micro phase separated gel that was predominantly WPI continuous and WS discontinuous. Findings from the *in vitro* starch hydrolysis component of that study showed a decreased amount of maltose equivalent liberated from binary WPI-WS gels in comparison to single WS systems.

While other authors agree that protein can hinder starch hydrolysis by the formation of disulphide bonds and physically blocking enzymes from accessing starch, there is further

complexity to consider with the introduction of chitosan in these systems. (Goni, Garcia-Alonso & Saura-Calixto, 1997; Oates, 1997; Singh, Dartois & Kaur, 2010). β-lactoglobulin in the presence of chitosan forms aqueous solutions, following pH adjustment to 5.5 and heating at 78°C for 10 min, where about half of the polymeric material is in the form of soluble complexes(Mounsey, Kennedy, Fenelon& Brodkorb, 2008). It was further established that in the presence of chitosan and by heating above the protein's denaturation temperature extensive aggregation can be eliminated.

In Chapter 5 of this Thesis, we followed the thermal transformation of whey protein and wheat starch in the presence of chitosan at pH 5.5. The storage modulus in shear of the 15 WPI-2 MMW CHT system did not increase dramatically after exceeding the denaturation temperature (77°C) of the protein. Texture profile analysis of the 15 WPI-2 MMW CHT recorded lower hardness values than for 15 WPI at the same experimental conditions. These findings, in conjunction with electron microscopy work, suggest that 15 WPI with 2MMW CHT did not aggregate to the same degree as the single protein preparation. Nonetheless, the addition of CHT to WPI-WS gels significantly enhances the effect of protecting starch from enzyme hydrolysis, as shown below from work in this chapter.

In the benign set up, a significant reduction in the amount of starch hydrolysed from WPI-WS gels containing 2 MMW CHT was seen throughout all time points of sampling. Figure 6.1 optimises the presentation of our work by illustrating only one set of results with error bars. The total maltose liberated from the 15 WPI-7.5 WS gel with and without 2 MMW CHT at 5 min is 42.2 and 64.9 mg/g, respectively. By the end of the experiment, maltose liberation in the presence and absence of chitosan corresponded to 47.0 and 69.0 mg/g. It appears that gels containing higher concentrations of WS did not affect the role played by the addition of 2 MMW CHT either. Thus in the presence of 2 MMW CHT, the 15 WPI-15 WS systems presented a greater degree of starch retardation from enzyme action than for whey protein-starch samples (Figure 6.2).

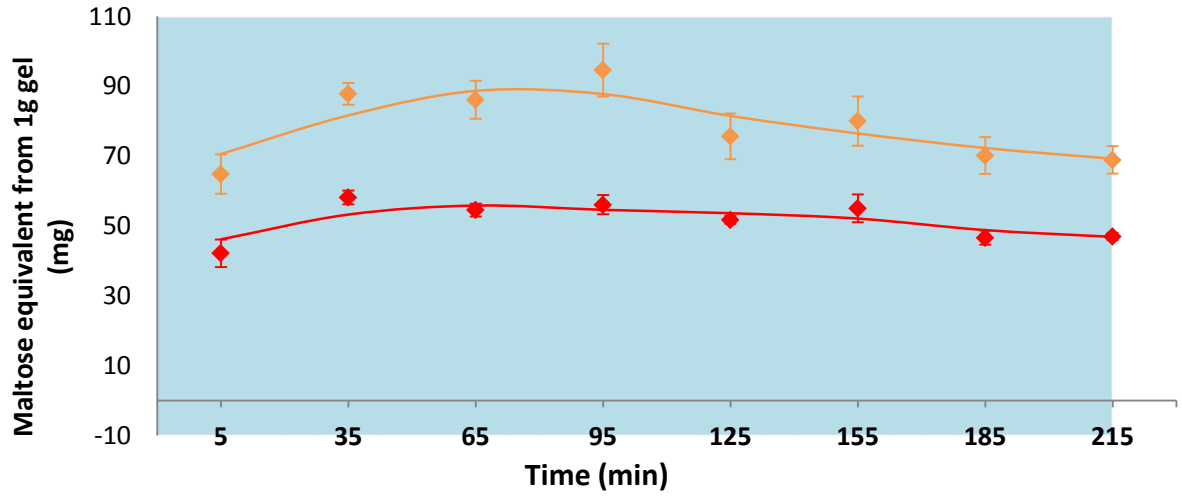

Figure 6.1 Total maltose equivalent and weighted moving average of total maltose equivalent liberated from 15% whey protein 7.5% wheat starch (♦)(-), and 15% whey protein 7.5% wheat starch with 2% medium molecular weight chitosan gel (♦)(-), during *in vitro* digestion at constant pH 6.9 condition.

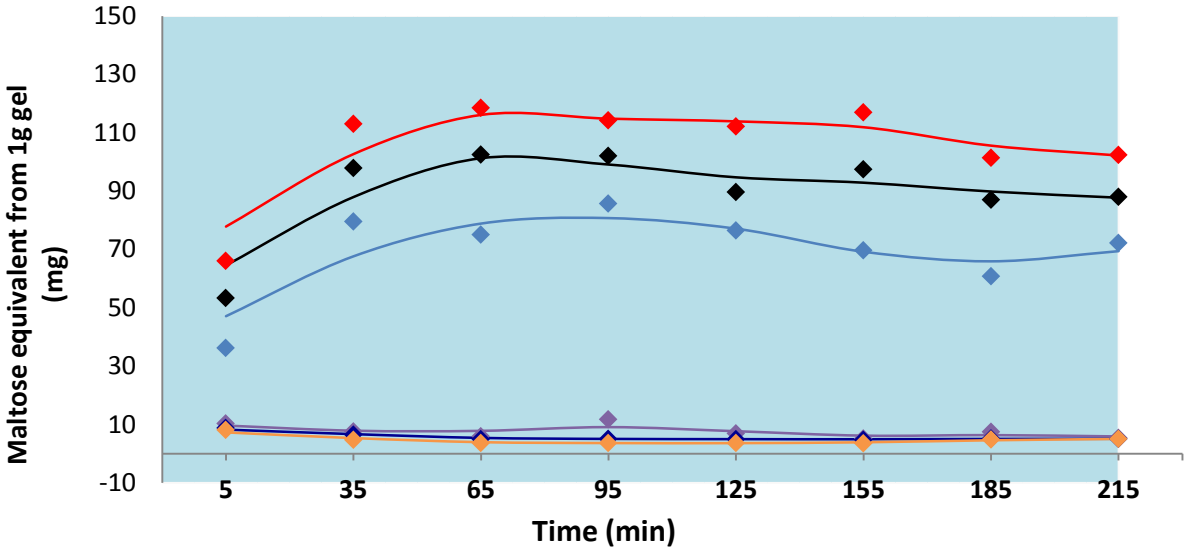

Figure 6.2 Total maltose equivalent and weighted moving average of total maltose equivalent liberated from gels of 2% medium molecular weight chitosan (♦)(-), 15% wheat starch (♦)(-), 15% whey protein (♦)(-), 15% whey protein with 2% medium molecular weight chitosan (♦)(-), 15% whey protein with 15% wheat starch (♦)(-) and 15% whey protein 15% wheat starch with 2% medium molecular weight chitosan (♦)(-), during *in vitro* digestion at constant pH 6.9 condition.

That was again true for all time points of analysis with the same quality of result variation (error bars are not shown in subsequent figures to avoid clutter). To be specific, the total maltose liberated from 15 WPI-15 WS gel with and without 2 MMW CHT at 5 min is 36.3 and 53.5 mg/g, respectively in Figure 6.2. At the 215 min mark, the 15 WPI-15 WS gel with and without 2 MMW CHT had been hydrolysed to a maltose equivalent of 72.3 and 88.0 mg/g. Although to a lesser extent, an overall reduction in hydrolysis of starch was also seen when we changed the formulation to low molecular weight chitosan. The total maltose liberated from the 15 WPI-15 WS with and without 2 LMW CHT at 215 min is 82.7 mg/g and 88.0 mg/g, respectively in Figure 6.3.

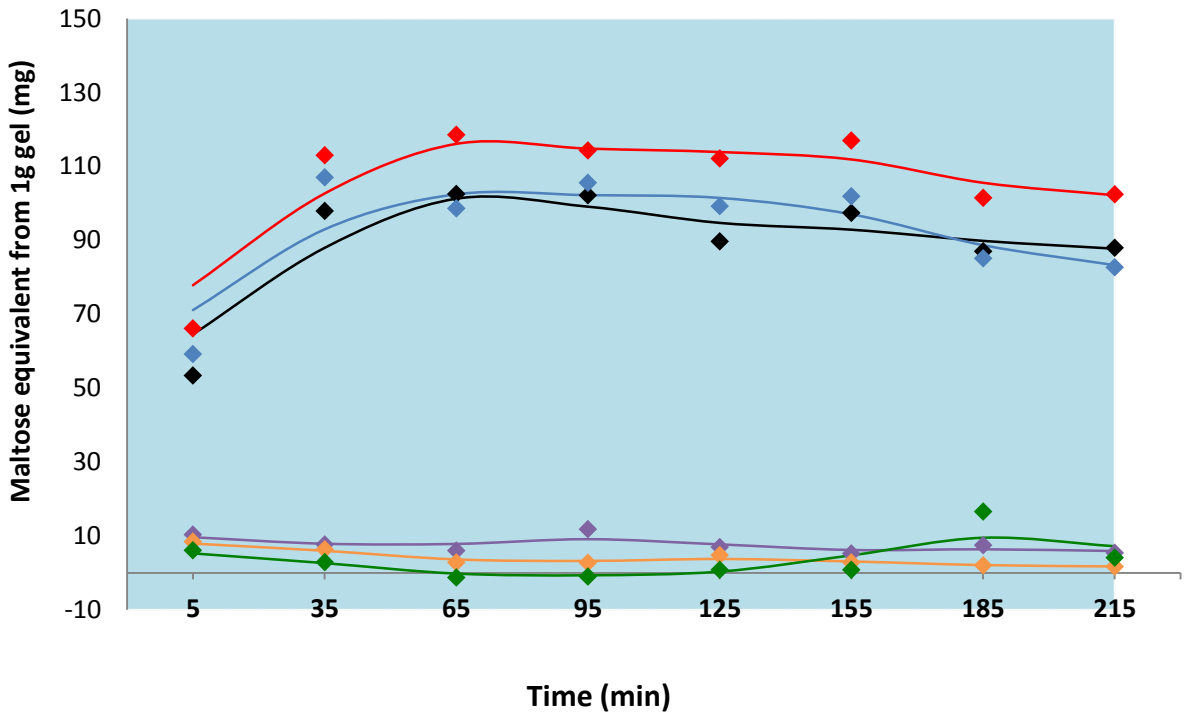

Figure 6.3 Total maltose equivalent and weighted moving average of total maltose equivalent liberated from gels of 2% low molecular weight chitosan (♦)(-), 15% wheat starch (♦)(-), 15% whey protein (♦)(-), 15% whey protein with 2% low molecular weight chitosan (♦)(-), 15% whey protein with 15% wheat starch (♦)(-) and 15% whey protein 15% wheat starch with 2% low molecular weight chitosan (♦)(-), during *in vitro* digestion at constant pH 6.9 condition.

The rate of hydrolysis in the benign set up for 15 WPI-15 WS gels with and without chitosan is presented in Figure 6.4. For all gels, the majority of starch degradation occurs within the first 65 min with a dramatic decrease thereafter. Rapid hydrolytic behaviour is the outcome of polymeric sites being exposed early to enzyme activity following the protocol of this investigation. However, the rate of hydrolysis was much higher in 15 WPI-15 WS gels at the first time interval of 30 min (Yang, Liu, Ashton, Gorczyca & Kasapis, 2013). The concentration corresponding to the highest rate of hydrolysis throughout the entire experiment is 15 WS. This is attributed to the full exposure of enzyme to substrate sites of starch in the absence of non-digestible polymer barriers. In the first 5 min of hydrolysis an equivalent of 13.2 mg maltose was liberated from each g of the 15 WS gel. On the other hand, only 7.3 mg maltose was released from each g of the 15 WPI-15 WS-2 MMW CHT gel. The latter exhibited the lowest rate of maltose release in comparison to all other samples.

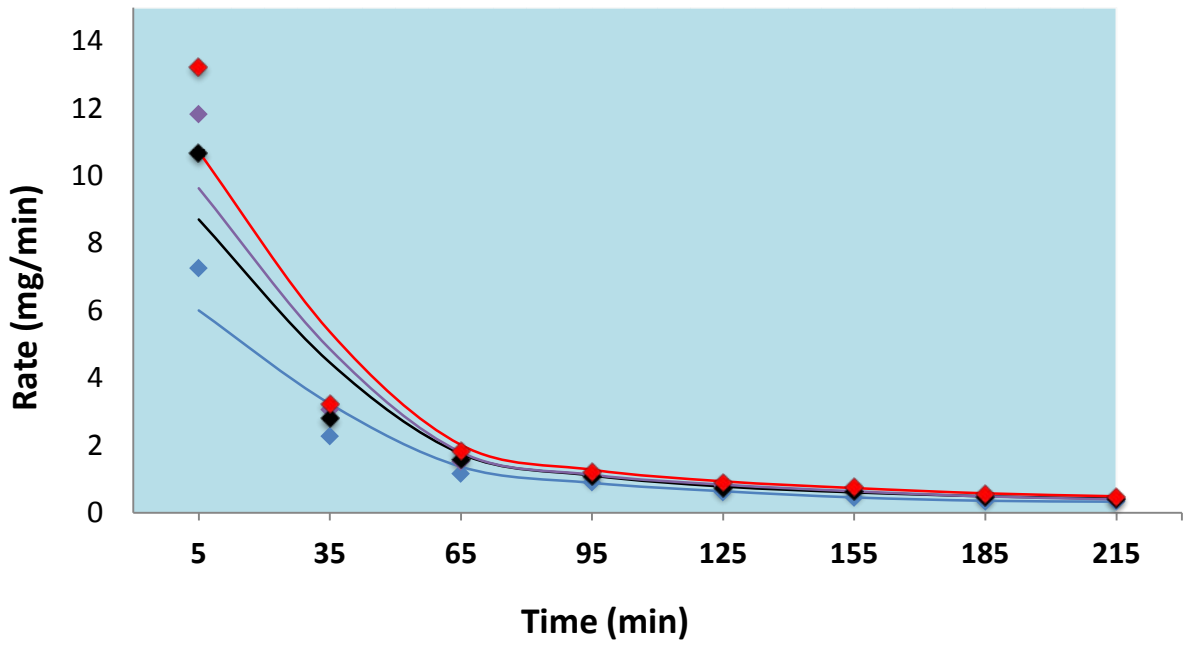

Figure 6.4 Rate of total maltose equivalent and weighted moving average of total maltose equivalent liberated from gels of 15% wheat starch (♦)(-),15% whey protein with 15% wheat starch (♦)(-), 15% whey protein 15% wheat starch with 2% medium molecular weight chitosan (♦)(-) and15% whey protein 15% wheat starch with 2% low molecular weight chitosan (♦)(-) during *in vitro* digestion at constant pH 6.9 condition.

The main reason for the relatively low amount and rate of maltose release from CHT incorporated systems is related to electrostatic associations of the two oppositely charged WPI and CHT components. This driving force has been extensively acknowledged in literature (Lee & Hong, 2009; Montilla et al., 2007; Thongngam & McClements, 2004; Yuan et al., 2013), and was documented in Chapter 5of this thesis using FTIR. Through the association, the WPI continuous phase, which was previously shown to protect starch from hydrolysis, is enhanced considerably. Moreover, Huang, Sun, Xiao & Yang (2012) observed, in SEM micrographs of soybean protein isolate and chitosan coacervates, noticeable vacuoles in the complex network. In our system, these pores would be equivalent to the location of wheat starch. The hydrolytic activity may also be hindered indirectly by interfering with starch gelatinisation. As noted by Tester & Sommerville (2003), a non starch polysaccharide like CHT could decrease the free volume and mobility of water molecules necessary in the gelatinisation process. This “antiplasticising” effect of CHT means that starch is not gelatinised to its full potential with a subsequent decrease in the amount available for enzymatic hydrolysis.

The disparity in structural functionality due to varying the molecular weight distribution of chitosan has been highlighted in literature (Roberts, 1992).Addition of high viscosity chitosan could immobilise water to delay starch gelatinisation and interact efficiently with whey protein at the right pH. A significant difference does exist between the amount of maltose liberated from CHT of medium and low molecular weight. In the first 5 min of hydrolysis, 15 WPI-15 WS-2 MMW CHT yielded 36.3 mg/g, as opposed to is 59.2 mg/g in 15 WPI-15 WS-2 LMW CHT (Figures 6.2 and 6.3, respectively). The amount of wheat starch that has been hydrolysed by 215 min from 15 WPI-15 WS-2 MMWCHT (72.3 mg/g) was also lower than for 15 WPI-15 WS-2 LMW CHT (82.7 mg/g) in the same illustrations.

Honary, Maleki & Karami (2009) studied chitosan of varying molecular weights and the impact on the release rate of prednisolone when complexed with alginate. It was found that limited contact (3 h) was sufficient in systems with high molecular weight chitosan to effectively reduce the rate of prednisolone release due to extensive electrostatic bonding between $-NH_3^+$groups of chitosan and $-COO^-$ of alginate. Low molecular weight chitosan required extra time to diffuse and react with the alginate (24 h), but maximum binding of the high molecular weight counterpart with alginate occurred within 4 h.

Preparation of gels in the present study took under 3h and that setting was held constant, but the time taken for CHT to interact with WPI will vary as a result of viscosity and experimental conditions in preparations. The low molecular weight material should have limited ability to bind effectively with whey protein, a difference that is magnified in the starch hydrolysis results. In fact, while the extent of starch degradation per unit of time corresponding to 15 WPI-15 WS-2 MMWCHT was the lowest, 15 WPI-15 WS-2 LMW CHT tended to be on par with that of 15 WPI-15 WS in the absence of chitosan (Figure 6.4).

6.4.2 The effect of chitosan on the retardation of starch hydrolysis in changing pH systems

By tweaking the pH value of the dissolution medium, the amount of maltose liberated from the gels for each experimental concentration in polymeric mixtures is variable, as shown in Figures 6.5 and 6.6. The amount of reducing sugar liberated from 15 WPI-15 WS, 15 WPI-15 WS-2 LMW CHT and 15 WPI-15 WS-2 MMW CHT in the first 5 min corresponds to 85.3, 68.0 and 81.4mg/g, respectively (Figure 6.6). In the benign set up, corresponding to the same treatment time and material concentration, these values are 53.5, 59.2 and 36.3 mg/gfrom data in Figures 6.2 and 6.3. Maltose liberated in the changing pH system was significantly higher in all aforementioned concentrations. Since the value of pH remained the same with earlier experimentation for the first 5 min, the disparity between the values of the two set up protocols could not originate from pH adjustment.

The two systems, however, vary in the composition of the external medium, with a phosphate buffer or a salt solution being the physicochemical environments of choice. Researchers have previously highlighted that the presence of NaCl can interfere with the formation of electrostatically charged complexes. For example, Thongngam & McClements (2004) noted that complexation of chitosan with the anionic surfactant sodium dodecyl sulfate (SDS) was noticeably weaker in the presence of 100mM NaCl. It was concluded that salt shielded charges on chitosan hence screening electrostatic interactions with SDS. Similarly, the soy protein isolate-chitosan coacervation was reduced within a salt solution (Huang, Sun, Xiao & Yang, 2012). It appears, therefore, that the competitive binding of NaCl reduces the strength of the protective barrier for WS by discouraging close proximity and direct electrostatic associations between whey protein and chitosan in our mixtures.

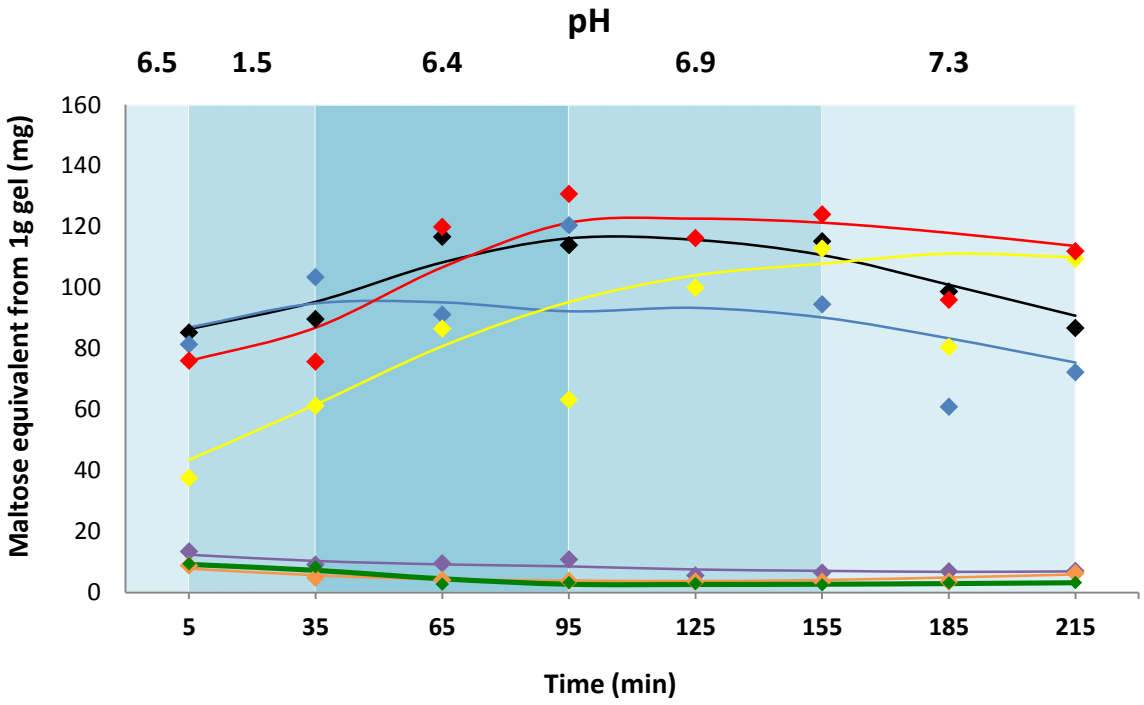

Figure 6.5 Total maltose equivalent and weighted moving average of total maltose equivalent liberated from gels of 2% medium molecular weight chitosan (♦)(-),15% wheat starch (♦)(-), 15% whey protein (♦)(-), 15% wheat starch with 2% medium molecular weight chitosan (♦)(-), 15% whey protein with 2% medium molecular weight chitosan(♦)(-), 15% whey protein with 15% wheat starch (♦)(-) and 15% whey protein 15% wheat starch with 2% medium molecular weight chitosan (♦)(-), during *in vitro* digestion with pH values mimicking those found in the human gastrointestinal tract.

Following the first 5 min of hydrolysis, the pH is reduced to 1.5 to mimic the acidity of the stomach and, at this interval, WPI is well below its pI and CHT below its pKa. Both polymers assume a positive net charge and electrostatic association is reduced. It is also important to note that as a response to low pH, the structure and active sites of WPI and *α*-amylase are prone to alteration. Indeed, the manufacturer has specified that *α*-amylase activity exists in a pH range of 5.5 to 10, which implies that at pH 1.5, α-amylase activity is at most minimal. This assumption is justified by comparing with the corresponding conditions in the benign system, where the increase in the amount of sugar liberated from the 5 to 35 min mark is consistently higher.

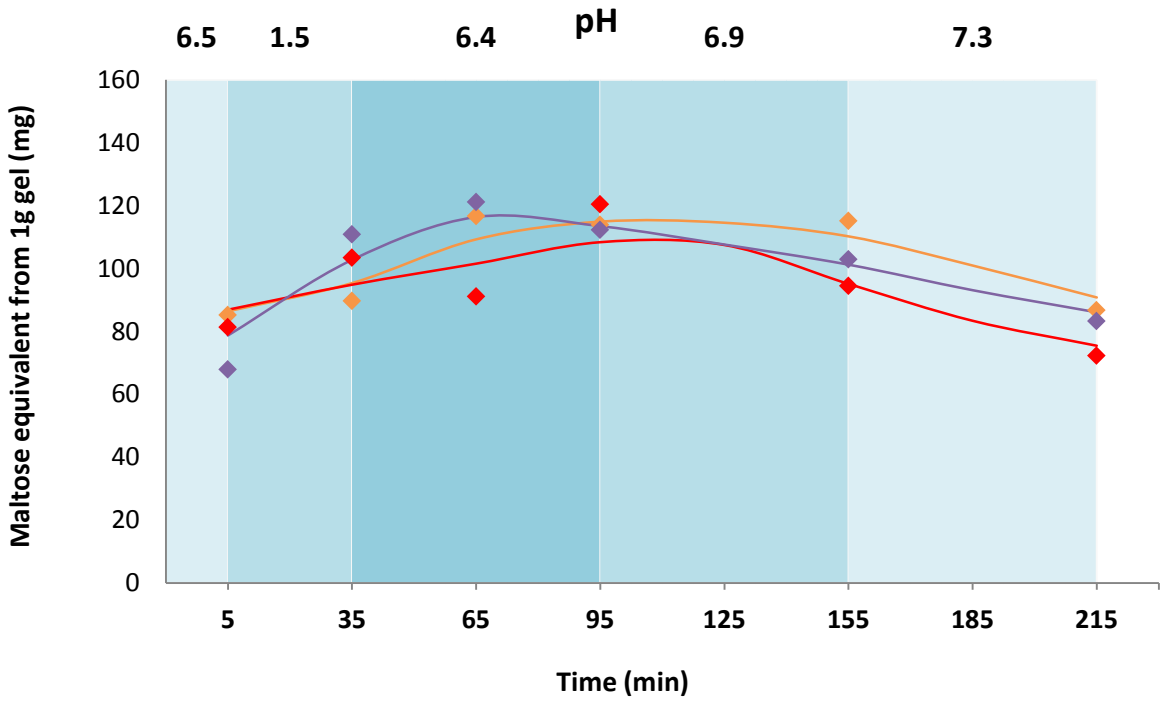

Figure 6.6 Total maltose equivalent and weighted moving average of total maltose equivalent liberated from gels of 15% whey protein 15% wheat starch (♦)(-), 15% whey protein 15% wheat starch with 2% medium molecular weight chitosan (♦)(-) and 15% whey protein 15% wheat starch with 2% low molecular weight chitosan (♦)(-), during *in vitro* digestion with pH values mimicking those found in the human gastrointestinal tract.

That was the case for all relevant concentrations, i.e. 15 WPI-15 WS, 15 WPI-15 WS-2 MMW CHT and 15 WPI-15 WS-2 LMW CHT. Thus, the incremental difference between 5 and 35 min in Figure 6.5, as the maltose equivalent was measured from the 15 WPI-15 WS gel in the pH dropping system, is only 4.5 mg/g. By comparison, the corresponding difference in the system with constant pH is 44.5 mg/g (Figure 6.2). The amount of starch hydrolysed from 5 to 35 min in the 15 WPI-15 WS-2MMW CHT gel is 22.1 mg/g (Figure 6.5), whereas in the benign system the latter corresponds to 43.3 mg/g (Figure 6.2). Since the maltose equivalent values between 5 to 35 min are still increasing, one may deduce that the diminishing protective effect of whey protein-chitosan mixture is downplayed by the reduced α-amylase activity.

Following the 35 min mark, at every hour the pH is adjusted to simulate conditions applicable to the duodenum (pH 6.4), jejunum (pH 6.9) and ileum (pH 7.3). In this part of the work, $NaHCO_3$ is used to increase the total volume and, in conjunction with HCl, adjust the pH at every hour interval. Hydrochloric acid reacts with $NaHCO_3$ and the nature of the reaction further fluctuates the pH. More specifically, at pH values below 7, the reaction of $NaHCO_3$ with HCl can increase the pH to about neutral, whereas when the pH of the medium is above 7, HCl addition decreases pH. The reaction causes pH mediated changes in charge density affecting the overall protection afforded from the WPI-CHT barrier against starch hydrolysis.

Environmental conditions related to small intestine dictate that the pH deviates from the pKa value of chitosan as digestion progresses. This is a critical issue documented in the literature by Hong & McClements (2007) when examining the stability of protein-coated lipid droplets with chitosan addition. Modulation of pH from 5 to 7 led to a steep decrease in zeta potential, which translated to increasing deprotonation of the charged amino groups. Montilla et al. (2007) also stressed the particular sensitivity of chitosan to changing acidity, and in our case it means that the effect of adjusting the pH from 6.4, 6.9 through to 7.3 would reduce the overall positive charge of chitosan.

The maltose equivalent liberated at the end of the experimental routine from the 15 WPI-15 WS-2 LMW CHT gel in the benign and changing pH systems is 82.7 and 82.3 mg/g, respectively, in Figures 6.3 and 6.6. The maltose liberated from 15 WPI-15 WS-2 MMW CHT at 215 min in the benign and changing pH set up is 72.2 and 72.4 mg/g, respectively, in Figures 6.2 and 6.5. Results indicate that medium molecular weight chitosan is a more efficient barrier to enzymatic hydrolysis of starch, as compared to the low molecular weight counterpart. By the end of the starch hydrolysis experiments, liberated maltose for both types of the polysaccharide is congruent in the benign and changing pH preparations. This outcome argues that the electrostatic interactions of chitosan and whey protein are reestablished to a good extent in the slightly acidic to alkaline environment of the small intestine following imitation of the highly acidic condition in the stomach.

6.5 Conclusions

Low to intermediate solid thermogels consisting of single, binary and tertiary systems of whey protein, wheat starch and chitosan were prepared and subjected to *in vitro* starch hydrolysis. A marked decrease in the total amount and rate of maltose equivalent liberated from the CHT incorporated WPI-WS gels was evident. While the protection of wheat starch by the CHT-WPI mixture was more consistent throughout the experiment in systems with constant near neutral pH, the trend could still be established in preparations with changing pH of the dissolution medium to imitate conditions from the mouth through the stomach to the small intestine in the human gastrointestinal tract. Fluctuations of liberated maltose measured inthe changing pH systemargue that the interactions between chitosan and whey protein are electrostatic in origin. In both hydrolysis scenarios, the medium molecular weight chitosan afforded greater starch protection than the low molecular weight counterpart. Reduction in starch hydrolysis by incorporating medium molecular weight chitosan into WPI-WS gels of changing pH from 1.5 to 7.3, to mimic conditions in the stomach and ileum, provides a good basis for future research in the development of low GI food products. This will require consideration of a more complete digestive environment including pepsin and bile salts present in the human gastrointestinal tract.

6.6 Acknowledgements

This research was fully supported under Australian Research Council's *Linkage Projects* funding scheme (project number LP100200617).

6.7 References

Belobrajdic, D.P., McIntosh, G.H. & Owens, J.A. (2009). A high-whey-protein diet reduces body weight gain and alters insulin sensitivity to red meat in wistar rats. *Tropical Journal of Pharmaceutical Research, 8,* 53-61.

Bernfeld, P. (1955). Amylases, α and β. In S.P. Colowick & N.O. Kaplan (Eds.), *Methods in enzymology* (pp. 149-158). New York: Academic Press.

Casal, E., Montilla, A., Moreno, F.J., Olano, A., & Corzo, N. (2006). Use of chitosan for selective removal of beta-lactoglobulin from whey. *Journal of Dairy Science, 89,* 1384-1389.

Franca, E.F., Freitas, C.G., & Lins, R.D. (2011). Chitosan molecular structure as a function of N-acetylation. *Biopolymers, 95,* 448-460.

Goni, I., Garcia-Alonso, A., & Saura-Calixto, F. (1997). A starch hydrolysis procedure to estimate glycemic index. *Nutrition Research, 17,* 427-437.

Health Insite, An Australian Government Initiative, Reviewed Sepetember 2008. "Diabetes Facts", Publisher: Nutrition Australia <http://www.healthinsite.gov.au/topics/Diabetes_Statistics>

Helgason, T., Weiss, J., McClements, D.J., Gislason, J., Einarsson, J.M., Thormodsson, F.R., & Kristbergsson, K. (2008). Examination of the interaction of chitosan and oil-in-water emulsions under conditions simulating the digestive system using confocal microscopy. *Journal of Aquatic Food Product Technology, 17,* 216-233.

Honary, S., Maleki, M., & Karami, M. (2009). The effect of chitosan molecular weight on the properties of alginate/chitosan microparticles containing prednisolone. *Tropical Journal of Pharmaceutical Research, 8,* 53-61.

Hong, Y., & McClements, D.J. (2007). Modulation of pH sensitivity of surface charge and aggregation stability of protein-coated lipid droplets by chitosan addition. *Food Biophysics, 2, 46-55.*

Huang, G., Sun, Y., Xiao, J., & Yang, J. (2012). Complex coacervation of soybean protein isolate and chitosan. *Food Chemistry, 135,* 534-539.

Jenkins, D.J.A, Kendall, C.W.C., Augustin, L.S.A., Franceschi, S., Hamidi, M., Marchie, A., Jenkins, A.L. & Axelsen, M. (2002). Glycemic index: overview of implications in health and disease. *The American Journal of Clinical Nutrition, 76,* 2665-2735.

Jenkins, D.J.A., Wolever, T.M.S, Taylor, R.H., Griffiths, C., Kizeminska, K., Lawrie, J.A., Bennett, C.M., Goff, D.V., Sarson, D.L., Bloom, S.R., (1982). Slow release dietary carbohydrate improves second meal tolerance. *American Journal of Clinical Nutrition, 35,* 1339-1346.

Kong, F. & Singh, R.P. (2008). Disintegration of solid foods in human stomach. *Journal of Food Science, 73,* 67-80.

Kong, M., Chen, X.G., Xing, K., & Park, H.J. (2010). Antimicrobial properties of chitosan and mode of action: A start of the art review. *International Journal of Food Microbiology, 144, 51-63.*

Lee, A., & Hong, Y. (2009). Coacervate formation of α-lactalbumin-chitosan and β-lactoglobulin-chitosan complexes. *Food Research International, 42,* 733-738.

Luhovyy, B.L., Akhavan, T., & Anderson, G.H. (2007). Whey proteins in the regulation of Food Intake and Satiety, *Journal of the American College of Nutrition, 26,* 704S-712S.

Miller, J.B. (1994). Importance of glycemix index in diabetes. *Americal Journal of Clinical Nutrition, 59* (Suppl.), S747-S752.

Mounsey, J.S., O'Kennedy, B.T., Fenelon, M.A. & Brodkorb, A. (2008). The effect of heating on β-lactoglobulin-chitosan mixtures as influenced by pH and ionic strength. *Food Hydrocolloids, 22,* 65-73.

Montilla, A., Casal, E., Moreno, F.J., Belloque, J., Olano, A., & Corzo, N. (2007). Isolation of bovine β-lactoglobulin from complexes with chitosan. *International Dairy Journal, 17,* 459-464.

Oates, C.G. (1997). Towards an understanding of starch granule structure and hydrolysis. *Trends in Food Science & Technology, 8,* 375-382.

Oomen, A.G., Rompelberg, C.J.M., Bruil, M.A., Dobbe, C.J.G., Pereboom, D.P.K.H. & Sips, A.J.A.M (2003). Development of an *in vitro* digestion model for estimating the bioaccessibility of soil contaminants. *Archives of Environmental Contamination and Toxicology, 44*, 281-287.

Rabe, S., Krings, U., & Berger, R.G. (2004). *In vitro* study of the influence of physiological parameters on dynamic in-mouth flavor release from liquids. *Chemical Senses, 29*, 153-162.

Roberts, G.A.F. 1992. Chitin Chemistry. London: The Macmillan Press Ltd.

Singh, J., Dartois, A., & Kaur, L. (2010). Starch digestibility in food matrix: A review. *Trends in Food Science & Technology, 8,* 375-382.

Tan, C., Xue, J., Eric, K., Feng, B., Zhang, X., & Xia, S. (2013). Dual effects of chitosan decoration on the liposomal membrane physicochemical properties as affected by chitosan concentration and molecular conformation. *Journal of Agricultural and Food Chemistry, 61*, 6901-6910.

Tester, R.F., & Sommerville, M.D. (2003). The effects of non-starch polysaccharides on the extent of gelatinisation, swelling and α-amylase hydrolysis of maize and wheat starches. *Food Hydrocolloids, 17,* 41-54.

Thongngam, M., & McClements, D.J. (2004). Characterisation of interactions between chitosan and an anionic surfactant. *Journal of Agricultural and Food Chemistry, 52,* 987-991.

Ulleberg, E.K., Comi, I., Holm, H., Herud, E.B., Jacobsen, M., & Vegarud, G.E. (2011). Human gastrointestinal juices intended for use in *in vitro* digestion models. *Food Digestion, 2,* 52-61.

Wang, Y.J., Assaad, E., Ispas-Szabo, P., Mateescu, M.A., & Zhu, X.X. (2011). NMR imaging of chitosan and carboxymethyl starch tablets: Swelling and hydration of the polyelectrolyte complex. *International Journal of Pharmaceutics*, *419*, 215-221.

Yang, N., Liu, Y., Ashton, J., Gorczyca, E., & Kasapis, S. (2013). Phase behaviour and *in vitro* hydrolysis of wheat starch in mixture with whey protein. *Food Chemistry, 137,* 76-82.

Yuan, Y., Wan, Z., Yin, S., Yang X., Qi, J., Liu, G., & Zhang, Y. (2013). Characterisation of complexes of soy protein and chitosan heated at low pH. *LWT Food Science and Technology, 50,* 657-664.

Zimmet, P., Alberti, G.M.M. & Shaw, J. 2001. Global and societal implications of the diabetes epidemic. *Nature, 414,* 782-787.

Chapter 7 - Conclusions and future work

The essence of starch hydrolysis is to provide metabolic value but concerns have been voiced over the high glycemic load, which involves rapid influx of glucose into the bloodstream. Consumption of high glycemic-index foods is associated with an increased risk of obesity and Type 2 diabetes, both diseases that are of global concern. Micro phase separation of protein and polysaccharide gels has previously provided an effective means of achieving the desired structure, texture and mouthfeel in food formulations that relate to the replacement of fat, sugar and gelatin. The basis of these macromolecular phenomena is thermodynamic incompatibility resulting in the segregation of distinct components and minimal mixing between counterparts in binary systems, which can be permanently captured in the matrix of gelling polymers. While micro phase separation has been effective for achieving desirable organoleptic traits, to the author's knowledge this is the first endeavour in trialling the fundamental basis of such to reduce the extent and rate of starch hydrolysis.

The experiments conducted in this thesis commenced with characterising the physicochemical properties of single and binary systems of whey protein isolate (WPI) and native wheat starch (WS). Low-to-intermediate solid concentrations of biopolymer mixtures proved to form micro phase separated gels that were WPI continuous and WS discontinuous, as deduced from a multidisciplinary approach of analysis. At the end of the heating (25-85°C) and cooling (85-5°C) regimes of 15 WPI 15 WS mixtures, the storage modulus (G') reflected a significantly higher gel strength than the sum of the individual components, an outcome which is evident of solvent partitioning and effective concentration of the two polymer phases. This trend was found to be qualitatively consistent upon measuring textural hardness of the gels subject to single cycle compression tests. From the differential scanning calorimetry studies, peaks reflecting starch gelatinisation and protein denaturation were detected and the absence of any other thermal events proved that no associative physicochemical interactions were apparent between polymers. In addition, mechanical experiments showed that the gelation of mixed systems occurred at heating temperatures (70°C) more closely aligned to the aggregation of protein (73°C) rather than the gelatinisation of starch (60°C). Upon subjecting gels to *in vitro* starch digestion, a considerable reduction in enzymolysis was demonstrated in WPI included WS gels providing a promising basis for formulations with reduced glycemic load.

Following the characterisation of binary networks, $CaCl_2$ at a wide range of concentrations (5-192 mM) was introduced into the system and analysed with similar techniques. In the rheology work, the significant increase in G' arising from protein aggregation after denaturation was detected at earlier temperatures in the presence of the counterion. As for DSC analysis, the presence of $CaCl_2$ in WPI systems did not significantly affect the temperature of the endothermic reactions indicating the influence of the electrolyte with WPI was concerned with the macromolecular network. The behaviour of the electrolyte on the network formed was concentration dependent and the protection of starch during *in vitro* digestion experiments was most effective at intermediate $CaCl_2$ levels. More specifically, binary polymer systems incorporating 48 mM $CaCl_2$ provided the optimum spatial structure against enzymatic starch degradation, but lower or higher concentrations were less ideal as such resulted in minimal or aggressive protein aggregation, respectively, leading to an inefficient network.

The third chapter of results furthers the conquest to protect starch *via* enhancing the protein coating with another polymer. It was hypothesised such was achievable with medium molecular weight chitosan (MMW CHT), as it was previously reported to exhibit a cationic character and interact with anionic polyelectrolytes under specific conditions. Thus, the physicochemical properties of the heteropolysaccharide were assessed at various concentrations and pH of practical interest. Since heating and cooling of 2% MMW CHT at pH of 5.5 corresponded to a smooth development of the highest network strength, it was the chosen combination for further analysis in composite systems. Mechanical spectra exemplified a clear interference in the thermal development of protein networks with the incorporation of MMW CHT otherwise evident with the protein alone. The DSC studies prove such disturbance was not a result of covalent bonding, since no “abnormalities” were detected in the thermogram of the mixture. ATR-FTIR was employed to identify the functional groups involved in possible physical interactions between chitosan and whey protein. In further validation of the DSC work, composite systems in the infrared spectra appeared as superposed but augmented species of the individual components. When the absorbance peaks was quantified, an increased peak area of absorbance in the amide II region was apparent in the MMW CHT incorporated WPI gels revealing a higher degree of morphological arrangement *via* electrostatic interactions. The absorbance peak was further intensified with the incorporation of WS, which provides evidence of effective polymer concentration, with starch being sterically excluded from the whey protein/chitosan phase.

The last set of experiments involved subjecting gels of the previously chosen 2% MMW CHT with WPI and WS to *in vitro* starch digestion. The experiments also involved a comparison of the MMW CHT with low molecular weight chitosan (LMW CHT). The digestion was set up in two ways, the first being a benign system with controlled pH at 6.9 throughout the entire experiment and the second that adjusted pH in synchronisation with conditions of the human gastrointestinal tract (mouth, stomach and small intestine). The incorporation of MMW and LMW CHT both resulted in a reduction of maltose equivalent liberated from the gel systems and the former proved to be consistently more effective. Although fluctuations in the measured sugar liberated from the pH adjusted model were clearly evident, the qualitative trend of retarding starch hydrolysis afforded by LMW and MMW CHT incorporation remained in effect, an outcome which is encouraging for applying this approach to systems imitating conditions of the GI tract.

The physicochemical properties of WPI, WS and CHT as a function of concentration, pH, added counteractions, temperature and time have been characterised. The macromolecular network formed by the low-to-intermediate solid systems has also been assessed on the effectiveness to minimise amylolytic attack and the specific conditions to achieve this have been pinpointed. The mimicking of the human gastrointestinal tract in so far as the pH, time and total volume to analyse starch containing samples has also been initiated. The findings of the thesis provides a stepping stone for the food industry interested in using WPI, WS, $CaCl_2$and CHT for the development of new products of potentially lowered glycemic load or as a reference to pre-existing products containing these materials. As the study presented in this thesis goes, it is suggested the next step is to assess the properties of tertiary systems combining whey protein, wheat starch and MMW CHT in the presence of added salts. The future work should also build on the present model mimicking the human gastrointestinal tract by progressive incorporation of further components, e.g. protease, bile salts, mucin for an improved picture of metabolic processes.

Appendices

Preparation of 3, 5-dinitrosalicylic acid reagent (DNSA)

For all the *in vitro* starch digestion experiments, DNSA assay was used. The preparation of the DNSA was as per Miller (1959) whereby approximately 3.15g of 3,5-dinitrosalicylic acid was dissolved into 500 mL of 0.5M NaOH. To this, the following ingredients were added: 91g rochelle salt, 2.5g phenol, 2.5g sodium bisulfite. The solution was mixed well and then diluted to 1L with de-ionised water. The DNSA was stored in brown glass bottle at room temperature, prepared 7 days before use and used within 2 weeks of preparation.

Maltose equivalent calculation

For every *in vitro* starch digestion experiment, a serial dilution of the maltose standard was prepared covering the concentration range from 0.025-0.125 mg/mL. This was read at an absorbance of 540 nm on the UV-VIS spectrophotometer and to draw a maltose standard curve such as the one below:

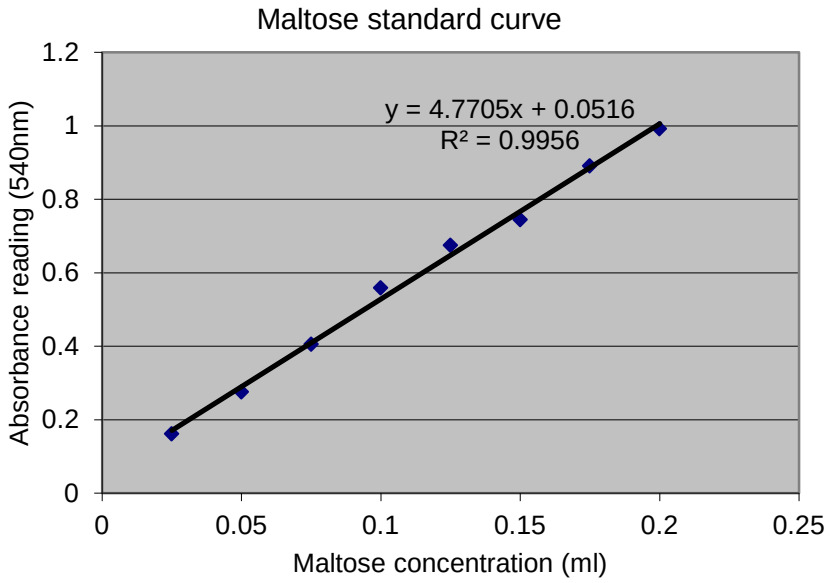

Sample aliquots were calculated against the maltose standard curve to measure the maltose equivalent in the sample. For example, column C & D are the absorbance readings of the sample. Column E is the average of the absorbance readings between replicates (C & D).Column F is the average of the absorbance reading divided by the maltose standard curve gradient. Column H, I, J and K is the respective amount of maltose equivalent within 0.6ml, in dialysis tube, in beaker and per gram of the gel sample.

A	B	C	D	E	F	G	H	I	J	K
21	Maltose equivalent of 15%WPI+0%Starch gel during 3hr hydrolysis									
	6g of 15%WPI+0%starch gel;12000U of alpha amylase from Aspergillus oryzae									
A	maltose equivalent in dialysis tubing									
	Time	Absorbance			Concentration in testing tube	Amount in 0.05ml	Amount in 0.6ml	Amount in dialysis tube (37ml)	Amount in beaker	Maltose quivalent from 1g gel
	(min)	1	2	AVE	(mg/ml)	(mg)	(mg)	(mg)	(mg/ml)	(mg)
	0	0.482	0.474	0.478	0.0901		0.4504	27.78	0.75	4.63
	0	0.454	0.453	0.454	0.0855		0.4274	26.35	0.71	4.39
	0	0.465	0.458	0.462	0.0870		0.4349	26.82	0.72	4.47
	30	0.457	0.453	0.455	0.0858		0.4288	26.44	0.71	4.41
	30	0.484	0.46	0.472	0.0890		0.4448	27.43	0.74	4.57
	30	0.443	0.441	0.442	0.0833		0.4165	25.69	0.69	4.28
	60	0.429	0.437	0.433	0.0816		0.4080	25.16	0.68	4.19
	60	0.427	0.413	0.420	0.0792		0.3958	24.41	0.66	4.07
	60	0.425	0.426	0.426	0.0802		0.4010	24.73	0.67	4.12
	90	0.395	0.402	0.399	0.0751		0.3755	23.16	0.63	3.86
	90	0.38	0.37	0.375	0.0707		0.3534	21.79	0.59	3.63

Journal publications (front pages)

Food Chemistry 137 (2013) 76–82

Contents lists available at SciVerse ScienceDirect

Food Chemistry

journal homepage: www.elsevier.com/locate/foodchem

Phase behaviour and *in vitro* hydrolysis of wheat starch in mixture with whey protein

Natasha Yang, Yingting Liu, John Ashton[1], Elisabeth Gorczyca, Stefan Kasapis*

School of Applied Sciences, RMIT University, City Campus, Melbourne, Vic 3001, Australia

ARTICLE INFO

Article history:
Received 2 August 2012
Received in revised form 19 September 2012
Accepted 4 October 2012
Available online 22 October 2012

Keywords:
Whey protein isolate
Native wheat starch
Phase separation
In vitro starch digestion

ABSTRACT

Network formation of whey protein isolate (WPI) with increasing concentrations of native wheat starch (WS) has been examined. Small deformation dynamic oscillation in shear and modulated temperature differential scanning calorimetry enabled analysis of binary mixtures at the macro- and microrheological level. Following heat induced gelation, textural hardness was measured by undertaking compression tests. Environmental scanning electron microscopy provided tangible information on network morphology of polymeric constituents. Experiments involving *in vitro* starch digestion also allowed for indirect assessment of phase topology in the binary mixture. The biochemical component of this work constitutes an attempt to utilise whey protein as a retardant to the enzymatic hydrolysis of starch in a model system with α-amylase enzyme. During heating, rheological profiles of binary mixtures exhibited dramatic increases in G' at temperatures more closely related to those observed for single whey protein rather than pure starch. Results from this multidisciplinary approach of analysis, utilising rheology, calorimetry and microscopy, argue for the occurrence of phase separation phenomena in the gelled systems. There is also evidence of whey protein forming the continuous phase with wheat starch being the discontinuous filler, an outcome that is explored in the *in vitro* study of the enzymatic hydrolysis of starch.

1. Introduction

In recent times, whey protein has become increasingly appreciated for its versatile functionality, superior nutritional value and significant bioactivity (Smithers, 2008). It is defined as the soluble proteins remaining in milk serum after coagulation of caseins at pH 4.6 and approximately 20 °C. The collective term mainly describes β lactoglobulin, α lactalbumin and bovine serum albumin (Considine et al., 2011). Thermogelation of whey protein is an example of a functional property considered important in the food industry. This occurs by a two-step process. Firstly, proteins must surpass the critical temperature causing denaturation and partial unfolding of the globular structure. Provided that the polymer concentration is high enough, association of individual molecules subsequently follows and inevitably leads to formation of a continuous three-dimensional structure (Aguilera & Rojas, 1996).

Native wheat starch mainly consists of linear amylose and highly branched amylopectin in the ratio of 1:3, which are α(1–4) and α(1–4)/α(1–6) glucose molecules, respectively (Copeland, Blazek, Salman, & Tang, 2009). The granule has been processed for all sorts of functional utility, including thickening and pasting properties. Heating in the presence of water leads to swollen granules, disruption of amylopectin double helices and migration of amylose out into the surrounding medium (Huang, Kennedy, Li, Xu, & Xie, 2007). Most importantly, heating must occur at or above the gelatinisation temperature for the aforementioned events to occur. Upon cooling, amylose associates to form a gel, followed by aggregation (known as retrogradation) mainly due to the amylopectin component (Hermansson & Svegmark, 1996).

The complexity comes about when heating of whey protein occurs in the presence of other biopolymers in aqueous systems. Knowledge of the phase morphology in polymeric mixtures is essential, since this largely determines the techno- and biofunctionality of materials used as components of commercial products. In the presence of high levels of water molecules, serving the role of a good quality solvent, heating and subsequent cooling results in a mixed system of denatured protein and gelatinised starch. These may form interpenetrating, conformationally or electrostatically coupled, and phase separated networks, depending on physicochemical environment and concentration of the two polymers (Morris, 1986; Turgeon & Beaulieu, 2001).

Mixed preparations above the minimum critical gelling concentration, and provided no overriding drive to heterotypic binding

* Corresponding author. Tel.: +61 3 992 55244; fax: +61 3 992 55241.
E-mail address: stefan.kasapis@rmit.edu.au (S. Kasapis).
[1] Address: Sanitarium Development and Innovation, Sanitarium Health Food Company, Cooranbong, NSW 2265, Australia.

0308-8146/$ - see front matter © 2012 Published by Elsevier Ltd.
http://dx.doi.org/10.1016/j.foodchem.2012.10.004

ARTICLE IN PRESS

Food Hydrocolloids xxx (2014) 1–9

Contents lists available at ScienceDirect

Food Hydrocolloids

journal homepage: www.elsevier.com/locate/foodhyd

Effect of calcium chloride on the structure and *in vitro* hydrolysis of heat induced whey protein and wheat starch composite gels

Natasha Yang [a], Jie Luan [a], John Ashton [a,b], Elisabeth Gorczyca [a], Stefan Kasapis [a,*]

[a] School of Applied Sciences, RMIT University, City Campus, Melbourne, Vic 3001, Australia
[b] Sanitarium Development and Innovation, Sanitarium Health Food Company, Cannonbong, NSW 2265, Australia

ARTICLE INFO

Article history:
Received 26 November 2012
Accepted 21 February 2014

Keywords:
Whey protein isolate
Native wheat starch
Calcium chloride
In vitro starch hydrolysis

ABSTRACT

The formation of heat induced whey protein isolate (WPI) and wheat starch (WS) gels in the presence of added calcium chloride (5–192 mM) has been examined. Thermal properties, including the onset temperature of starch gelatinization and protein denaturation, are defined by low amplitude oscillation on shear and modulated temperature differential scanning calorimetry. Upon heating and subsequent cooling, comparison of the storage modulus values bear information on the enhancement of protein aggregation by the electrolyte and the occurrence of phase separation phenomena between the two polymeric constituents in the mixture. Further confirmation of observed trends has been provided by measurements on textural hardness of gels in single cycle compression tests. Porous and aggregated microstructures are identified upon visual examination by environmental scanning electron microscopy. The gels were subjected to *in vitro* enzymatic hydrolysis and the role of calcium in reducing the extent of starch degradation by α-amylase has been established. It is evident from the results that ionic strength in the form of added calcium ions largely influences gelation kinetics of whey protein leading to significant variability in the hydrolytic potential of α-amylase on wheat starch.

1. Introduction

The superior nutritional value, granted GRAS status, and versatile functionality of whey proteins are a part of the appeal in utilizing the additive in many food formulations (Smithers, 2008). Manufacturers most commonly take advantage of its gelation mechanism and emulsification properties to manipulate bulk and interfacial features thus affecting organoleptic properties in end products (Doi, 1993).

Effective incorporation of whey protein is achievable by developing products on a sound technological basis and could directly benefit consumers by providing a healthy alternative to a range of popular convenience foods (Hongsprabhas & Barbut, 1996). This is particularly important as it has been estimated that in excess of a million Australians have obesity and Type 2 diabetes, and about half of those are not aware that they have the condition (Health Insite, 2008). The current society is suffering from 'diseases of choice' where few seem inclined to change their nutritional habits. Food directly influences blood glucose concentrations and response. However, this response is influenced by many factors such as the food form (whole or ground), cooking and processing, particle size and structure.

Heat induced protein gelation primarily occurs via partial unfolding of the corpuscular molecule and exposure of non polar and sulfhydryl groups (Iupano & Gonzalez, 1999; Matsudomi, Rector, & Kinsella, 1991; Steventon, Gladden, & Fryer, 1991; Verheul & Roefs, 1998). Aggregation subsequently follows, involving disulphide and non-covalent interactions, i.e. electrostatic and van der waals forces, hydrogen and hydrophobic bonds (Britten & Giroux, 2001; Damodaran, Parkin, & Fennema, 2008; Hoffmann & Van Mil, 1997; Kinsella & Whitehead, 1989; Shimada & Cheftel, 1988; Verheul & Roefs, 1998). The characteristics of the heat set protein gel depends on a multitude of factors including heating rate, holding time and temperature, pH, ionic strength, mineral content and presence of other hydrocolloids forming a rather complex physicochemical environment (Barbut, 1995; Damodaran et al., 2008; Ju & Kilara, 1998; Kuhn, Cavalieri, & Cunha, 2010; Muhrhill, Rector, & Kinsella, 1990; Verheul & Roefs, 1998). Calcium salts are known to be especially effective at enhancing thermal stability and increasing protein aggregation (Kuhn et al., 2010).

* Corresponding author. Tel.: +61 3 992 55244; fax: +61 3 992 55248.
E-mail address: stefan.kasapis@rmit.edu.au (S. Kasapis).

http://dx.doi.org/10.1016/j.foodhyd.2014.02.022
0268-005X/

Please cite this article in press as: Yang, N., et al., Effect of calcium chloride on the structure and *in vitro* hydrolysis of heat induced whey protein and wheat starch composite gels, *Food Hydrocolloids* (2014), http://dx.doi.org/10.1016/j.foodhyd.2014.02.022

References

Miller, G. L. (1959). Use of dinitrosalicylic acid reagent for determination of reducing sugar. *Analytical chemistry, 31*, 426-428.